ORGANIC CHEMISTRY FRONTIERS

REVIEW

View Article Online
View Journal

Cite this: DOI: 10.1039/d5qo01417d

Radical reactivity of aryl thianthrenium salts

Ryan A. Pohorenec [a] and Shiqing Xu *[a,b]

Functionalization of the C(sp^2)–H bond is a challenging yet highly useful synthetic task due to its relative inertness and commonality among functional groups. Arene thianthrenation is an emerging C(sp^2)–H bond activation strategy featuring high chemo- and regioselectivity in the modification of structurally diverse substrates. The resultant aryl thianthrenium (Ar–TT^+) salts exhibit divergent single- and two-electron reactivity modes, which have enabled new C(sp^2)–bond formation to the main group elements through mechanistically distinct routes. This review complements the existing literature on the two-electron behavior of Ar–TT^+ salts by highlighting the enhanced control of radical reactivity achieved in the site-selective thianthrenation of arenes and subsequent C(sp^2)–S bond homolysis to generate aryl radicals. Discussion of the structural and electronic properties of Ar–TT^+ salts promoting single-electron reactivity under mild conditions, functional group tolerance, enhanced platform cross-compatibility, and increased potential for sustainability through catalysis is a thematic focus throughout. Identification of these prior methodological advancements culminates in a prospectus on the opportunities for future reaction development.

Received 12th October 2025,
Accepted 17th December 2025
DOI: 10.1039/d5qo01417d
rsc.li/frontiers-organic

1. Introduction

A fundamental goal of synthetic chemistry is to exert precise control over bond scission and formation. Primary challenges encountered therein include the selectivity (*e.g.* chemo-, regio-, and stereo-) and efficiency of a given transformation. Among the most useful yet challenging bond types to selectively and efficiently manipulate is the carbon–hydrogen (C–H) bond. Therefore, innovation of C–H activation platforms is a matter of longstanding research interest due to the comparative ubiquity and inertness of this bond type relative to other functional groups. Significant advancements in C–H activation (scission, polarization) and functionalization (replacement) were made in the last century.[1–8] Nonetheless, opportunities for the refinement of known methods and exploration of novel techniques remain with respect to the overarching goals of synthetic chemistry and modern reaction design.[9–11]

Thianthrenation as a C–H activation strategy features high chemo- and regioselectivity in the modification of structurally

[a]*Department of Chemistry, College of Arts and Sciences, Texas A&M University, College Station, TX 77843, USA. E-mail: shiqing.xu@tamu.edu*
[b]*Department of Pharmaceutical Sciences, Irma Lerma Rangel College of Pharmacy, Texas A&M University, College Station, Texas 77843, USA*

Ryan A. Pohorenec

Ryan Pohorenec received BS (2022) and MS (2023) degrees from the University of Rochester, where he studied organometallic chemistry under the guidance of Prof. William D. Jones. He now continues graduate studies in chemistry through joint training as a physician scientist (MD-PhD). His current research interests include synthetic methodology and homogeneous catalysis.

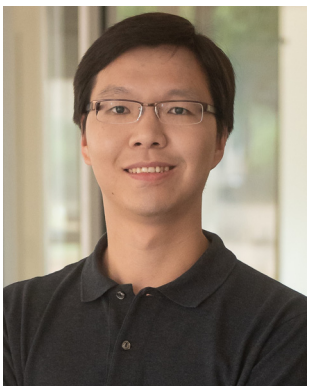

Shiqing Xu

Shiqing Xu received his PhD in Medicinal Chemistry from Fudan University under the mentorship of Professors Peng Xia and Ying Chen. He subsequently completed postdoctoral training and worked as a research scientist in Chemistry at Purdue University with Professor Ei-ichi Negishi. He joined the faculty at Texas A&M University and started his independent career in 2023. His research interest focuses on synthetic organic chemistry and medicinal chemistry.

diverse substrates under mild reaction conditions.[12] Activation of C_{sp^3}–H, C_{sp^2}–H, and C_{sp}–H bonds by this approach has enabled new carbon bond formation to the non-metallic main group elements through multiple mechanistically distinct pathways. Further, this strategy enables reactivity complementary to other "onium"-based C–H functionalization platforms[13] with superior selectivity and scope of compatible substrates.

Earlier accounts from the pioneering Ritter[14] and Wang[15] laboratories provided overviews of aryl sulfonium salt reactivity, and Ritter has recently expanded their work to highlight the recent growth in the synthetic utilization of C_{sp^n}-substituted thianthrenium salts.[12] Shu has similarly outlined the synthesis and reactivity of C_{sp^n}-substituted thianthrenium reagents.[16] Alkene C_{sp^2}-substituted thianthrenium salts display a wide range of distinct and synthetically valuable reactivity modes,[17–30] as recently reviewed by Wickens.[31] Chen reviewed the access to aryl radical intermediates from a variety of sulfonium salts.[32] The field has continued to advance rapidly, with substantial progress made in understanding and exploiting the radical chemistry of thianthrenium salts. In this review, we focus specifically on the reactivity of aryl thianthrenium salts as aryl radical precursors, with an emphasis on the enhanced control of carbon-centered radical reactivity enabled by stepwise site-selective thianthrenation and subsequent functionalization. By providing a mechanistically focused overview of recent advances, we aim to clarify reactivity patterns and inspire continued innovation in this rapidly expanding area of research.

1.1 Arene thianthrenation

Organic sulfur ("organosulfur") compounds, containing a carbon–sulfur (C–S) bond, exhibit diverse structures and reactivity enabled by the range of accessible oxidation states and availability of unoccupied sulfur d-orbitals.[33] Expansive discussion of organosulfur compounds is available elsewhere.[34–36] Additional evidence for the practical utility of these compounds is demonstrated by the diversity in industrial applications of organosulfurs across the pharmaceutical,[37] agricultural,[38] polymer,[39] and electronics[40] industries. Organosulfur compounds serve important biologic functions as radical scavengers, atom- and group-transfer reagents (*e.g.* *S*-adenosyl methionine, SAM), structural moieties of biopolymers, and functional units of proteolytic enzymes.[41] Given their compatibility with various synthetic platforms (thermochemistry, transition-metal catalysis, photochemistry, electrochemistry), organosulfurs have emerged as useful reagents in modern organic synthesis.[42–45]

Synthetic access to and utilization of various subclasses of sulfonium salts have been recently reviewed.[46,47] It is useful to distinguish cyclic sulfoniums, in which the sulfur atom contributes to a ring system, from their acyclic counterparts, as well as to refer to the most labile and reactive bond between sulfur and its substituents (*e.g.* "C_{sp^n}-substituted"), as reactivity patterns are distinct among these groups. While many sulfonium salts currently utilized synthetically are carbon-substituted, heteroatom-substituted sulfonium reagents have also been prepared.[48] Among the common cyclic sulfonium salts are those constructed on the thianthrene (TT), dibenzothiophene (DBT),[49] and phenoxathiin backbone. Notable transformations of C_{sp^2}- and C_{sp}-substituted sulfoniums also involve cycloaddition reactions.[46] Various cross-couplings of organosulfoniums have been reported, including Suzuki–Miyaura, Mizoroki–Heck,[50] and Sonogashira reactions.[51] Computational (DFT) study of the lowest unoccupied molecular orbital (LUMO) of aryl thianthrenium salts revealed antibonding character of the exocyclic C_{sp^2}–S bond, promoting selective reactivity at this site.[52] Accordingly, the BDE of the exocyclic C_{sp^2}–S bond in Ph–TT^+ has been calculated by DFT as 64.2 kcal mol^{-1}.[53] Endocyclic C_{sp^2}–S cleavage occurring through a ring-opening attack by a strong nucleophile, such as a carbanion equivalent, has been observed.[54,55]

The redox profile of thianthrene includes two reversible single-electron oxidations with $E_{ox}(TT^+/TT)$ = +1.26 V and $E_{ox}(TT^{2+}/TT^+)$ = +1.77 V in MeCN *vs.* SCE.[56] The singly-oxidized radical cation (TT^+) was found to be air and water stable after 13 days in a solution of 96% H_2SO_4, as demonstrated by Shine and Petite's ultraviolet-visible (UV-vis) spectroscopic analysis. Early experimental evidence for the formation of thianthrene radical cation resulted from the first accurate EPR studies in 1962, undertaken by independent groups of Shine and Petite,[57] Kinoshita,[58] and Lucken.[59] These experiments demonstrated five-line spectrum with isotropic hyperfine splitting of magnitude 1.32 G, consistent with spin-nuclear interactions with four equivalent hydrogen atoms. Characterization by single-crystal X-ray diffraction of the thianthrenium tetrachloroaluminate salt was achieved in 1994 by Bock and colleagues.[60]

Despite the early foundations set forth by these studies, thianthrenium salts were synthetically underutilized until only recently. A PubMed search on 24 November 2025 for "thianthrene cation" or "thianthrenium" or "thianthrenation" yielded 202 total results, with marked growth in annual reports since the year 2019 (Fig. 1). A structure-based search of the Reaxys database for aryl thianthrenium compounds on 16

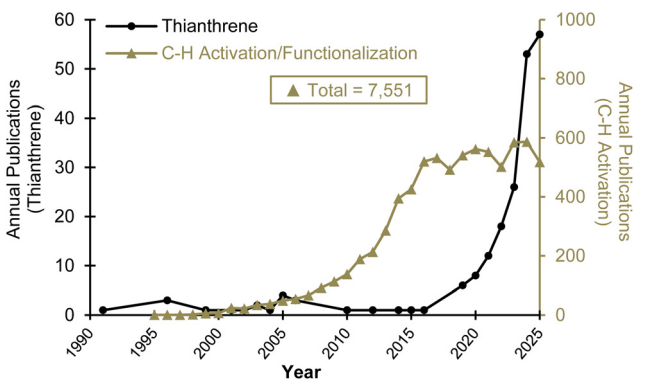

Fig. 1 Trends in C–H activation/functionalization and thianthrenium chemistry. Data collected from the PubMed database on 24 November 2025 using the search terms "thianthrene cation" OR "thianthrenium" OR "thianthrenation"; "C–H activation" OR "C–H functionalization".

August 2025 yielded results for 973 substances and 1321 reactions, as reported within 1973 documents divided among 215 primary or review articles and 1765 patents. The recently renewed interest in thianthrenation as a C–H functionalization strategy has largely been driven by the development of synthetic approaches to thianthrenium salt precursors, accompanied by mechanistic insights, recognition of favorable redox activity, compatibility with all major platforms for energy input, and demonstrated versatility in new-bond construction under mild conditions.

Following the preliminary works of the middle 20th century, a relative paucity in work occurred until the Dawn of the 21st century. Nine years after their unambiguous spectral characterization of thianthrene radical cation salts, the Shine group prepared aryl thianthrenium compounds by reaction of the explosive thianthrenium perchlorate salt with methylbenzene, methoxybenzene, and anisole.[61] This work was extended to disubstituted benzenes three years later in 1974.[62] Two decades later, [3 + 2] cycloadditions between the thianthrenium radical cation and olefins[63,64] as well as additions to alkynes were observed.[65,66] Cycloadducts of thianthrenium perchlorate salts and alkenes were later shown to decompose to oxazolines in the presence of acetonitrile and water,[67] with a subsequent report demonstrating the capability for electrochemical reactivity and potential for regeneration of thianthrene upon formation of decomposition products.[68] A paucity in new annual reports on the synthetic use of thianthrenium salts ensued, until 2019 (Fig. 1), presumably due to hazards associated with the perchlorate salts and difficulty in their purification. The preparation of the less hazardous thianthrenium tetrafluoroborate salt was described in 1988.[69]

The breakthrough came in 2019 when the Ritter group reported a new synthetic strategy that enabled continued development of the thianthrenation platform for C_{sp^2}–H activation and functionalization.[70] When treated with trifluoroacetic anhydride (TFAA), (tetrafluoro)thianthrene (TFT or TT), and tetrafluoroboric acid (HBF_4), (tetrafluoro)thianthrene *S*-oxide (TFTSO or TTSO), various arenes were readily converted to the corresponding thianthrenium tetrafluoroborate salts *via* C_{sp^2}–H thianthrenation. In the presence of the monosubstituted arenes such as ethylbenzene, high *para*-selectivity (>99%) was observed for C_{sp^2}–H thianthrenation. A similar result was obtained in the direct electrolysis of TFT in the presence of arene. Numerous synthetic applications were demonstrated in this report, including Suzuki, Negishi, Mizoroki–Heck, and Sonogashira couplings, in addition to carbonylation, halogenation, phosphonylation, and borylation. The initial mechanistic proposal for the formation of aryl thianthrenium salts involved the formation of a TFT^{+}–/TT^{+}–TFA adduct that, or TT, generated the radical cation (TFT$^{\bullet+}$ or TT$^{\bullet+}$), which subsequently reacts with arene to produce a dicationic Wheland intermediate prior to a selectivity-determining irreversible deprotonation event.[70]

Additional experimental and computational evidence later suggested that the dication (TT^{2+}) is the reactive species toward arene, and it is generated by heterolysis of a TT^{+}–TFA adduct (Scheme 1). Single electron transfer (SET) between TT^{2+} and arene affords a radical ion pair between TT$^{\bullet+}$ and arene (Ar$^{\bullet}$), which by comproportionation with a second equivalent of TFT subsequently undergoes radical recombination to form a dicationic Wheland intermediate. Reversibility of this radical recombination step, promoted by the relative stability of TT$^{\bullet+}$ to other sulfur radicals, is permissive of thermodynamically controlled selection for the lowest energy regioisomer of the Wheland intermediate.[71] In the case of monosubstituted arenes, steric considerations support a relative ordering in ΔG of *ortho-* > *meta-* ~ *para-*, while the electronics of radical addition support ΔG *meta-* > *ortho-* ~ *para-*. Taken together, an explanation for the generally observed exceptional *para*-selectivity in thianthrenation emerges based on arene stereoelectronics. Notably, an alternative pathway for generation of the Wheland intermediate *via* a concerted S_EAr mechanism was

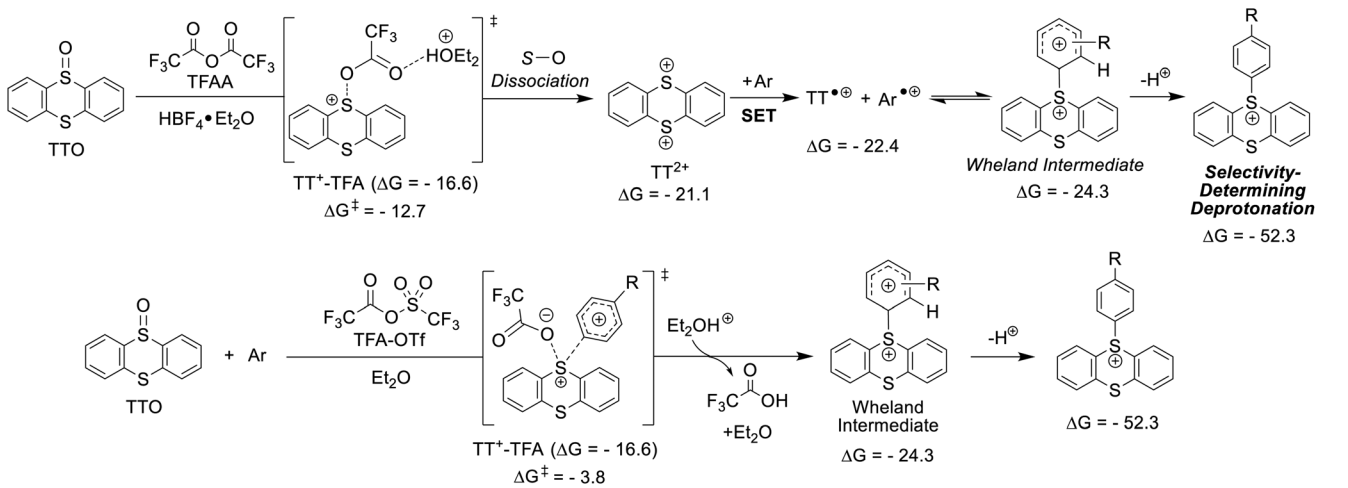

Scheme 1 Mechanistic basis for regioselectivity in thianthrenation. DFT-calculated Gibbs free energies are reported in kcal mol^{-1} with respect to TTO, where Ar = toluene and R = CH_3.[71]

considered operant in the absence of Brønsted acid, which proceeds through a higher energy transition state ($\Delta\Delta G^{\ddagger}$ = 8.9 kcal mol^{-1}) than formation of TT^{2+}. In addition to the conditions used, dependence on the electronic nature of the arene influences the mechanistic trajectory, with stronger nucleophiles computationally favoring direct substitution on TT^{+}–TFA.[71]

In 2020, Wang reported a strategy for the efficient synthesis of aryl thianthrenium triflate salts. Thianthrene *S*-oxide (TTSO) was reacted with triflic anhydride (Tf_2O). High *para*-selectivity was observed in the thianthrenation of toluene as a model monosubstituted arene. A preliminary mechanistic hypothesis supported by computational investigation suggested that the dication TT^{2+} is the reactive species toward arene, which is generated by heterolysis of a TT^{+}–OTf adduct. Experimentally observed regioselectivity was suggested to result from the electronics of the radical addition in combination with electrostatic interactions among accumulated charge on the arene and thianthrenium in formation of the Wheland intermediate, which together favor an *exo*-conformation leading to *para*-product formation.[72] Given the mechanistic studies undertaken by the Ritter laboratory,[71] a direct substitution pathway between arene and TT^{+}–OTf adduct may be additionally considered for the formation of the Wheland intermediate.

Recently, distinct sets of thianthrenation conditions have been developed based on the electron density and acid–base sensitivity of the substrate to be functionalized, adapted for arenes that strongly activated (electron-rich) to those that are weakly activated (electron-deficient). Reported limitations include the undesirable reactivity of certain functional groups with the strong acids (*e.g.* TfOH, TFAA) added to enhance the efficiency of thianthrenation among weakly activated arenes, as well as a general incompatibility between deactivated arenes and any of the described sets of standard conditions.[73] While few reports demonstrating the isolation of Ar–TT^{+} salts generated by the direct electrochemical conversion of arenes and thianthrene are available in the literature,[74,75] this approach confers opportunity for the one-pot activation and functionalization of C_{sp^2}–H bonds as well as the catalytic reuse of substoichiometric quantities of thianthrene. Given the advantageous step- and resource economy of this method, we anticipate the increased future prevalence of this method of Ar–TT^{+} salt utilization. In addition to C_{sp^2}–H thianthrenation, alternative strategies have been developed to access a broader range of arylthianthrenium (Ar–TT^{+}) salts.

These include Cu-mediated thianthrenation of (hetero)aryl boronic acids[76] and photoinduced decarboxylative thianthrenation of (hetero)aryl carboxylic acids,[77] which enable the synthesis of electron-deficient Ar–TT^{+} salts that are typically inaccessible *via* direct C–H thianthrenation.

Considering the remarkable selectivity observed in arene thianthrenation, its demonstrated versatile synthetic utility in C_{sp^2}–H activation, recent reviews have discussed the subject.[12,14–16,31,32,46,51] Herein, we focus on the recent synthetic utilization of aryl thianthrenium (Ar–TT^{+}) salts as aryl radical (Ar$^{\bullet}$) precursors. Several routes to aryl radicals[78–80] have been studied under thermal, photochemical, and electrochemical conditions, including aryl halides, aryldiazonoium salts,[81] diaryliodonium salts, and aryl pyridinium salts.[13] Compared to aryl halides (E_{red}(PhX/PhX$^{\bullet-}$) = −2.97, −2.80, −2.44, and −2.24 V *vs.* SCE for X = F, Cl, Br, and I, respectively),[82] Ar–TT^{+} salts are more reducible (E_{red}(Ph–TT^{+}/Ph–$TT^{\bullet}$) = −1.55 V *vs.* SCE in MeCN),[52] enabling milder conditions and enhanced functional group tolerance among transformations of the latter. Aryl diazonium salts (E_{pc}(PhN_2^{+}/$PhN_2^{\bullet}$) = −0.06 V *vs.* SCE)[83] are highly reactive and therefore require special handling and storage precautions.[84] Diaryliodonoium salts (E_{pc}($PhIPh^{+}$/$PhIPh^{\bullet}$) = −0.96 V *vs.* SCE)[85] tend more reactive than Ar–TT^{+} salts, though their preparation usually proceeds with lower regioselectivity or by less direct routes than thianthrenation.[86,87]

2. Radical reactivity of aryl thianthrenium salts

Homolysis of the exocyclic C_{sp^2}–S bond of an Ar–TT^{+} salt yields an aryl radical, a useful synthetic intermediate. To date, bonds to diverse non-metal elements have been constructed using this approach, representing a versatile and accessible transformation space (Fig. 2). Compatibility with major reaction platforms – transition metal catalysis,[88,89] photochemistry,[90] electrochemistry, and dual catalysis – further demonstrates the versatility of this synthetic approach. Integration of thianthrenation with the established and emerging strategies among these platforms is reflected by the recent reports featuring multicomponent reactions, visible-light photoredox catalysis, generation of sulfonium salt EDA complexes,[91,92] and the catalytic recycling of thianthrene in one-pot reactions.

2.1 Group 1

C_{sp^2}–D bond formation. Substitution of arene C_{sp^2}–H bonds for deuterium (^{2}H, D) or tritium (^{3}H, T) is useful for mechanistic studies of chemical transformations and tracing metabolites in biological systems. For some applications of hydrogen isotope exchange (HIE) reactions, regioselective mono-substitution strategies are desirable yet challenging frontiers. Various transition metal catalysts were reported to facilitate HIE, while capable of achieving high regioselectivity and isotope incorporation, demonstrate a propensity for multiple (≥2) bond replacement and dependency on substrate or ligand sterics for control of site-selectivity.[93,94] To address these limitations and enable finer chemo- and regio-control, a strategy combining the site-selectivity of thianthrenation with heterogeneous palladium catalysis has been developed.[95,96]

Within the single-electron regime, deuteration of a variety of mono-, di-, and tri-substituted aryl thianthrenium salts in the presence of a CD_3OD, base (Cs_2CO_3), and light (λ = 380–385 nm, P = 50 W) proceeded with moderate efficiency (up to 80% yield) and high regioselectivity, and high deuterium incorporation (up to 99%).[97] Late stage functionalization of

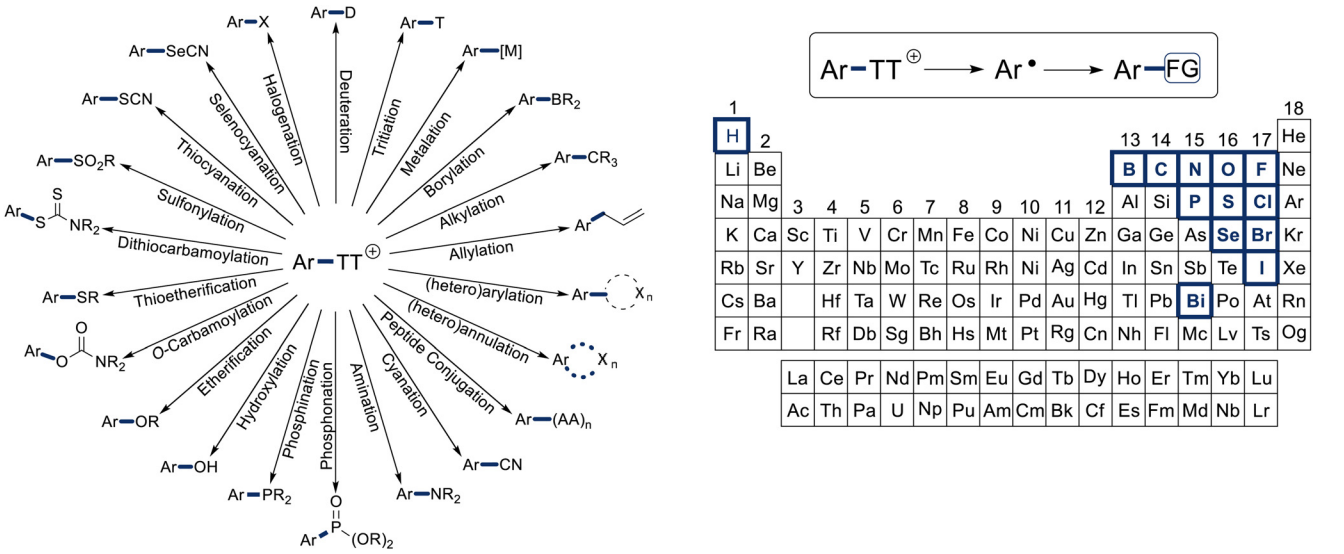

Fig. 2 Synthetic utilization of aryl thianthrenium salts as aryl radical precursors.

bioactive compounds of the agrochemicals pyriproxyfen and boscalid was reported therein. Mechanistic insights from experiments with the radical scavengers (2,2,6,6-tetramethylpiperidin-1-yl)oxyl (TEMPO), 2,6-di-*tert*-butyl-4-methylphenol (BHT), and1,1-diphenylethylene (DPE) suggested the formation of radical intermediates by observation of a significant reduction in yield when added to standard conditions (Scheme 2). While the mechanistic details remain unclear, observations on the extent of deuterium incorporation with varying solvent isotopomers suggested that the deuterium atom is sourced primarily from the CD_3-group of CD_3OD. This result is consistent with cleavage of the weakest D–X bond in methanol (C–H BDE = 96.1 ± 0.3 kcal mol^{-1} and the O–H BDE = 104.6 ± 0.7 kcal mol^{-1}).[98]

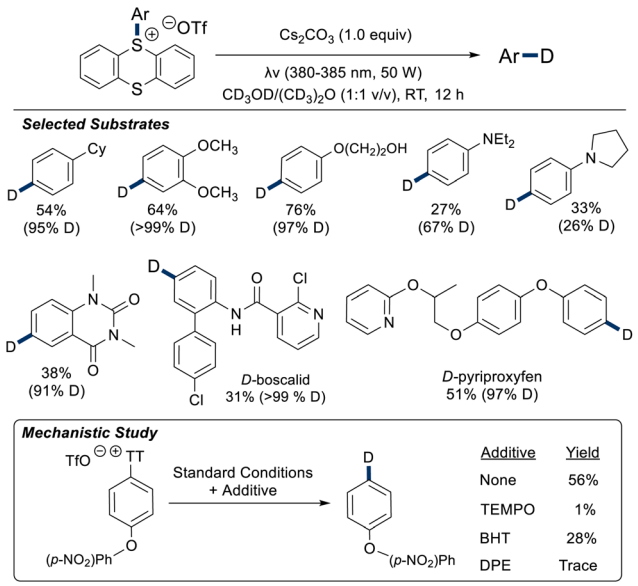

Scheme 2 Hydrogen isotope exchange. TEMPO = (2,2,6,6-tetramethylpiperidin-1-yl)oxyl, BHT = 2,6-di-*tert*-butyl-4-methylphenol, DPE = 1,1-diphenylethylene.

An organic photoredox-catalyzed deuteration of Ar–TT$^+$ salts was reported by Yu in 2024.[99] Under aerobic conditions and visible light irradiation (λ = 427 nm, P = 40 W; PS = 2,3,4,5,6-penta(carbazol-9-yl)benzonitrile, 5CzBN) in an aqueous medium, substituted biphenyl derivatives and (hetero)arenes were transformed.

Several bioactive and pharmaceutical compounds were functionalized with high deuterium incorporation (≥90%) from an inexpensive and widely available deuterium source ($CDCl_3$) in a demonstration of applications in LSF. Select examples of extension of this approach to the borylation, cyanation, and selenocyanation of Ar–TT$^+$ salts were described. Robust mechanistic study of the system was undertaken, which supports an energy transfer (EnT) pathway for the generation of aryl radicals; the first observation of this mode of activation of Ar–TT$^+$ salts. Photoexcitation of the photosensitizer (PS) reflected increasingly less intense fluorescence with increasing concentration of the chosen model substrate, biphenylthianthrenium tetrafluoroborate, suggesting the capacity for Ar–TT$^+$ salts to quench PS*. The triplet state (T_1) of this substrate, resulting from an EnT interaction with PC*, has a calculated (DFT) energy of E_{T1} = 60.9 kcal mol^{-1}, and reaction yields increased as E_{T1}(PS*) approached and superceded this value (Scheme 3). The observation that reactivity does not depend as strongly on the relative magnitudes of E_{red}(PC$^{\bullet+}$/PC*) and E_{red}(Ar–TT$^+$) as it does on those of E_{T1}(PS*) and E_{T1}([Ar–TT$^+$]*) is suggestive of an EnT mechanism. Additional support for an EnT mechanism was the observation of an absorption feature attributable to TT$^+$ by transient absorption spectroscopy (TAS), where TT is the expected byproduct of reductive SET. Absent significant overlap between the PS* emission spectrum and substrate absorption spectrum,

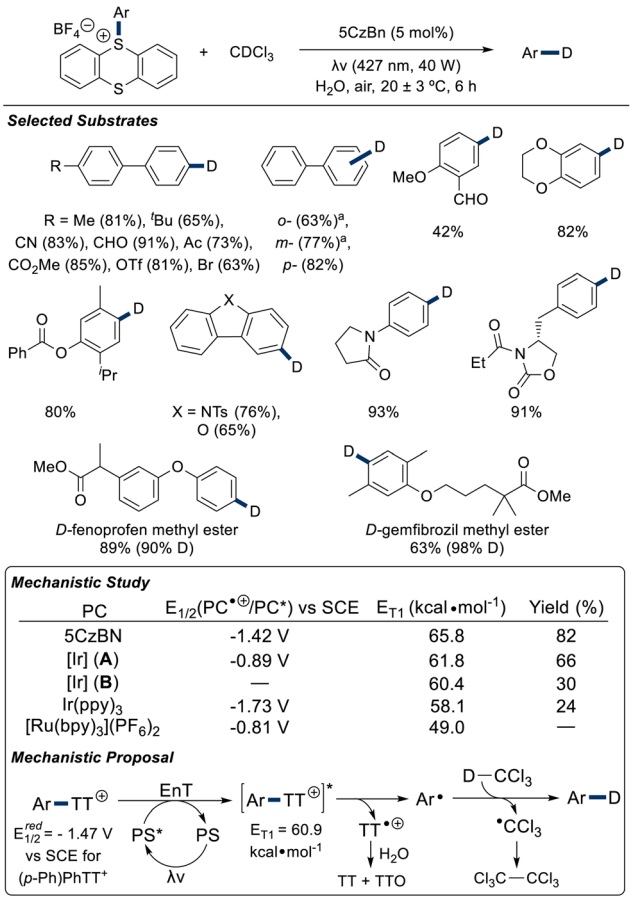

Scheme 3 EnT-promoted deuteration of aryl thianthrenium salts. [a]reaction time = 24 h. Deuterium incorporation is > 99% unless otherwise indicated. [Ir] (A) = $[Ir(dF(CF_3)ppy)_2(dtbbpy)]PF_6$, [Ir] (B) = $[Ir(dF(CF_3)ppy)_2(bpy)]PF_6$.

Förester resonance energy transfer (FRET) was deemed less likely than a Dexter-type EnT mechanism.[100] Addition of the radical scavengers TEMPO, BHT, and DPE led to the detection of the corresponding adducts by HRMS analysis. Excluding a radical chain mechanism through on–off studies, and a mechanistic proposal was generated. An advantageous feature of this system is mitigation of the need for addition of exogenous redox reagents to restore the resting PS.

2.2 Group 13

C_{sp^2}–B bond formation. Organoboron compounds are well-established cross-coupling partners in Suzuki–Miyaura reactions,[101] though their preparation by direct conversion of arene C_{sp^2}–H bonds to the corresponding C_{sp^2}–B bond has traditionally relied on transition metal catalysts wherein regioselectivity is promoted by sterics or the use of directing groups.[102–104] Dual catalysis strategies reported for this transformation have been similarly limited by regioselectivity challenges in direct C_{sp^2}–H functionalization.[105] A room-temperature photoredox-catalyzed synthesis (λ = 450 nm, P = 60 W; PC = $[Ru(bpy)_3][PF_6]_2$) of the aryl boronic ester derivative of thianthrenated pyriproxyfen (76% yield) was reported by Ritter in 2019, making advantageous use of the selectivity conferred by thianthrenation.[70] Later, an expanded set of electron-rich Ar–TT^+ salts were borylated in up to 89% yield under visible-light ($\lambda\nu$ = blue LED) organic photoredox conditions (PC = 2,4,5,6-tetra(carbazol-9-yl)benzene-1,3-dicarbonitrile, 4-CzIPN) in the presence of 4-dimethylaminopyridine (DMAP) base.[72] An alternative approach to the visible-light organic photoredox-catalyzed (λ = 420–430 nm; PC = 1,4-diazabicyclo[2.2.2]octane, DABCO) borylation of Ar–TT^+ salts was described by Song in 2025 (Scheme 4).[106] Their strategy featured substrate activation by the formation of an EDA complex with the inexpensive DABCO at ambient temperatures in the presence of pyridine as a Lewis base. Notably, arenes bearing electron-withdrawing substituents (–C(O)R, –C(O)OR, –CN, $–CF_3$, $–SO_2Me$), halogens, and an aldehyde were well-tolerated.

2.3 Group 14

C_{sp^2}–C_{sp} bond formation. Various transition-metal-catalyzed arene cyanation reactions have been reported.[107] In 2023, Ding reported the Ni-catalyzed cyanation of electron-rich arenes by treatment of Ar–TT^+ substrates with $NiCl_2{\cdot}6H_2O$, (9,9-dimethyl-9*H*-xanthene-4,5-diyl)bis(diphenylphosphane) (Xantphos), Zn$(CN)_2$, and Zn^0 at 120 °C in dimethylformamide (DMF) under N_2.[108] Various *mono*- and *di*-substituted arenes were functionalized in fair to good yields, including the agrochemicals famoxadone and pyriproxyfen (Scheme 5). Their mechanistic propo-

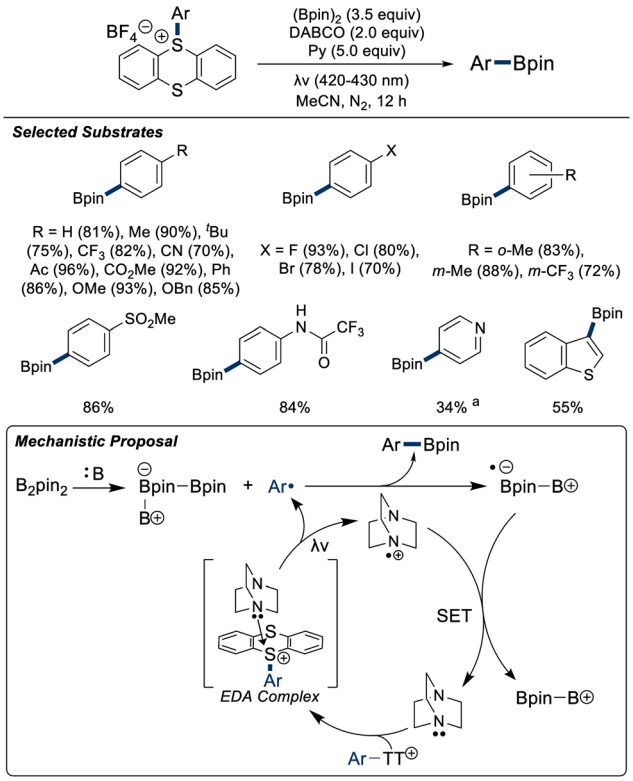

Scheme 4 Borylation of aryl thianthrenium salts. [a]Counteranion to Ar–TT^+ is $^-$OTf.

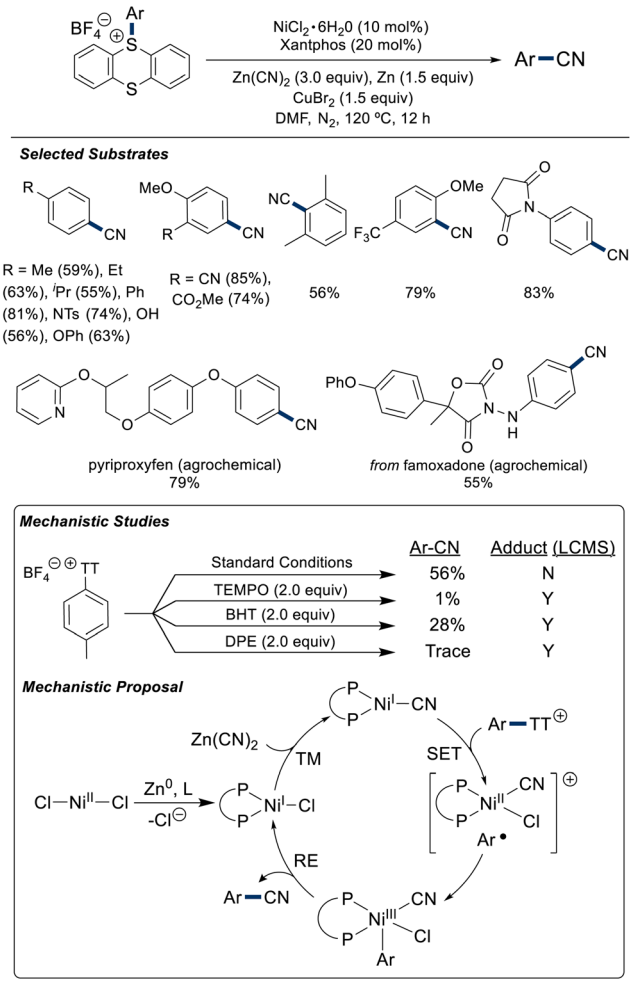

Scheme 5 Cyanation of aryl thianthrenium salts.

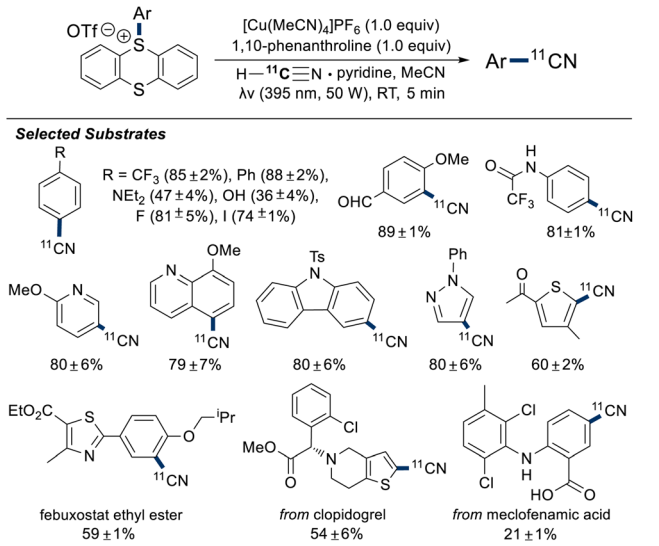

Scheme 6 [^{11}C]-cyanation of aryl thianthrenium salts. Non-decay-corrected radiochemical yields are shown as the average of at least two reaction trials, as determined by radiochemical TLC and HPLC analysis.

sal suggests activation of the precatalyst through reduction by Zn^0 to generate [Ni^I–Cl], followed by transmetalation with $Zn(CN)_2$ to generate a Ni^I–CN complex that donates an electron to substrate *via* SET. Radical rebound of the resultant radical ion pair yields a Ni^{III}-complex which reductively eliminates product and regenerates the resting state of the catalyst. Support for the generation of aryl radicals was obtained by observation of radical recombination products with the radical scavengers TEMPO, BHT, and DPE by LC-MS. $CuBr_2$ additive was suggested to enhance yield by interception of the aryl radical and subsequent [Cu]-catalyzed reactivity. Use of suprastoichiometric quantities of transition metals (Zn, Cu) and elevated temperature represents limitations of this system.

Sanford and Scott later reported the visible-light promoted, Cu-mediated [^{11}C]-cyanation reaction of aryl thianthrenium salts under aerobic conditions at ambient temperature.[109] A variety of electron-rich and electron-poor substrates were functionalized, including N-, O-, and S-heterocycles (Scheme 6). Functionalization of the pharmaceuticals febuxostat ethyl ester (xanthine oxidase inhibitor) and clopidogrel ($P2Y_{12}$ inhibitor) was reported. Competing fragmentation of the endocyclic C–S bond during radical generation was detected by radio-HPLC analysis for some substrates. In consideration of applications of [^{11}C]-radiolabeled compounds in pharmaceutical development,[110] a low-cost assembly of an automation module was designed and implemented in the functionalization of febuxostat ethyl ester.

C_{sp^2}–C_{sp^3} bond formation. Traditional methods for arene cross-coupling reactions in biaryl synthesis generally require pre-activation of one or both arenes to promote reactivity and regioselectivity, often with addition of excess base or oxidant.[111] Thianthrenation confers high regioselectivity in functionalization and subsequent transformation, and through careful design can be carried out by one-pot methods with recycling of $Na_2S_2O_8$ (Scheme 7). Multi-substituted aryl thianthrenium salts were functionalized, as well as S- and N-heterocyclic coupling partners. The bioactive molecules boscalid, pyriproxyfen, and famoxadone (55%), as well as the cyclooxygenase 1 and 2 (COX1/2) thianthrene byproduct (discussed later). In 2021, Ritter reported late-stage (hetero)arylations of aryl thianthrenium salts in an aqueous medium.[112] Aryl radicals were formed by the reduction of aryl thianthrenium salts *via* α-aminoalkyl radicals, which were generated *in situ* by reaction of excess $^nBu_3N$ with inhibitor indomethacin (41%) and the antifungal bifonazole were functionalized in moderate yields. Poor regioselectivity in the addition of aryl radicals to heteroaryl substrates was observed in some cases. Tolerance to air and water is an advantageous feature of this system.

Patureau reported the direct photochemical (λ = 285 nm, P = 144 W) (hetero)arylation of aryl thianthrenium salts soon after.[113] Electron-rich arenes were furanylated or conjugated to other N- or S-heterocyclic substrates under an inert atmosphere (N_2) in DMSO (Scheme 8). Introduction of radical sca-

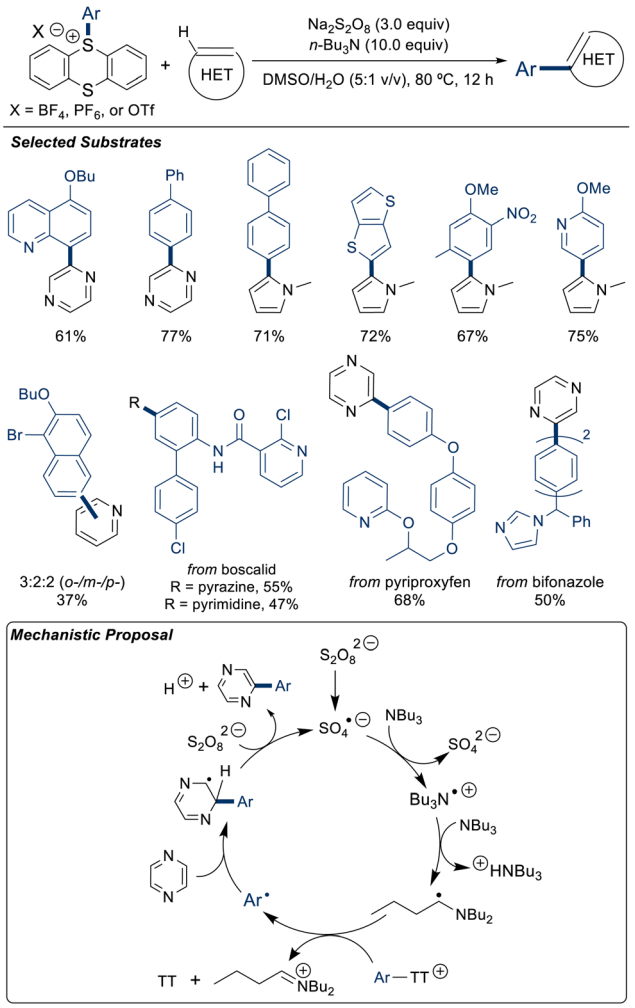

Scheme 7 Thermally-promoted (hetero)arylation of aryl thianthrenium salts.

vengers TEMPO and 1,4-dinitrobenzene led to a significant reduction (>35%) in yield when 5-(3-fluoro-4-methoxyphenyl)-thianthrenium tetrafluoroborate was irradiated in the presence of furan. Light-induced homolysis of the exocyclic C–S bond and subsequent addition of Ar to unsaturated substrate is proposed to precede SET from TT^+ to the radical adduct, furnishing a cationic adduct that is reduced by BF_4^-. Reductions in yield were observed when the reaction was carried out under air and in organic solvents other than DMSO (including MeCN, THF, and DMF). Advantages of this system include the regeneration of neutral thianthrene, operational simplicity, and lack of sacrificial redox agents.

Sun and Yu achieved the site-selective, organic photoredox-catalyzed (λ = 457 nm, P = 10 W; PC = 4-CzIPN) arylation of 2-aryl-2*H*-indazoles at room temperature.[114] Several electron-rich, mono- and di-substituted aryl thianthrenium salts were compatible with the transformation (yields 53–87%). Electron-donating substitutions on the *N*-phenyl group were well-tolerated (yields 55–83%), as were similar modifications to the indazole backbone (yields 71–83%) using *p*-tolylthianthrenium

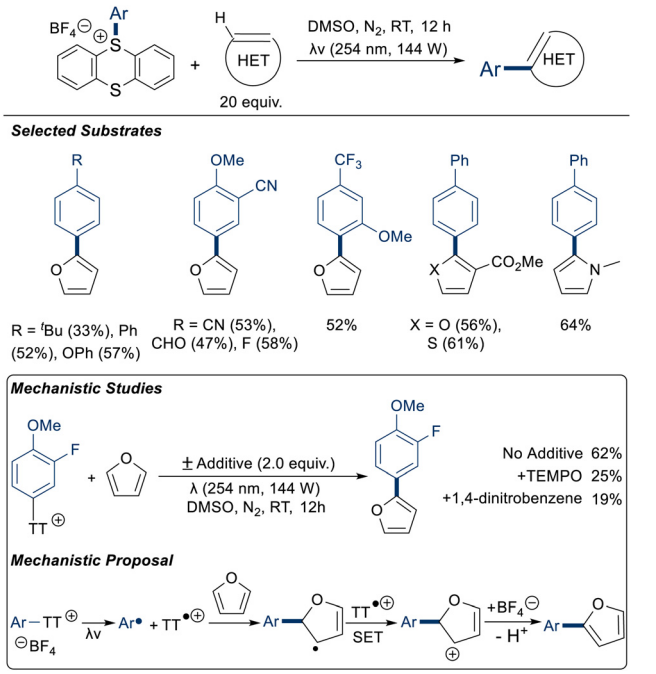

Scheme 8 Direct photochemical (hetero)arylation of aryl thianthrenium salts.

tetrafluoroborate salt coupling partners (Scheme 9). A prodrug of the COX1/2 inhibitor flurbiprofen and the agrochemical pyriproxyphen (71%) were thianthrenated and conjugated to

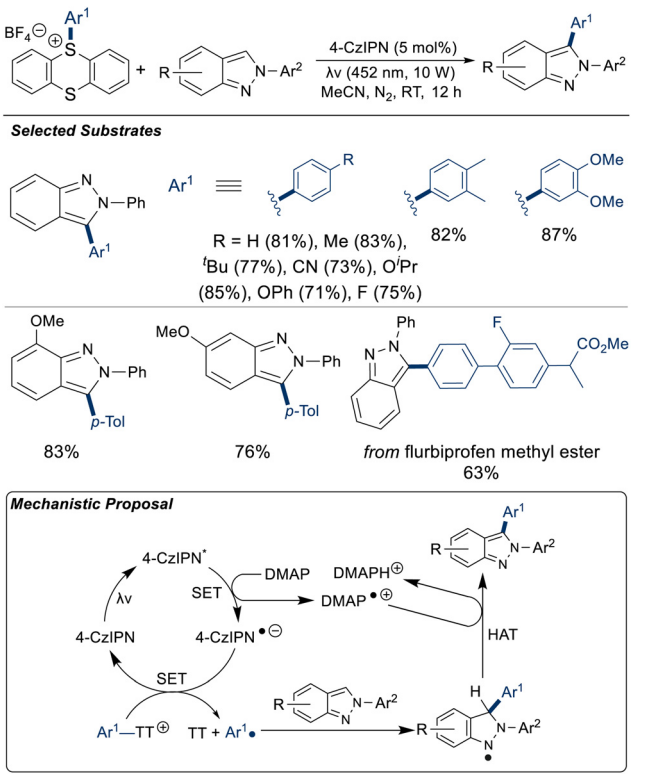

Scheme 9 Organic photoredox-catalyzed arylation of 2-phenyl-2*H*-indazoles.

2-phenyl-2*H*-indazole. Treatment of the model substrates, 2-phenyl-2*H*-indazole and *p*-tolylthainthrenium tetrafluoroborate with radical scavengers under optimized reaction conditions abolished yield, and the corresponding TEMPO and BHT adducts were detected by high-resolution mass spectrometry (HRMS). Further, the reaction did not proceed in the dark or in the absence of PC, suggesting formation of radical intermediates. In consideration of redox potentials of the reactants and PC, a mechanistic proposal was generated in which aryl radicals are generated through SET with $PC^{\bullet-}$ prior to addition to indazole and subsequent DMAP-mediated HAT. Scalability was demonstrated by using model substrates in an attempted gram-scale synthesis (68% yield), as was the sustainable use of natural sunlight as an irradiation source (61% yield). Primary advantages of this system include functional group tolerance and operational simplicity.

The C2-arylation of azoles was achieved by metallaphotoredox-catalyzed (λ = 420 nm, P = 10 W, M = CuI) coupling to Ar–TT^{+} salts in 2025.[115] Benzoxazoles were conjugated to electron-rich arenes in moderate yields at ambient temperature using LiO^{t}Bu as base under an inert (N_2) atmosphere. From the absence of an observed kinetic isotope effect (KIE) upon C2-deuteration, it was suggested that C2–H bond cleavage is not the rate-limiting step. Radical trap experiments with TEMPO or DPE led to the detection of adducts with the arene substrate by HRMS along with a marked reduction in reaction yield, suggesting the intermediacy of aryl radicals. Base-mediated ligation of azole substrate to [Cu], followed by SET and coordination to the arene with subsequent reductive elimination of product, was proposed as the operant mechanism. A one-pot synthesis was demonstrated by the thianthrenation of ethylbenzene followed by addition of benzoxazole, [Cu], and base under irradiation in 54% yield.

In 2022, visible-light photoredox catalyzed (λ = 429 nm, P = 10 W; PC = DABCO) arylation of 6-azauracil derivatives (Scheme 10) and quinoxalin-2(1*H*)-ones was described by Yu.[116] A wide scope of arenes were conjugated to the N-heterocyclic scaffolds. Bioactive compounds, including a derivative of the norepinephrine transporter (NET) inhibitor atomextine, flurbiprofen methyl ester, several nucleoside derivatives (38–71%), pyriproxyfen (64%), and boscalid (71%) were arylated in fair to good yields. Model substrates, 2,4-dibenzyl-1,2,4-triazine-3,5(2*H*,4*H*)-dione and *p*-tolyl-thianthrenium tetrafluoroborate, were selected for attempts at gram-scale synthesis (63%) using natural sunlight irradiation as energy source (79%). Treatment of the model system with the radical scavengers TEMPO and DPE led to observation of trapped adducts by HRMS and a significant reduction in reaction yield, suggesting formation of radical intermediates. UV-Vis absorption spectra recorded for independent and combined solutions of *p*-tolyl-thianthrenium tetrafluoroborate and 1,4-diazabicyclo[2.2.2]octane (DABCO) provided evidence for formation of an *in situ* generated EDA complex by observation of an absorption feature that is red-shifted compared to the stand-alone solutions. Taken with control experiments demonstrating a lack of reactivity in the absence of DABCO or light, a

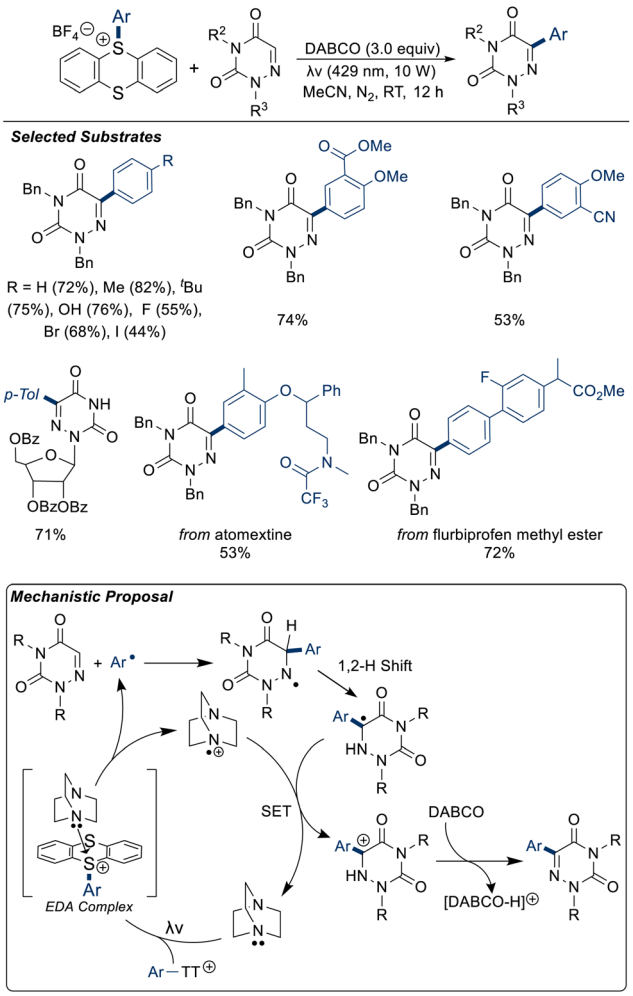

Scheme 10 Arylation of 6-azauracil derivatives *via* visible-light promoted EDA complex formation.

mechanism was proposed. Aryl radicals generated through SET within an EDA complex undergo radical addition to N-heterocyclic substrates. The resultant radical is oxidized by $PC^{\bullet+}$ to generate a formal cationic species prior to HAT with DABCO to furnish product. This strategy offers the advantage of functionalizing nucleobase derivatives and bioactive compounds under mild conditions.

In 2025, Wu reported the cyclization of 2-isocyanobiphenyls initiated by the radical addition of aryl radicals derived from Ar–TT^{+} salts to afford the corresponding 6-aryl-phenanthridines (Scheme 11).[117] Under visible light irradiation (λ = 450–455 nm, P = 30 W) and inert (N_2) atmosphere at ambient temperature in the presence of DBU, the N-heterocyclic products were formed in moderate to fair yields within 12 h. Addition of either 1,4-dioxane or a diarylphosphine oxide to the reaction mixture formed the 6-alkylated or 6-phosphorylated product *via* HAT with Ar$^{\bullet}$ prior to radical addition to the isocyanide. Thianthrenation of the bioactive compounds pyriproxyfen (46%) and boscalid (44%) for use in the reaction was demonstrated as a LSF strategy. Analysis of the system by

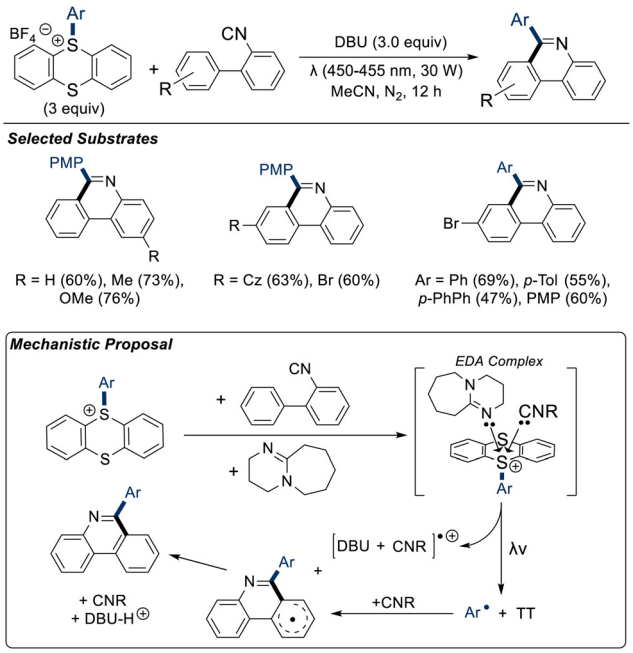

Scheme 11 6-Aryl-phenanthridine synthesis *via* radical cyclization. PMP = *p*-methoxyphenyl.

UV-Vis spectroscopy indicated the strongest bathochromic shift in the absorption profile upon combination of a 2-isocyanobiphenyl substrate, Ar–TT$^+$ salt, and DBU, suggesting the formation of a trimolecular EDA complex whose stoichiometry was further probed by Job's method. Electronic perturbations within the Ar–TT$^+$ salt were also detected *via* ^{1}H NMR spectroscopy upon addition of DBU and 4′-bromo-2-isocyanobiphenyl. Radical trap experiments with TEMPO, BHT, or DPE led to HRMS observation of the trapped adducts for the proposed alkyl, aryl, and phosphoryl radical intermediates. Radical cyclization under mild reaction conditions is advantageous to the efficient increase in molecular complexity through establishment of two new bonds in a single step.

C_{sp^2}–C_{sp^3} bond formation. Arene trifluoromethylation was demonstrated by Ritter in 2019.[118] Using a metallaphotoredox catalysis strategy (λ = blue LED, P = 34 W; PC = [Ru(bpy)$_3$](PF$_6$)$_2$, bpy = 2,2′-bipyridine), (hetero)aryl thianthrenium salts bearing electron-neutral and electron-donating groups were functionalized by reaction with suprastoichiometric quantities of an *in situ* generated [Cu-(CF$_3$)] species. The system was reportedly incompatible with carboxylic acids, phenols, and nitro compounds. Application of this strategy to the anti-inflammatory drug indomethacin methyl ester (59%), antilipemic drugs clofibrate methyl ester (81%) and gemfibrozil methyl ester (56%), as well as the agrochemical etofenprox (69%) was described. A radical trap experiment did not produce TEMPO-CF$_3$ adducts, decreasing the likelihood of trifluoromethyl radical formation. Diminished yield of trifluoromethylated arene (<1%) observed in the absence of light or photocatalyst supported a photoredox mechanism.

An organic photoredox-catalyzed (λ = blue LED, P = 24 W, PC = eosin Y) hydroarylation of azine-substituted enamides was reported in 2021 by Wang.[119] Electron-rich (hetero)arenes were investigated, as were substrates bearing substituted azines (Scheme 12). This strategy was extended to the functionalization of azine-substituted alkenes (52–63%) and the LSF of flurbiprofen (49%) and pyriproxyfen. A radical trap experiment with TEMPO was consistent with formation of aryl radicals, and incorporation of deuterium was observed when CD_3OD was used solvent. Absence of PC or *N*,*N*-diisopropylethylamine (DIPEA) produced indeterminate yield. On this basis, a mechanism was proposed in which aryl radicals are generated *via* SET between Ar–TT$^+$ and PC$^{\bullet-}$, with subsequent radical addition to enamine. The resultant α-amino radical can either undergo HAT with DIPEA$^+$ or sequential reduction by PC$^{\bullet-}$ and protonation by solvent to furnish product.

Difunctionalization of electron-deficient alkenes by irradiation (λ = white LED, P = 40 W) of methyl acrylate in the presence of aryl thianthrenium salts, *N*-phenyl-benzo[*b*]phenothiazine (PTH) as photocatalyst, and *tert*-butylammonium bromide (TBAB) at low temperature (−20 °C) was described by Ritter in 2022.[120] Highly regio-selective alkene functionali-

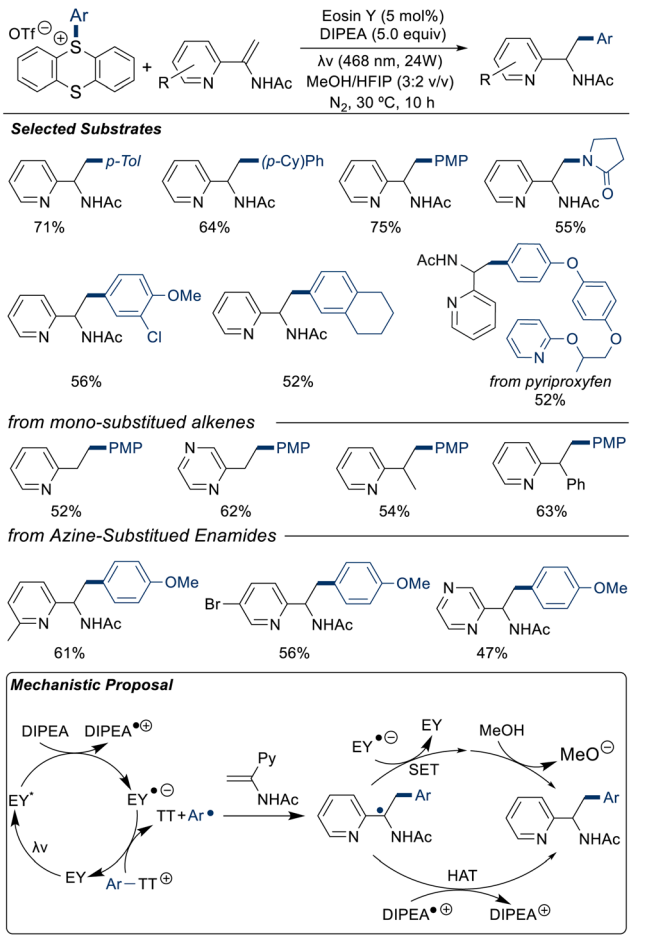

Scheme 12 Organic photoredox-catalyzed hydroarylation of enamides. PMP = *p*-methoxyphenyl.

zation was observed, with aryl radical addition biased toward the least substituted olefinic carbon to produce a radical intermediate stabilized by the electron-withdrawing ester. Site-selective thianthrenation of flurbiprofen (66%), diclofenac amide (COX1/2 inhibitor), indomethacin, nimesulide (COX2 inhibitor), meclofenamic acid (COX1/2 inhibitor, 70%), and benzbromarone (URAT1 inhibitor, 46%) enabled their use as precursors for this reaction (Scheme 13). Further reactivity of the newly furnished C_{sp^3}–Br bond was demonstrated by treatment with various N-, O-, S-, and P-nucleophiles. No evidence for EDA complex formation between Ar–TT$^+$ and PTH was observed in the UV-vis absorption spectra. Support for quenching of PC* by Ar–TT$^+$ was obtained through Stern–Volmer analysis. Reduction of Br^- to Br_2 by PTH$^{\bullet+}$ was observed indirectly by addition and halogenation of 1,3,5-trimethoxybenzene. Based on these results, a mechanistic proposal involving the formation of aryl radicals was generated. Photoexcited PTH* transfers an electron to Ar–TT$^+$, producing Ar$^\bullet$ and TT. Aryl radicals add to alkene substrates, followed by radical abstraction of bromine formed by reaction with PTH$^{\bullet+}$.

A Cu-catalyzed three-component coupling of Ar–TT$^+$ salts, sodium azide, and alkenes under visible light irradiation (λ = 453 nm, P = 40 W) generated 1,2-difunctionalized products under mild conditions and inert atmosphere (N_2).[121] A diverse substrate scope was evaluated, including N- and S-heterocyclic arenes, multi-substituted alkenes, and bioactive compounds (Scheme 14). Among the latter are included the pharmaceuticals diclofenac amide, flubiprofen, and meclofenamic acid, as well as agrochemicals boscalid (69%), cloquintocet-mexyl, and pyriproxyfen (60%). Stern–Volmer analysis suggested the role

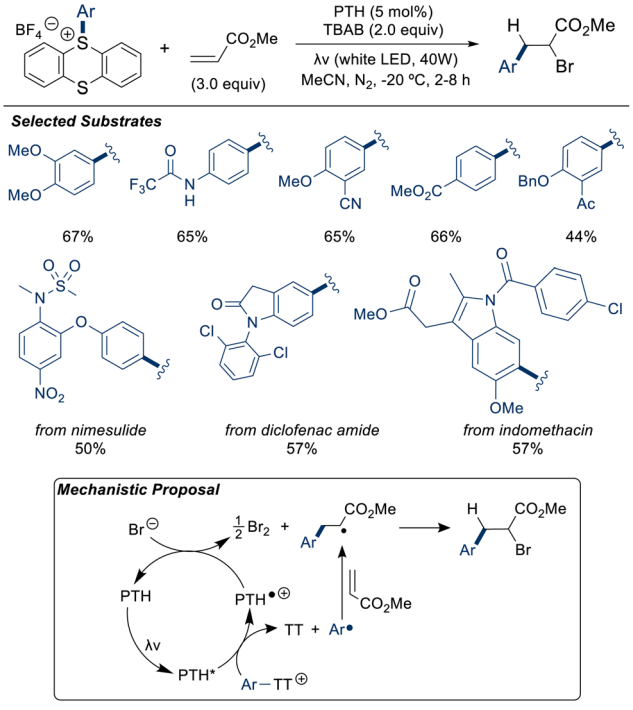

Scheme 13 Photoredox-catalyzed bromoarylation of methyl acrylate.

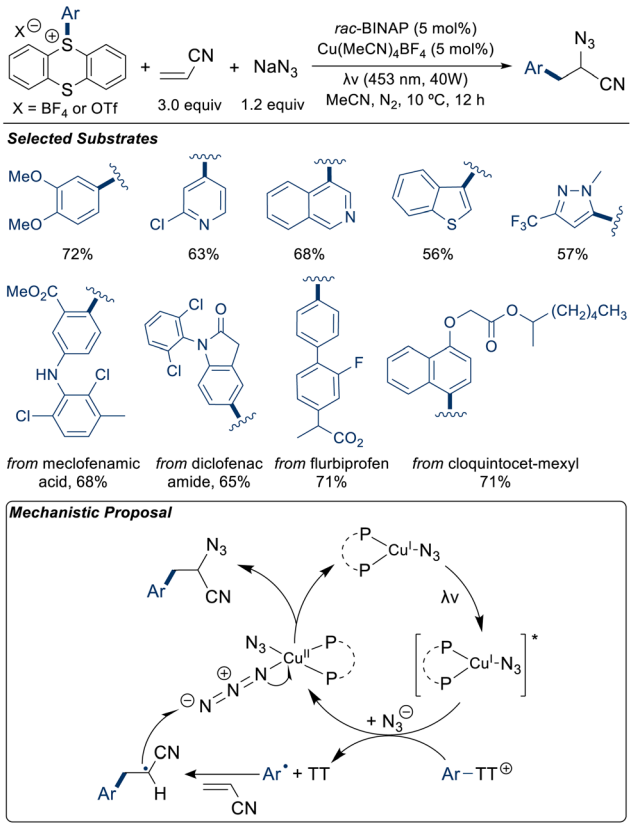

Scheme 14 Three-component azidoarylation of alkenes.

of [Cu^{I}(*rac*-BINAP)(N$_3$)] (BINAP = racemic 2,2′-bis(diphenylphosphino)-1,1′-binaphthalene) as a photocatalyst on the basis of observed quenching by Ar–TT$^+$ salts. Experimental evidence for the reactivity of the dimer [Cu$_2$(*rac*-BINAP)$_2$(μ-N$_3$)$_2$] with Ar$^\bullet$ was obtained by formation of azidoarylation product when the complex was treated with benzoyl peroxide at 80 °C. Light-induced excitation of the PC and subsequent SET to Ar–TT$^+$ was proposed to generate aryl radicals, which add to acrylonitrile to furnish an intermediate is α-cyano radical. Radical abstraction of an azide group from [Cu^{II}(*rac*-BINAP)(N$_3$)$_2$] ensues, forming product and regenerating the active catalyst. Attempts at enantioselective synthesis using (*R*,*R*)-BINAP ligand provided comparable yields with low enantiomeric excess (≤8% ee), purportedly due to the spatial separation of ligand from the site of *enantio*-determining radical abstraction. Nonetheless, high regioselectivity in the aryl radical addition to alkene was observed, presumably due to radical stabilization conferred by the electron withdrawing α-cyano group. Installation of the azido group enables further reactivity.

Difunctionalization of ethylene through a radical polar crossover pathway enabled by EnT-mediated activation of Ar–TT$^+$ salts was reported by Ritter in 2025.[53] Visible-light irradiation (λ = 390 nm, P = 40 W; PS = thioxanthone, TXO) of arenes under an atmosphere of ethylene gas led to the facile formation of 1,2-difunctionalized intermediates which, without isolation, are further transformed by the addition of

various (C-, N-, P-, O-, S-, Se-, F-, Cl-, Br-, I-) nucleophiles (Scheme 15). Stern–Volmer analysis demonstrated the quenching ability of Ar–TT$^+$ salts on PS*. Correlation of the reaction yield with E_T(PS), and not the redox potential of the PC that would be expected in a SET-mediated process, was suggestive of an EnT mechanism. Additional support for EnT was generated through observation of a TAS absorption feature attributable to TT$^{\bullet+}$. Certain properties of TXO favor EnT over SET, such as highly efficient intersystem crossing from S_1 to T_1 (ϕ_{ISC} = 0.99)[122] and a long triplet lifetime (τ = 95 μs in MeCN).[123] An overall quantum yield of Φ = 0.12 was observed from a measured EnT efficiency of 0.33 and quantum yield of homolytic cleavage following EnT of Φ_{EnT} = 0.36 when phenylthianthrenium triflate was used as substrate, demonstrating the efficient photophysical properties of this system. Exclusion of a radical chain mechanism was supported by this finding. Computational (DFT) study enabling consideration of the nature and spatial arrangement of the PS* HOMO relative to the substrate LUMO provided evidence for a hypothesized Dexter-type EnT mechanism. Further, the geometry of this interaction was suggested to impart chemoselectivity in EnT to the thianthrenyl moiety over other functional groups present in the arene.

Radical cascade cyclization reactions increase structural complexity by promoting multiple bond scission and formation events in a single reaction step. Initiation of an inter-intramolecular radical cyclization cascade *via* irradiation (λ = 390 nm, P = 30 W) of Ar–TT$^+$ salts in the presence of *N*-methyl-*N*-aryl-methacrylamide led to formation of benzyl oxindoles under mild conditions and an inert atmosphere (Ar).[124] Electron-rich, -neutral, and -poor arenes were studied, as were *N*-phenyl-substituted acrylamides (Scheme 16). Addition of TEMPO inhibited product formation suggesting formation of radical intermediates, and UV-vis absorption spectroscopy supported the formation of an EDA complex between Ar–TT$^+$ and K_2CO_3 by observation of a spectral red-shift when a combined solution is prepared. Addition of aryl radicals, formed through EDA-complex-mediated SET, to acrylamides yields radical intermediates that undergo intramolecular cyclization. Cyclized radical intermediates can donate an electron to a second equivalent of Ar–TT$^+$, thus initiating another cascade and generating a cationic product precursor converted to neutral form *via* deprotonation. The measured quantum yield of 6.1 supports the SET activation of the second Ar–TT$^+$ equivalent by a radical intermediate.

Organic photoredox-catalyzed (λ = 427 nm, P = 30 W; PC = eosin Y) arene allylation by addition of aryl radicals to electron-deficient alkenes was reported in 2024.[125] Electron-rich

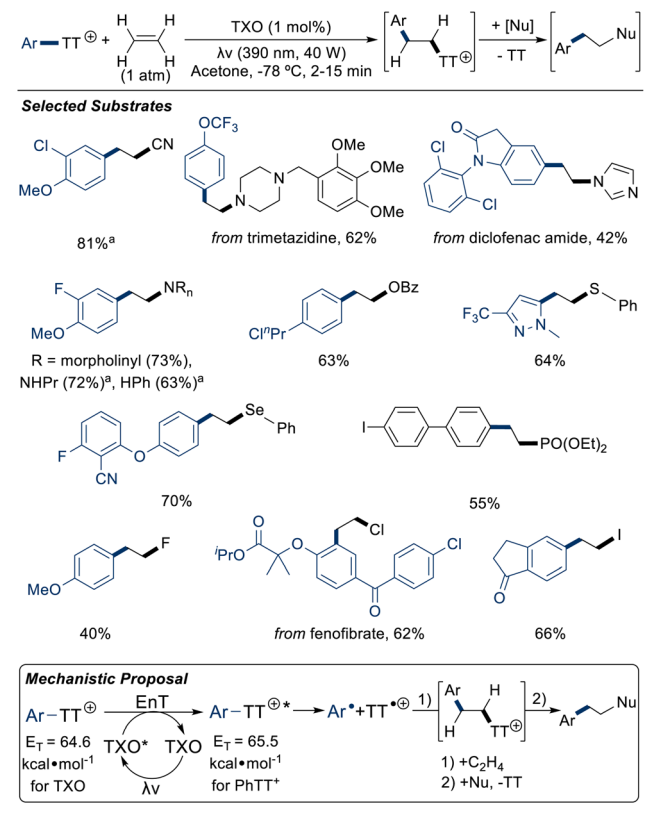

Scheme 15 EnT-promoted aryl radical formation in olefin difunctionalization. Counter anion to Ar–TT$^+$ is either BF_4^- or OTf^-. Reaction time extended by 12 h, and solvent manipulated for select substrates, upon addition of nucleophile. [a]TBAB (1.2 equiv.) added in the first step.

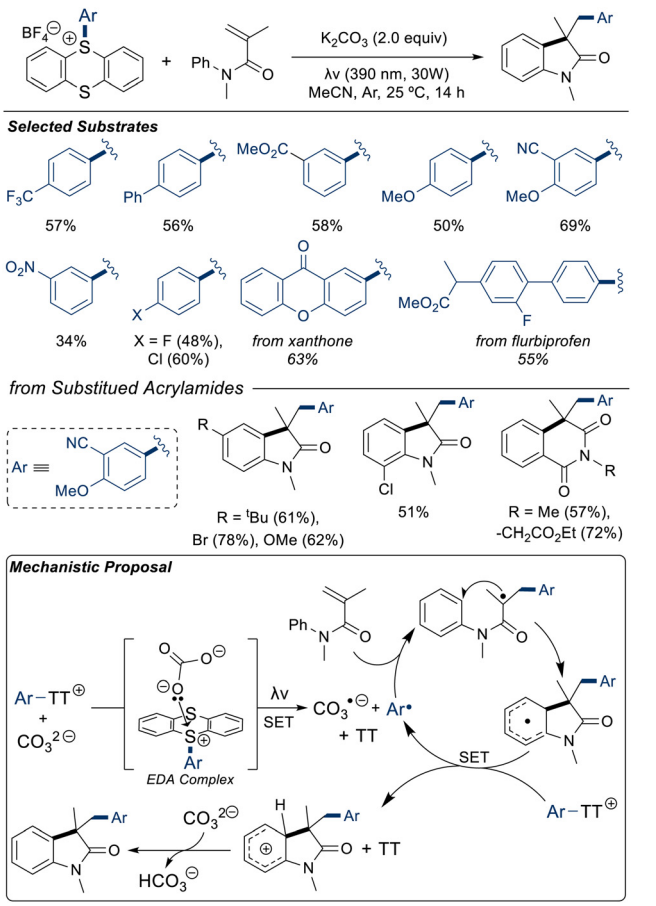

Scheme 16 Radical cascade cyclization of acrylamides with aryl thianthrenium salts.

(hetero)arenes and *gem*-disubstituted alkenes were transformed in moderate to good yields (Scheme 17). The reaction did not proceed in the absence of light or PC, nor in the presence radical scavengers TEMPO and BHT, suggesting the formation of radical intermediates. Homolytic cleavage of the aryl thianthrenium salt promoted by SET with PC* generates aryl radicals that undergo addition to the alkene coupling partner at the sterically least hindered carbon, producing an intermediate radical adduct stabilized by the electron-withdrawing α-methyl ester. Decarboxylative loss of CO_2 and $^tBuO^\bullet$ furnishes product. For some substrates, the decarboxylation step proceeds with moderate to high *E*/*Z*-stereoselectivity.

A Cu-catalyzed three-component reaction of Ar–TT^+ salts, alkenes, and trimethylsilyl cyanide (TMSCN) under visible light irradiation (λ = 455 nm, P = 15 W) and inert atmosphere (N_2) at low temperature (5 °C) generated 2,3-diarylpropionitrile products.[126] Various electron-rich styrene derivatives and Ar–TT^+ salts were coupled, and the LSF of several bioactive compounds was demonstrated (Scheme 18). Site-selective thianthrenation of ibuprofen (COX1/2 inhibitor), oxaprozin (COX1/2 inhibitor), and gemfibrozil enabled difunctionalization of *p*-phenyl styrene, or *p*-methoxystyrene in the case of flurbiprofen (83%) and pyriproxyfen (60%). Gram-scale coupling of model substrates *p*-methoxystyrene and biphenylthianthrenium tetrafluoroborate afforded product in 60% yield with efficient recovery of TT (89%). Independent and combined solutions of biphenylthianthrenium tetrafluoroborate, dibutamine (DBA), and TMSCN were analyzed by UV-vis absorption spectroscopy, which suggested formation of a trimolecular EDA complex by the observation of a spectral red shift and the appearance of an absorption feature at λ = 375–450 nm that is attributable to a charge-transfer band present only when all three analytes were combined. Trapping of radical intermediates upon addition of TEMPO was detected by HRMS, and the alkene difunctionalization product was formed in trace quantities. A control experiment in the absence of light annihilated reactivity to further support a radical mechanism. Activation of CuOAc precatalyst by ligation of *rac*-BINAP and reaction with TMSCN yields the resting catalyst, [Cu^I(*rac*-BINAP)(CN)]. After photoexcitation, [Cu^I(*rac*-BINAP)(CN)]* undergoes SET with [TMSCN-DBU]$^{\bullet+}$, formed from SET within the EDA complex, to produce [Cu^{II}(*rac*-BINAP)$(CN)_2$]. Alkyl radical intermediates formed by the addition of thianthrenium salt-derived aryl radicals to styrene substrates add to the [Cu^{II}] complex, generating a [Cu^{III}] complex from which product is reductively eliminated.

Another three-component, metallaphotoredox-catalyzed (λ = 390 nm, P = 15 W, PC = PTH, [M] = $Cu(MeCN)_4PF_6$, L = 2,2′-bipyridine (bpy), B = KH_2PO_4) system involving TMSCN and 1,3-enynes provided access to the tetrasubstituted allenyl nitriles in 2025.[127] The arene scope largely consisted of elec-

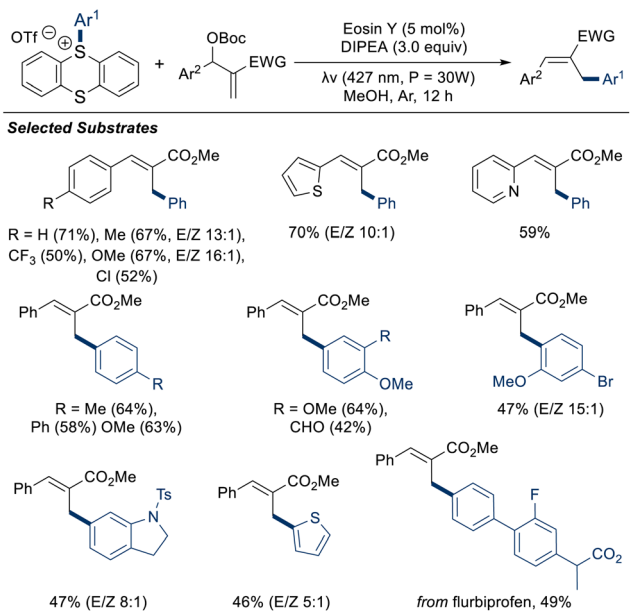

Scheme 17 Allylation of aryl thianthrenium salts.

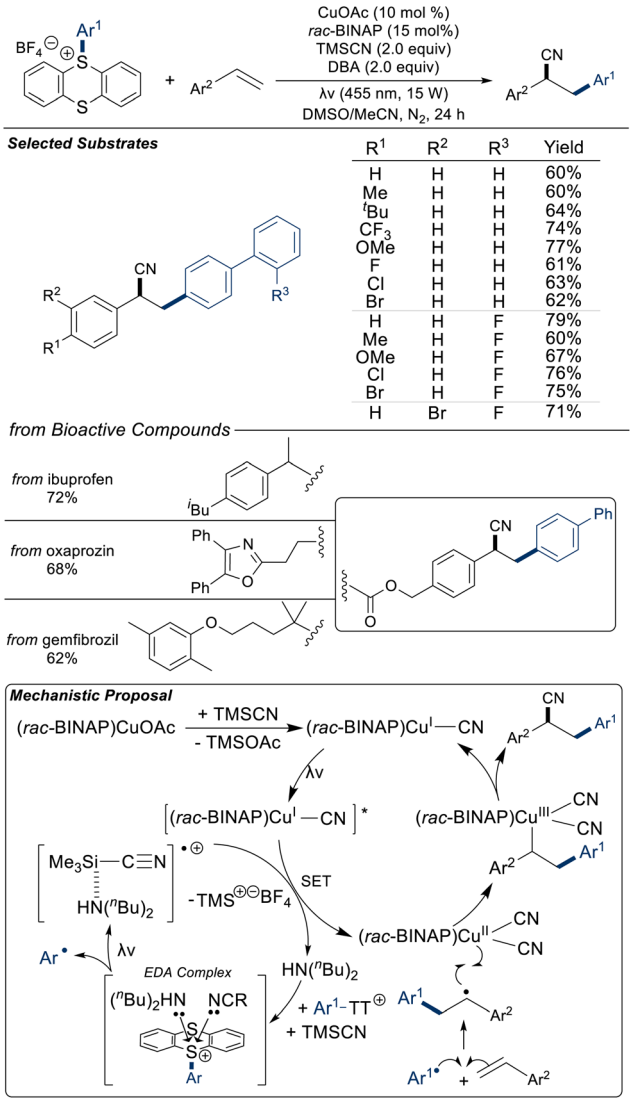

Scheme 18 Three-component arylcyanation of alkenes.

tron-rich substrates, although a few examples of disubstituted arenes bearing an ester substituent were included.

Mechanistic insight from radical trap experiments, Stern–Volmer analysis, and the UV-vis characterization of combined and independent solutions of reaction components enabled a proposal for the product formation pathway. Aryl radicals generated from the interaction of Ar–TT$^+$ salts and PC* undergo radical addition to the terminal alkene site of the 1,3-enyne, and the progargyl radical resonance form of the adduct may ligate a [Cu^{II}(bpy)(MeCN)$_2$] species to then reductively eliminate product. This system features the advantageous use of visible-light irradiation, inexpensive and earth-abundant metal catalyst, and ambient temperature.

Aryl radical addition to nonnatural amino acids (NAAs) derived from dehydroalanine (Dha) was reported by Noël in 2024 and represents an LSF strategy enabled by thianthrenation.[128] Common to the NAAs studied is a modified N-terminus, incorporating a phthalimide moiety, and an α,β-unsaturated side chain and C-terminus. Under mild photocatalytic conditions (λ = 456 nm, PC = eosin Y) and inert atmosphere (N_2), functionalization of peptides and bioactive compounds was achieved in batch and flow apparatus. Pharmaceutical compounds benzbromarone (62%), bifonazole, flurbiprofen, meclofenamate (64%), and the agrochemicals boscalid and pyriproxyfen (67%) were functionalized. Aryl thianthrenium salts bearing N- and O-heterocyclic or electron-donating substituents were well-tolerated (Scheme 19). The reaction was most efficient when run in a cosolvent system of MeCN/hexafluoroisopropanol (HFIP) (7 : 1 v/v) and with DIPEA as terminal reductant. Extension of this approach to the merger of Dha incorporation into proteins[34] with the reactivity of Ar–TT$^+$ salts represents a potential application in bioconjugate chemistry and a new route toward the selective modification of complex biomolecules under mild conditions.

Difunctionalization of the ring-strained tricyclic hydrocarbon [1.1.1]propellane by a metallaphotoredox catalysis (λ = 450–460 nm, P = 3 W, PC = Ir(ppy)$_3$, [M] = Cu(acac)$_2$, L = 2,2′-bis(dicyclohexylphosphino)-1,1′-biphenyl, B = DBU) approach was described by Zhang in 2025.[129] Phenylacetlyenes with electron-donating aryl substituents and electron-rich Ar–TT$^+$ salts were transformed in fair yields (45–60%) at ambient temperature under inert (Ar) atmosphere. On the basis of mechanistic studies involving radical trap and on–off experiments, it was hypothesized that formation of aryl radicals derived from Ar–TT$^+$ salts following interaction with PC* enabled a strain-relieving radical addition to [1.1.1]propellane, where the resultant radical adduct is intercepted by a [Cu$^{(II)}$(alkynide)] species to form a [Cu$^{(III)}$] intermediate from which the 1-alkynyl-3-ary-

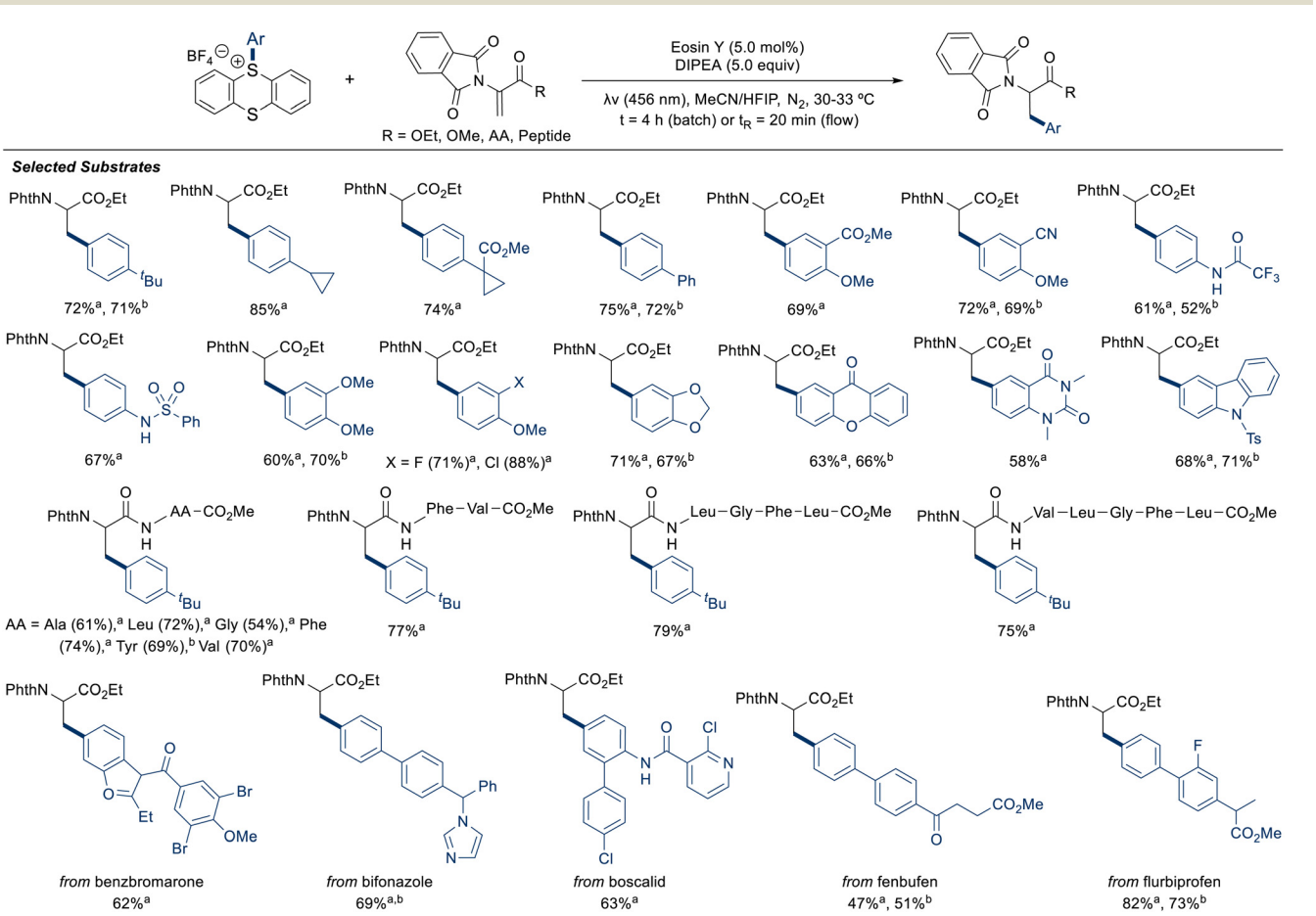

Scheme 19 Arylation of nonnatural, dehydroalanine-derived amino acids. [a]Batch reaction, [b]Continuous flow reactor. AA = amino acid.

lated product is reductively eliminated. Extension of this work to other ring-strained systems high in sp^3 character may increase access to single-electron reactivity among these substrates under mild conditions.

A three-component coupling of substituted styrenes, (hetero)aromatic aldehydes, and Ar–TT$^+$ salts using a visible-light (λ = 460–465 nm, P = 65 W) induced, NHC-catalyzed approach led to formation of the corresponding 1,2-arylacylated products (Scheme 20).[130] The reaction was most efficient using sterically accessible and aldehydes with electron-withdrawing aryl substituents, electron-rich Ar–TT$^+$ salts, and electron-rich olefins. Evidence for the generation of aryl radical intermediates was obtained from the addition of TEMPO to standard reaction conditions, as radical-trapped adducts were detected by HRMS and the desired product was not detected. Addition of base promotes the formation of an NHC(C2)-aldehyde adduct known as a Breslow intermediate, which provides access to enol-based precursors of persistent ketyl radicals after SET.[131] Here, the radical combination of this ketyl radical and the radical intermediate formed upon addition of Ar$^\bullet$ to the olefinic substrate furnishes a new C_{sp^2}–C_{sp^3} bond and regenerates the active NHC organocatalyst. The use of a thiazole-based NHC organocatalyst enhances the scalability and sustainability of the transformation, while the formation of multiple bonds is beneficial from a step-efficiency standpoint.

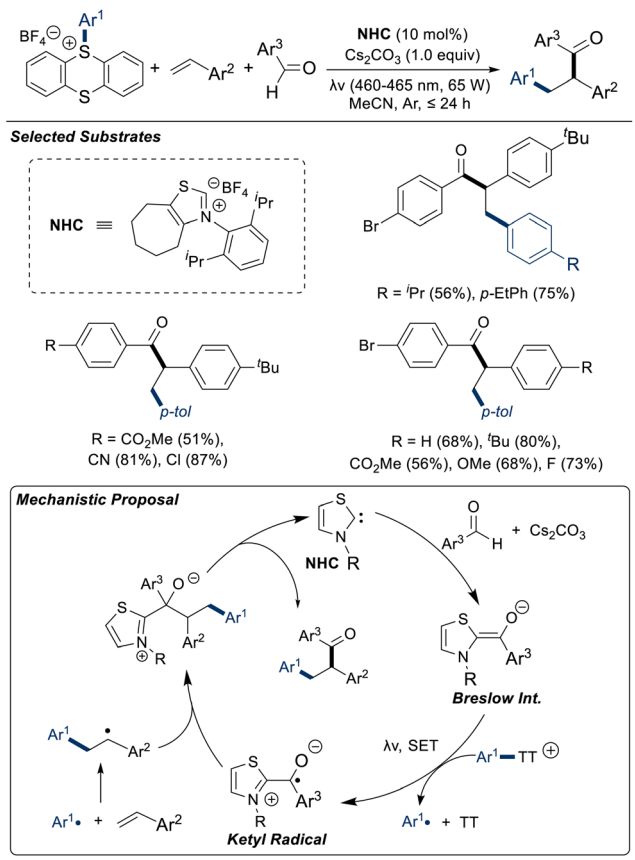

Scheme 20 Three-component 1,2-arylacylation of olefins.

Exploration of generality of this transformation among other structural classes of aldehydes and olefins represents an opportunity for future investigations.

2.4 Group 15

C_{sp^2}–N bond formation. In 2019, Ritter demonstrated a metallaphotoredox approach to the amination of arylthianthrenium salts under visible light irradiation (λ = 450 nm, P = 60 W; PC = Ir(ppy)$_3$ or [Ru(bpy)$_3$](PF$_6$)$_2$, ppy = 2-phenylpridine and bpy = 2,2′-bipyridine).[132] Primary and N-heterocyclic amines were conjugated to *p*-phenoxyphenylthianthrenium tetrafluoroborate in moderate to good yields (up to 87%). Functionalization of the pharmaceutical scaffolds of rivaroxaban (anticoagulant), nefiracetam (CNS agent), and indomethacin was achieved (Scheme 21), along with the agrochemicals etofenprox and pyriproxyfen. It was suggested that homolytic fragmentation of Ar–TT$^+$ salts following SET with PC* generates aryl radicals which may undergo oxidative ligation to [Cu^{II}], with subsequent reductive elimination of product from [Cu^{III}], analogously to a proposal later put forth by Jiang (*vide infra*).

Amination of aryl thianthrenium salts under photochemical conditions (λ = 450 nm, P = 30 W; PC = [Ir(dtbbpy)(ppy)$_2$]PF$_6$, dtbbpy = 4,4′-di-*tert*-butyl-2,2′-dipyridine) using ammonia as a nitrogen source was reported by Jiang in 2023.[133] Electron-rich Ar–TT$^+$ salts, including those bearing N- and O-heterocyclic or aryl halide substituents, were transformed in up to 86% yield (Scheme 22). The bioactive compounds bifona-

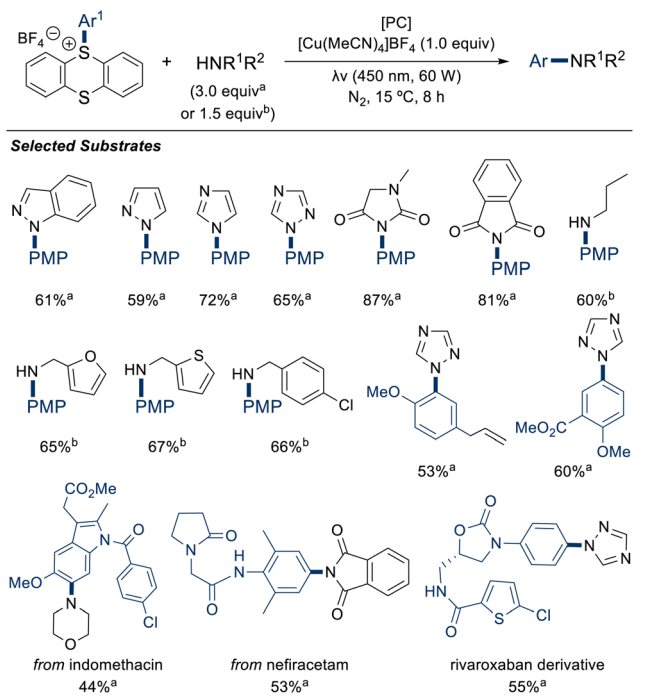

Scheme 21 Amination of aryl thianthrenium salts. (a) PC = [Ru(bpy)$_3$](PF$_6$)$_2$ (5 mol%), additive = NMe$_4$OH or NaH (3.0 equiv.), solvent = MeCN/DMSO (1 : 1 v/v); (b) PC = Ir(ppy)$_3$ (3 mol%), [Cu(MeCN)$_4$]BF$_4$ (1.0 equiv.), K$_2$CO$_3$ (2.0 equiv.), solvent = MeCN. PMP = *p*-methoxyphenyl.

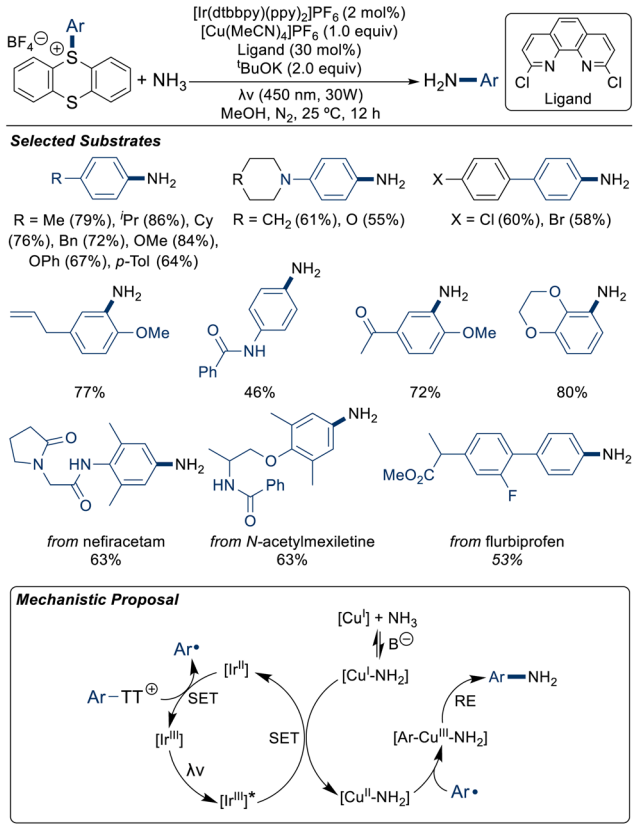

Scheme 22 Aniline synthesis *via* aryl thianthrenium salts.

zole, estradiol, fenbufen (COX1/2 inhibitor), flurbiprofen, and *N*-acetylmexiletene (antiarrhythmic), in addition to the agrochemical pyriproxyfen, were site-selectively functionalized. When *p*-tolylthianthrenium tetrafluoroborate was treated with TEMPO under standard conditions, trace amount of *p*-toluidine product was formed and the TEMPO adduct 2,2,6,6-tetramethyl-1-(*p*-tolyloxy)piperidine was detected by HRMS analysis, suggesting the formation of aryl radical intermediates. Stern–Volmer analysis demonstrated the ability of [Cu$(CH_3CN)_4$]PF_6 to quench PC*. Taken together, a mechanistic proposal was generated in which the reduced form of the PC, [Ir^{II}], engages in SET with Ar–TT^+ to furnish Ar$^\bullet$ and the resting PC, [Ir^{III}]. Upon photoexcitation, PC* oxidizes [$Cu^I(L)_2(NH_3)$]PF_6 (L = 2,9-dichloro-1,10-phenanthroline) *via* SET and the resultant [Cu^{II}] complex intercepts Ar$^\bullet$ and subsequently reductively eliminates aminated product from a transient [Cu^{III}] complex. Although the precatalyst can theoretically be regenerated by reductive elimination, a reduction in yield from 83% to 67% was observed when the quantity of [Cu] was reduced from 1.0 equivalent to 0.6 equivalents with respect to *p*-tolylthianthrenium tetrafluoroborate, suggesting catalyst deactivation.

In extension of their prior work, the Ritter group reported visible-light-promoted (λ = white or blue LED), Ni-catalyzed aminations of Ar–TT^+ salts in 2024.[134] Under ambient conditions and inert atmosphere (Ar), several electron-rich arenes and N-nucleophiles were efficiently coupled by earth-abundant and inexpensive catalysts (Scheme 23). When used in suprastoichiometric (≥2 equiv.) quantities relative to Ar–TT^+ salts, substrate amine can serve as an endogenous base and reductant. Alternatively, exogenous DABCO or 2-*tert*-butyl-1,1,3,3-tetramethylguanidine (BTMG) was used to serve these functions. Late-stage functionalization of the bioactive compounds amoxapine (SNRI, serotonin-norepinephrine reuptake inhibitor), desloratadine (H_1-receptor antagonist), fenbufen (54%), flurbiprofen, and the structurally complex (−)-strychnine (GlyR and AchR antagonist) was accomplished through reactivity of piperidine or piperazine moieties. Based on evidence of electron paramagnetic resonance spectroscopic evidence of Ni(I) formation under light irradiation and control experiments in the absence of light, a mechanistic proposal was generated. Coordination of N-nucleophiles to Ni^{II}-sources, such as $NiCl_2$ or $NiBr_2$, may precede the formation of amine radicals *via* light-induced ligand-to-metal charge transfer (LMCT) and subsequent SET from the resultant [Ni^I] complex to Ar–TT^+. Oxidative ligation of Ar$^\bullet$ followed by a subsequent reductive elimination formed product. Notably, the system is tolerant to added H_2O (5.0 equiv.), producing a modest reduction in yield

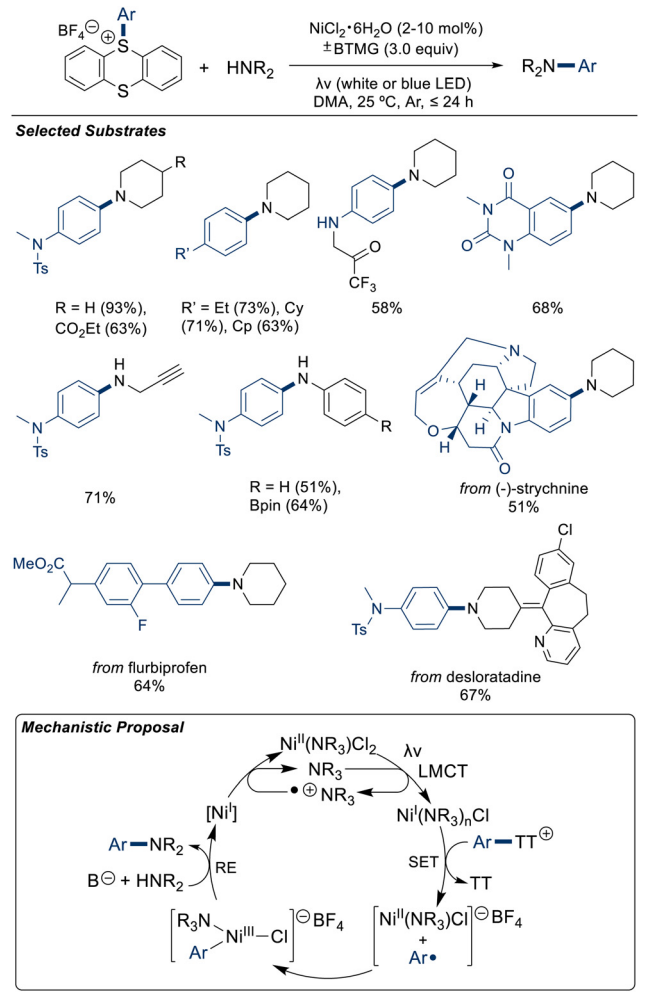

Scheme 23 Nickel-catalyzed amination of aryl thianthrenium salts.

of ~10% for the model substrates piperazine and 5-(4-((*N*,4-dimethylphenyl)sulfonamido)phenyl)-thianthrenium tetrafluoroborate.

C_{sp^2}–P bond formation. Direct phosphonation of aryl C_{sp^2}–H bonds using a visible-light-promoted (λ = 455 nm, P = 25 W), EDA complex strategy was reported by Yang in 2023.[135] Combination of electron-rich, -neutral, and -poor Ar–TT$^+$ salts with phosphonate esters ($P(OR)_3$; R = Me, Et, ^{i}Pr), and 1,4-dimethylpiperazine (DMP) as base led to site-selective transformation in the absence of a photocatalyst (Scheme 24). Agrochemicals pyriproxyfen and bifenthrin were suitable substrates. An attempt at gram-scale transformation of thianthrenated pyriproxyfen produced product in 54% yield, with 94% recovery of thianthrene as a recyclable byproduct. Natural sunlight irradiation of 5-([1,1′-biphenyl]-4-yl)-thianthrenium tetrafluoroborate, triethyl phosphite, and base produced phosphorylated arene in 94% yield, demonstrating the efficacy of a green energy input in this system. Addition of TEMPO or DPE to these model substrates under standard conditions led to HRMS observation of the corresponding biphenyl adducts and trace product formation, suggesting the presence of radical intermediates. UV-Vis spectroscopic analysis suggested EDA complex formation by a red-shifted absorption profile upon combination of DMP and the model Ar–TT$^+$ salt and Job's method indicated a 1 : 1 stoichiometry. It was hypothesized that formation of Ar$^\bullet$ from the EDA complex enables radical addition to phosphonate esters prior to sequential oxidation of the phosphoranyl radical intermediate by DMP$^{\bullet+}$ and hydrolysis of the phosphonium ether to furnish product. Other tertiary amines screened in DMSO solvent, including DABCO, *N*,*N*,*N*′,*N*′-tetraethylenediamine (TMEDA), and 1,3,5-trimethyl-1,3,5-triazacyclohexane (TMTAC) provided comparable yields (within 6%) to DMP.

Granados reported the phosphonation of Ar–TT$^+$ salts by a visible-light-promoted (λ = 390 nm, P = 30 W) EDA complex strategy with a P-donor.[136] At ambient temperature under an inert atmosphere (Ar), electron-rich and electron-poor arenes were converted to aryl phosphonate esters in an acetonitrile solution of triethylphosphite and $KHCO_3$ (Scheme 25). Alternative solvents (acetone and DCM), bases (DABCO, K_2CO_3, and K_3PO_4), irradiation wavelengths (456 nm), and phosphines (trimethyl-, triisopropyl-, and triphenyl phosphite) demonstrated compatibility for this transformation, with yields generally within 10% of the optimized conditions. Irradiation of the 5-(3-cyano-4-methoxyphenyl)thianthrenium or 5-(4-fluorophenyl)thianthrenium tetrafluoroborate salts with natural or simulated sunlight, respectively, provided the phosphonate products in 82% and 79% yield, demonstrating an opportunity for green energy input. Late-stage functionalization of fenbufen (74%), flurbiprofen (88%), gemfibrozil (65%), and clofibrate was described. Mechanistic insight from UV-vis spectroscopy suggested EDA complex formation, and a radical trap experiment with TEMPO indicated the presence of radical intermediates. The result of measurement of the quantum yield (Φ =

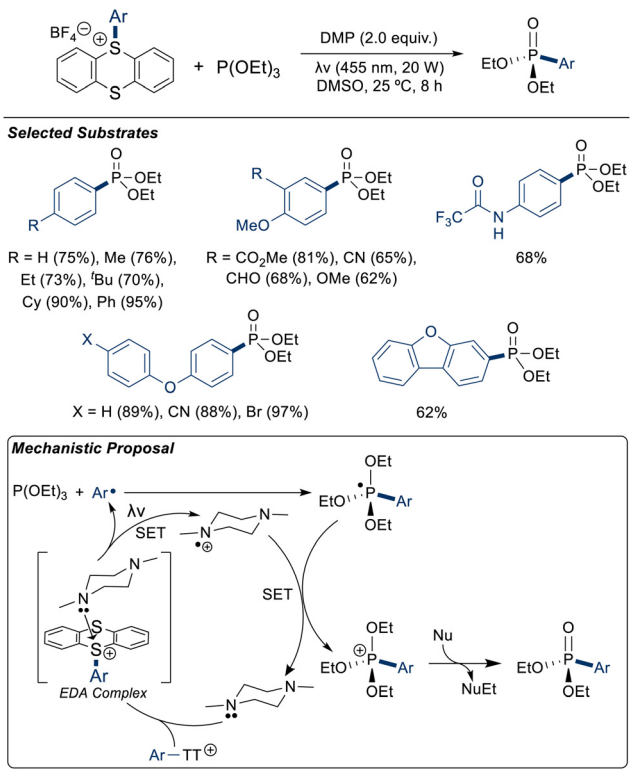

Scheme 24 Phosphonation of aryl thianthrenium salts promoted by a N-donor EDA complex.

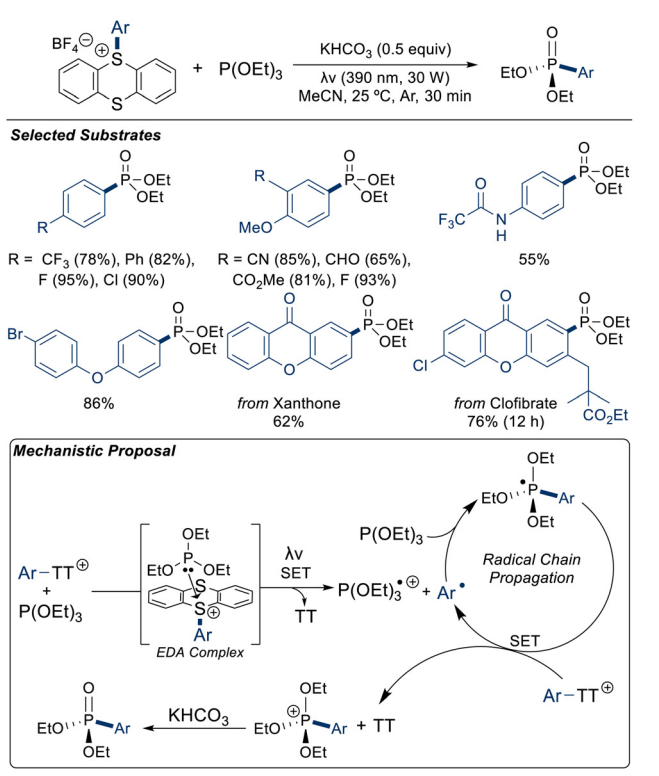

Scheme 25 Phosphonation of aryl thianthrenium salts promoted by a P-donor EDA complex.

118) suggested a radical chain mechanism. Fragmentation of the EDA complex to generate aryl radicals with subsequent addition to phosphites generates a radical intermediate that is oxidized to the cation *via* SET with an additional equivalent of Ar–TT$^+$. Formation of the phosphonium intermediate was supported by ^{1}H-^{31}P HMBC NMR and HRMS. An Arbuzov-type dealkylation step may then furnish product.

Ou and Su reported phosphination of Ar–TT$^+$ salts under visible light irradiation (λ = 420 nm, P = 15 W) at room temperature by leveraging the capacity for an EDA complex with K_2CO_3 to generate aryl radicals.[137] Treatment of electron-rich arenes with diaryl phosphines afforded asymmetrically substituted triaryl phosphines in moderate yields (Scheme 26).

Observation of a red-shifted UV-vis absorption spectrum upon combination of Ar–TT$^+$, PR_3, and K_2CO_3 provided experimental evidence for the formation of an EDA complex. A chemical shift was observed for thianthrenium ^{1}H nuclei only in a combined solution of these three components, further supporting this hypothesis. Computational (DFT) studies identified an optimized ground state structure with intermolecular interactions between Ar–TT$^+$ and phosphine as well as phosphine and K_2CO_3. On this basis, it was suggested that deprotonation of phosphine promotes SET within the EDA complex, forming aryl and phosphoryl radicals that recombine to form the product.

C_{sp^2}–Bi bond formation. Cornella described the addition of aryl radicals derived from Ar–TT$^+$ salts to *N*,*C*,*N*-bismuthinidenes in 2023 (Scheme 27).[138] Irradiation of 5-(4-methoxyphenyl)thianthrenium triflate with visible-light (λ = 395, 420, 465, 550, and 650 nm) at room temperature afforded aryl-Bi(III) complexes in ≥85% isolated yield. Treatment of thianthrenated pyriproxyfen with red light (λ = 650 nm) furnished the Bi(III) complex in 85% NMR yield. A spin trapping experiment analyzed by *in situ* EPR upon addition of 5,5-dimethyl-1-pyrroline *N*-oxide (DMPO) suggested the formation of aryl radical

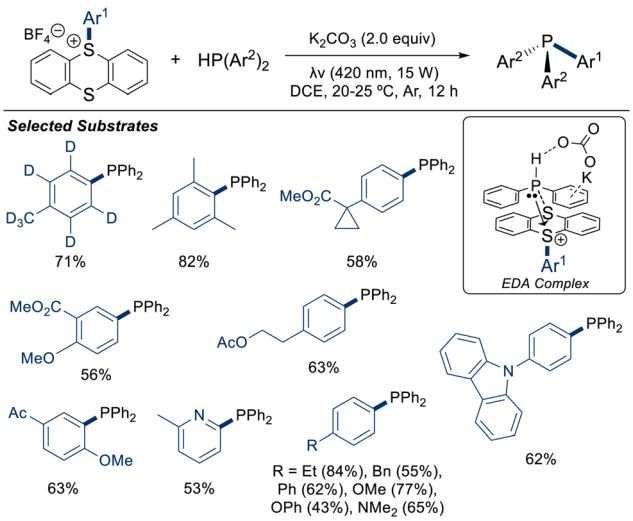

Scheme 26 Phosphorylation of aryl thianthrenium salts promoted by an EDA complex.

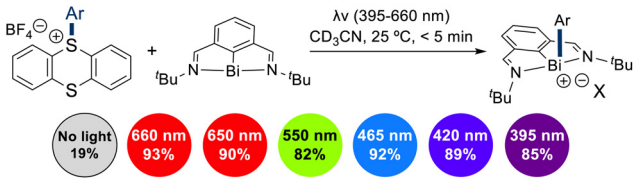

Scheme 27 Oxidative addition of aryl thianthrenium salts to Bi(I). Ar = *p*-methoxyphenyl.

intermediates by observation of a spin adduct. The spatial dependency of H_β–N EPR hyperfine coupling on the dihedral angle with the nitrogen p-orbital is the basis for this analysis. A control experiment in the absence of light led to a significant reduction in yield, which is consistent with light-induced formation of aryl radical species.

2.5 Group 16

C_{sp^2}–O bond formation. Hydroxylation and etherification of Ar–TT$^+$ salts using a visible-light metallaphotoredox catalysis ($\lambda\nu$ = blue LED, P = 34 W; PC = [Ir(dF(CF$_3$)ppy)$_2$(dtbpy)]PF$_6$) strategy was reported by Ritter 2019.[139] In the presence of water and CuO_2/dimethylglyoxime or CuTC (TC = thiophene-2-carboxylate), electron-rich, -neutral, and -poor arenes were transformed (Scheme 28) under argon atmosphere at 30 °C. Application to the late-stage hydroxylation of the agrochemicals boscalid (57%), etofenprox (62%), pyriproxyfen (49%) was demonstrated. Stern–Volmer analysis supported the reductive quenching of PC* by TT, and the resultant TT$^{\bullet+}$ was proposed to oxidize [Cu^{I}–OH] to [Cu^{II}–OH] prior to the oxidative ligation of Ar$^\bullet$ and reductive elimination of hydroxylated product. A radical trap experiment performed by addition of TEMPO to (*R*)-4-(4-hydroxy-benzyl)-3-propionyloxazolidin-2-onetetrafluorothianth-renium tetrafluoroborate, PC, and [Cu] led to isolation of the corresponding radical adduct. Conditions for the thioetherification of a limited scope of arenes were also described. Reducing the equivalency of [Cu^{I}] reduced substrate conversion, and the substitution of Cu_2O for either CuI or [Cu(MeCN)$_4$]BF$_4$ significantly reduced yields. The former observation suggests a limited TON for [Cu^{I}] prior to deactivation, despite the theoretical potential for catalyst regeneration following reductive elimination of product. Increasing the equivalency of DMG ligand to from 10 mol% to 50 mol% led to a reduction in yield of hydroxylated biphenyl from ≥80% to 38% and an increase in hydrodefunctionalized product formation.

Patureau reported the direct photochemical (λ = 254 nm, P = 144 W) synthesis of phenols using (4-oxo)-TEMPO as an oxygen atom source in 2022.[140] Substituted biaryls, including haloarenes, were functionalized in addition to O-/S-/N-heteroarenes (Scheme 29). Late-stage functionalization of flurbiprofen (56%) and bifonazole (62%) was reported.

Addition of the radical scavengers BHT, DPE, and 1,4-dinitrobenzene to the model system using biphenyl thianthrenium tetrafluoroborate as substrate led to a >40% reduction in phenol yield, suggesting the formation of an aryl radical intermediate. With thianthrenated fluorenone as substrate, a

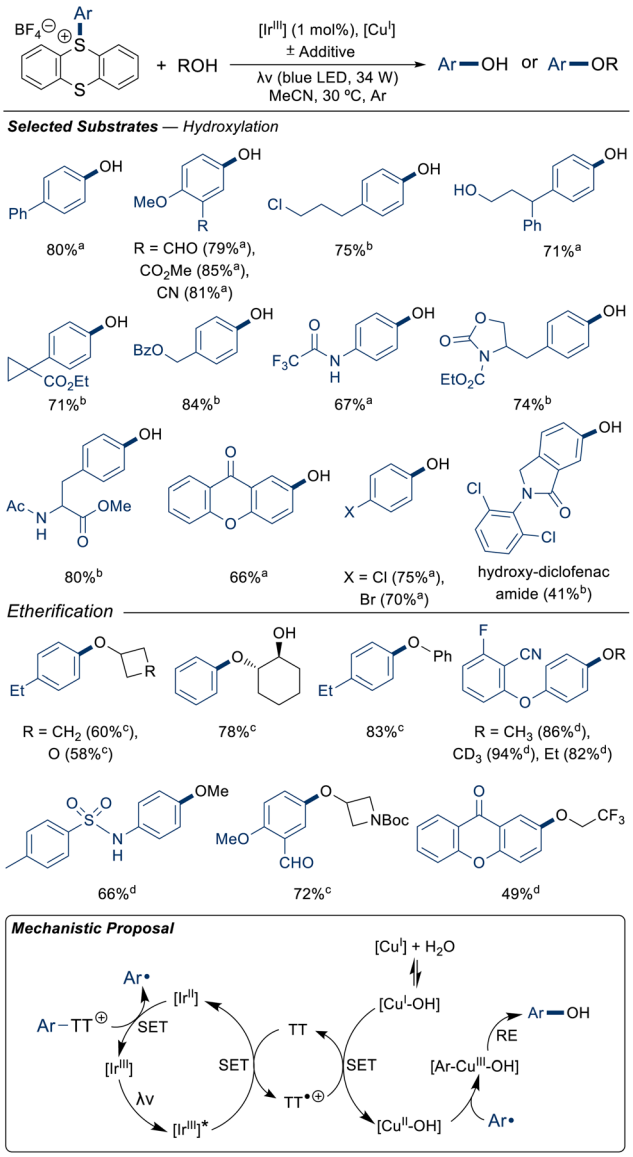

Scheme 28 Hydroxylation and etherification of aryl thianthrenium salts. [a][Cu^{I}] = Cu_2O (0.8 equiv.), solvent = MeCN/H_2O (10/3 v : v), additive = dimethylglyoxime (10 mol%), 16 h; [b][Cu^{I}] = CuTC (1.5 equiv.), ROH = H_2O (20 equiv.), 16 h; [c][Cu^{I}] = CuTC (1.0 equiv.), ROH (2 equiv.), additive = Na_2CO_3 (1.0 equiv.), 2 h; [d][Cu^{I}] = CuTC (1.0 equiv.), 16 h. [Ir^{III}] = [Ir(dF(CF$_3$)ppy)$_2$(dtbpy)]PF$_6$ (1 mol%).

TEMPO adduct was isolated and characterized by single-crystal X-ray diffraction, supporting the intermediacy of arene-TEMPO adducts formed by radical recombination after light-induced homolysis of Ar–TT^{+} salts. Subsequently, fragmentation of the N–O bond within the adduct may furnish an oxygen-centered phenol radical capable of abstracting hydrogen to generate product.

A three-component coupling of amines, carbon dioxide, Ar–TT^{+} salts to produce *O*-aryl carbamates under metallaphotoredox conditions (λ_{max} = 450 nm, P = 30 W; PC = [Ir(dtbbpy)(ppy)$_2$]PF$_6$) was reported by Qi in 2023.[141] The reaction was most efficient using secondary amines, electron-rich arenes,

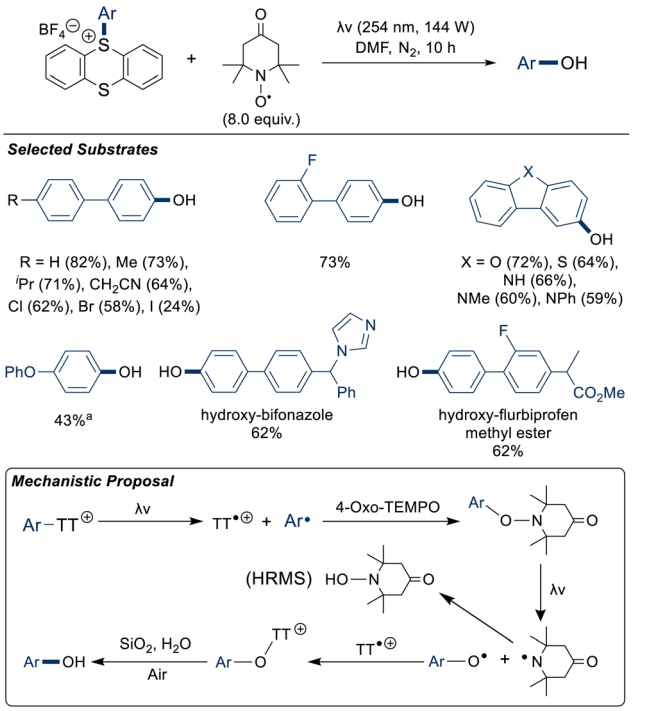

Scheme 29 Hydroxylation of biaryl thianthrenium salts. [a]Hydroxyl source is TEMPO (20 equiv.).

DABCO as base, suprastoichiometric quantities of [Cu(MeCN)$_4$]PF$_6$, and BF_3·OEt additive (Scheme 30). Radical trap experiments combining biphenyl thianthrenium tetrafluoroborate and TEMPO or DPE under optimized conditions led to observation of radical-trapped adducts and a ≥44% reduction in *O*-aryl carbamate product yield, suggesting formation of aryl radicals. Stern–Volmer analysis was consistent with the reduction of PC* by DABCO, supporting the following mechanistic proposal. Base-mediated deprotonation of amines facilitates carbamato complex formation with [Cu^{I}] prior to its oxidation by DABCO$^{\bullet+}$ to [Cu^{II}]. Oxidative ligation of Ar$^{\bullet}$ generates a [Cu^{III}] complex from which product may be reductively eliminated. Increased product yield and suppression of hydrodefunctionalized product formation was observed upon increasing the molar equivalency of [Cu^{I}] from 5 mol% to 40 mol%, which further improved with the use of a suprastoichiometric quantity (3 equiv.) of [Cu^{I}] under the optimized conditions. This suggests a low TON for [Cu^{I}] prior to its deactivation or off-cycling.

C_{sp^2}–S bond formation. Molander reported room-temperature arene sulfonylation reactions mediated by an EDA complex in 2022.[142] Combination of (hetero)aryl thianthrenium salts, (hetero)aryl or alkyl sulfinate salts, and Cs_2CO_3 base in DMSO under visible-light irradiation (λ_{max} = 390 nm, P = 30 W) and inert atmosphere (Ar) afforded the corresponding sulfones in moderate to good yield (Scheme 31). Application of this strategy to LSF of the pharmaceuticals bifonazole (methylsulfonylation, 50%), flurbiprofen (methyl- or tolyl-sulfonylation; 53%), and gemfibrozil (phenylsulfonylation, 42%) was

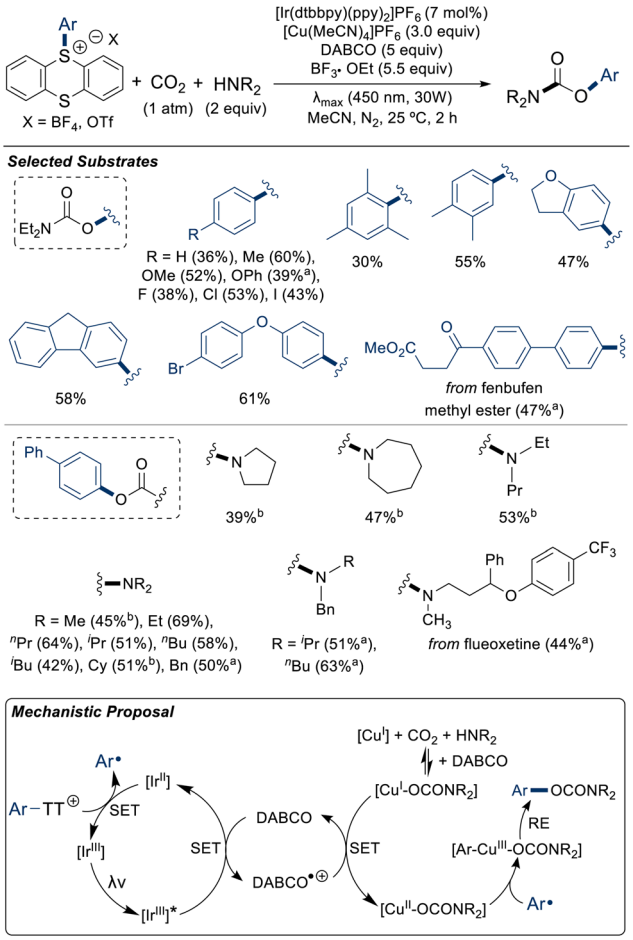

Scheme 30 Synthesis of *O*-aryl carbamates. [a]Reaction time = 6 h. [b]Quinuclidine instead of DABCO.

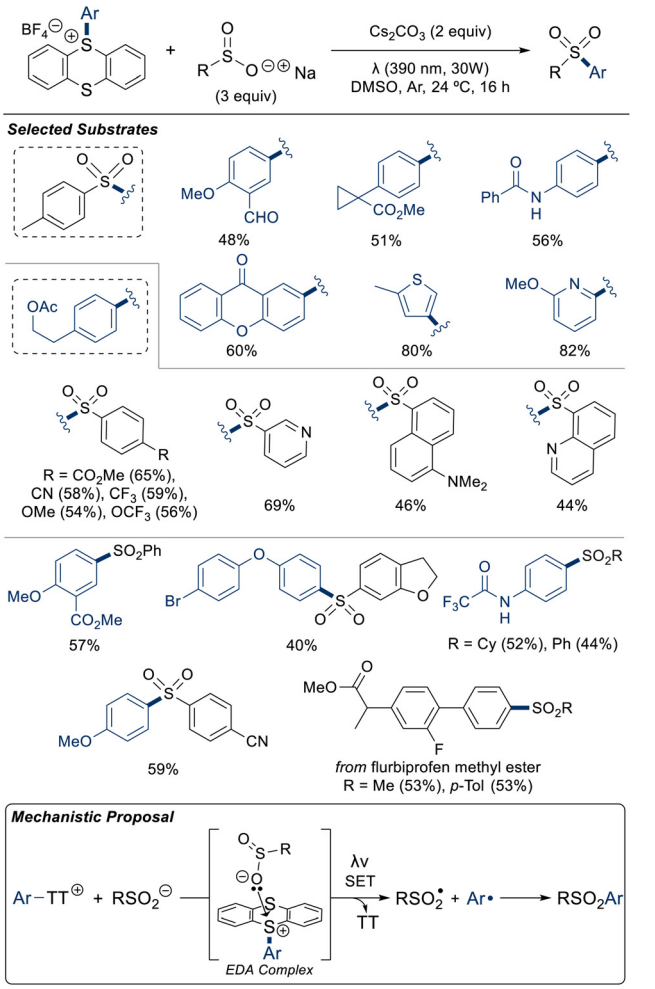

Scheme 31 Arene sulfonylation promoted by an *O*-donor EDA complex.

described. In the UV-vis absorption spectra of combined and independent solutions of the reaction components, a bathochromic shift was observed upon combination of the Ar–TT$^+$ and sulfinate salts that was further enhanced by the addition of Cs_2CO_3, suggesting the formation of a bimolecular or trimolecular EDA complex. However, the absence of a red-shifted absorption profile in a solution of the Ar–TT$^+$ salt and Cs_2CO_3 is inconsistent with the formation of a bimolecular EDA complex of these components, further supporting the role of sulfinate as a donor species. Experimental evidence for the intermediacy of aryl radicals was obtained through radical trapping experiments with TEMPO and BHT, where upon their addition the desired product yields were markedly decreased.

A photoredox-catalyzed (λ_{max} = 460–470 nm, P = 30 W; PC = Ir(ppy)$_3$) three-component coupling of Ar–TT$^+$ salts, [SO_2], and silyl enol ethers was reported by Wu in 2022.[143] At ambient temperatures under inert atmosphere (N_2), electron-rich arenes and silyl enol ethers were coupled *via* a sulfone bridge to generate the corresponding (α,α-difluoro-)β-keto-arylsulfones in moderate to good yields (Scheme 32). Thianthrenated forms of the bioactive compounds estrone methyl ether, indomethacin methyl ester, and pyriproxyfen were successfully functionalized using this strategy. Recycling of thianthrene in 90% recovery was demonstrated for the model substrates 1-phenyl-1-trimethylsiloxyethylene and *p*-tolylthianthrenium triflate. Quenching of PC* by the model Ar–TT$^+$ salt was observed in a Stern–Volmer analysis. Radical adducts were observed by HRMS when TEMPO or BHT were added to the model system, suggesting the formation of aryl radical intermediates. On this basis, it was hypothesized that aryl radicals formed upon SET with PC* undergo addition to [SO_2] equivalents to generate an intermediate S-centered radical species, which may in turn add to silyl enol ether. The resultant C-centered radical is then oxidized to the corresponding cation, regenerating the resting PC, prior to desilylation to furnish product. Avoidance of sacrificial redox agents is established by two synthetically useful SET events between photocatalyst and these intermediates, although the redox involvement of DABCO in this system cannot be ruled out.

Arenesulfonohydrazides were synthesized *via* three-component coupling of Ar–TT$^+$ salts, [SO_2], and hydrazines under photoredox conditions ($\lambda\nu$ = blue LED, P = 30 W; PC = Ir(ppy)$_3$)

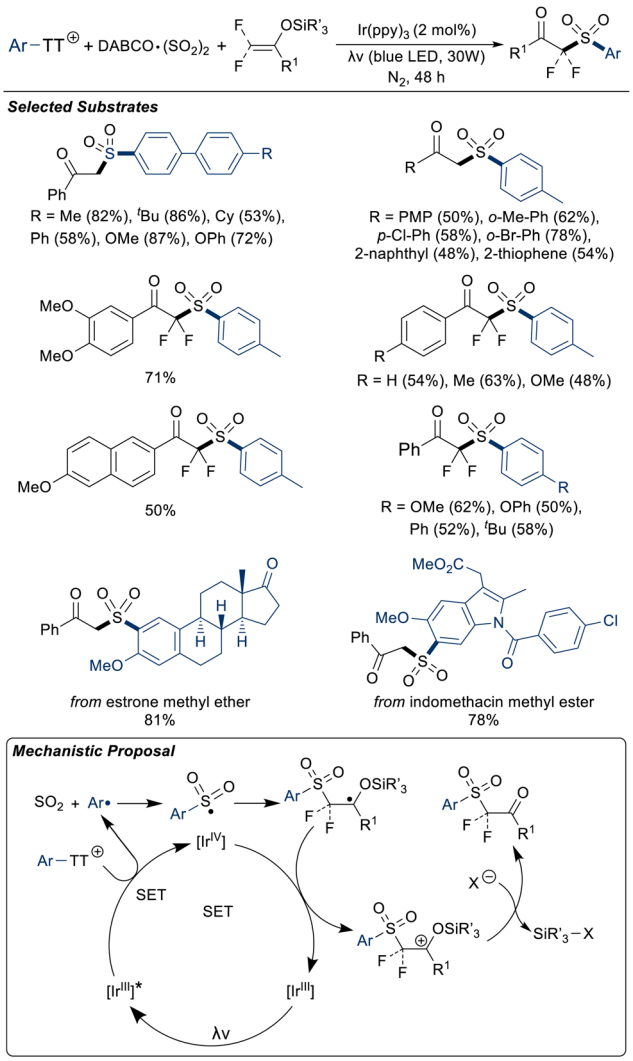

Scheme 32 Synthesis of β-keto-arylsulfones. For trimethylsilyl enol ether: Ar–TT$^+$ (1.5 equiv.), DABCO·$(SO_2)_2$ (12 equiv.), solvent = MeCN/THF (1/1 v : v); for 2,2-difluoro-1-triethylsilyl enol ether: Ar–TT$^+$ (2 equiv.), DABCO·$(SO_2)_2$ (1 equiv.), solvent = DCE.

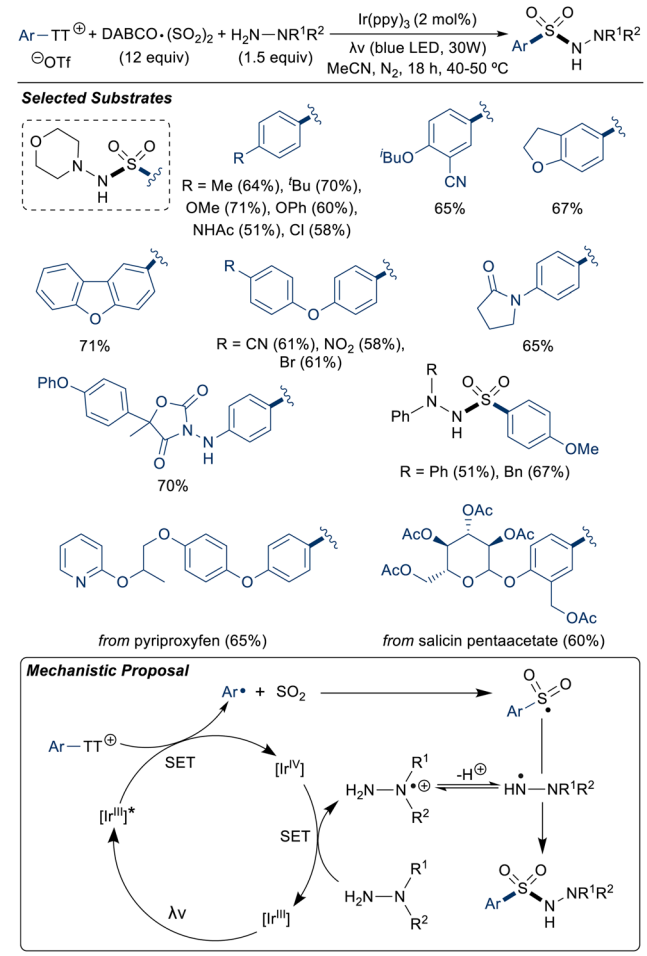

Scheme 33 Three-component synthesis of sulfonyl hydrazides.

by Wu in 2022.[144] Electron-rich arenes were functionalized (Scheme 33), including a demonstration of the LSF of pyriproxyfen and the protected carbohydrate salicin pentaacetate using morpholine as the hydrazine substrate. Mechanistic insight gained by addition of the radical scavenger TEMPO to the model system suggested the intermediacy of aryl radicals, corroborating the results of control experiments conducted in the absence of light or PC.

Quenching of PC* by the model Ar–TT$^+$ salt, *p*-methoxyphenyl thianthrenium triflate, was indicated by Stern–Volmer analysis. On this basis, a mechanistic hypothesis was proposed. Aryl radicals engage [SO_2] to yield S-centered radical adducts that couple with a hydrazine radical, formed in the reduction of [Ir^{IV}] to [Ir^{III}], to generate product.

Cao reported a three-component fluorosulfonylation of Ar–TT$^+$ salts under galvanostatic electrochemical conditions (*I* = 8 mA, ϕ = 1.5–2.0 V, cylindrical carbon felt electrodes [10 mm × 10 mm × 0.3 mm], electrolyte = *n*-Bu_4NClO_4) in 2023.[145] Combination of electron-rich (hetero)aryl thianthrenium salts, DABSO·SO_2, and potassium bifluoride (KHF_2) in an undivided cell at room-temperature under inert atmosphere (N_2) afforded the corresponding fluorosulfonylated arenes in moderate to good yields (46–86%) (Scheme 34). Application to the LSF of gemfibrozil methyl ester (42%) and the steroid epiandrosterone was demonstrated. A one-pot method in which the model Ar–TT$^+$ salt, *p-tert*-butylphenyl thianthrenium triflate, was sequentially thianthrenated and fluorosulfonylated, generating product in 69% yield. A gram-scale experiment of the model system (4 mmol Ar–TT$^+$) gave 81% yield, comparable to the 0.2 mmol-scale yield of 81%. Further, recovery of TTSO (85%) by exposure of the model system to air and extension of the reaction time was shown and did not affect product yield. Cyclic voltammetry studies supported the redox activity of the Ar–TT$^+$ salt, with an irreversible reduction observed at E_{pc} = −0.95 V *vs.* Ag/Ag^+. A radical trap experiment using TEMPO led to detection of S–O–N and C_{sp^2}–O–N radical-trapped adducts by HRMS and trace product formation, suggesting the intermediacy of S- and C-centered radicals. When the model system

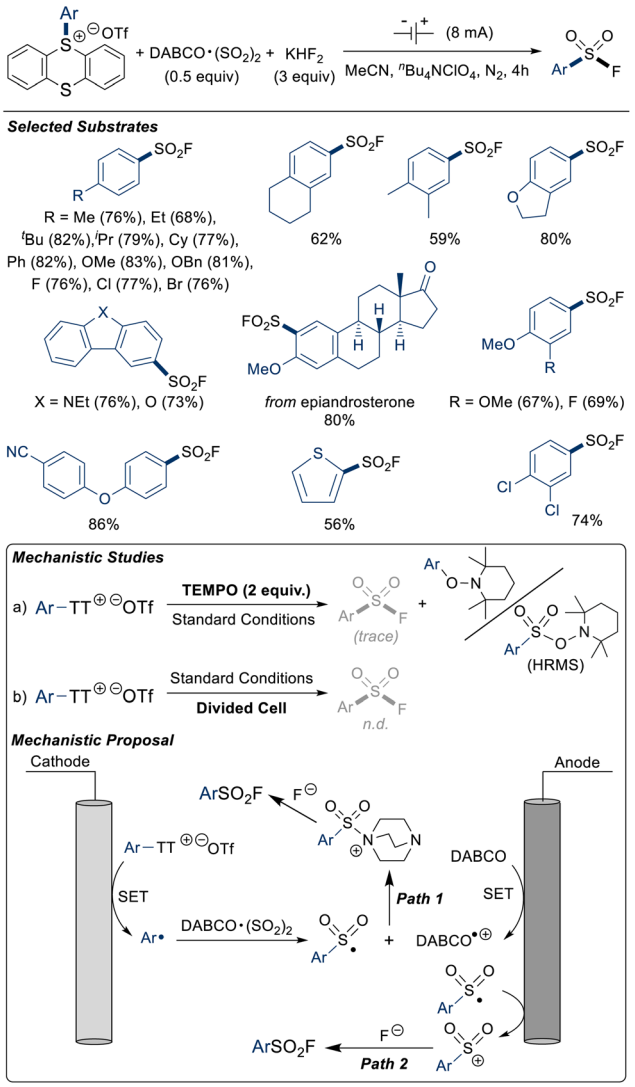

Scheme 34 Electrochemical fluorosulfonylation of aryl thianthrenium salts.

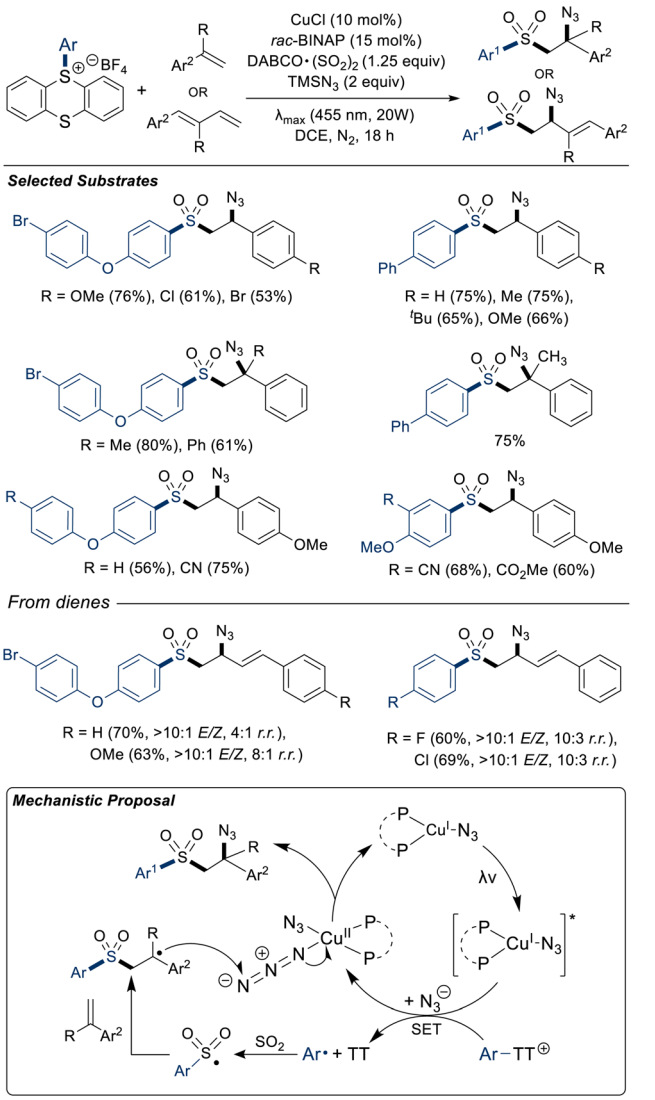

Scheme 35 Four-component azidosulfonylation of alkenes.

was probed for activity in a divided cell, no product formation was observed by GC-MS analysis, suggesting synthetically productive interactions of species generated at both the cathode and anode. A mechanistic proposal was generated in which aryl radicals are formed by the cathodic reduction of the Ar–TT^+ salt, which undergoes addition to [SO_2] to produce a S-centered radical intermediate. This intermediate may then either combine with anodically generated $DABCO^{\bullet+}$ or itself undergo anodic oxidation, followed by nucleophilic attack of F^- to generate product in both cases.

Yang reported a visible-light-promoted (λ_{max} = 455 nm, P = 20 W), Cu-catalyzed, four-component coupling of Ar–TT^+ salts, alkenes, trimethylsilyl azide ($TMSN_3$), and [SO_2] in 2024.[146] Difunctionalization of aryl-substituted alkenes generated the corresponding β-azido-arylsulfone products, which contain a reactive functional group capable of further transformation (Scheme 35). For instance, conversion of the β-azido moiety into a triazole by a Cu-catalyzed click reaction or reduction to primary amine was demonstrated in select cases; the latter was utilized in the synthesis of an apremilast (PDE_4 inhibitor) analogue. High stereoselectivity and good regioselectivity was observed in the azidosulfonylation of some 1,3-butadiene substrates. Enhanced UV-vis absorption was observed upon addition of *rac*-BINAP to a solution of CuCl, suggesting the role of a [Cu^I(*rac*-BINAP)] complex as a photoactive species. Radical trapping experiments with TEMPO and BHT led to observation of S–O–N and C_{sp^2}–O–N radical-trapped adducts by HRMS, along with a significant reduction in product yield. Photoexcitation of Cu^I(*rac*-BINAP)(N_3) enables SET to Ar–TT^+, generating aryl radicals which may undergo addition to [SO_2] and, subsequently, addition to alkene substrates. Outer-sphere radical abstraction of azide from Cu^{II}(*rac*-BINAP)(N_3)$_2$ then furnishes product and regenerates the catalyst. A similar system was reported by Wu in 2023 using Ir(ppy)$_3$ as PC.[147]

Thioetherification of Ar–TT$^+$ salts mediated by an EDA complex under aerobic conditions and visible light irradiation (λ = 427 nm, P = 30 W) was reported by Molander in 2022.[148] Coupling of (N-hetero)aryl thiols and electron-rich Ar–TT$^+$ salts was demonstrated (Scheme 36) in addition to the LSF of the bioactive compounds fenbufen, flurbiprofen, gemfibrozil, salicin, and xanthone. Longer irradiation wavelengths ($\lambda\nu$ = 455 nm/40 W or 525 nm/44 W) increased the formation of undesired thiolate dimerization products. Experimental evidence for the formation of an EDA complex was obtained by UV-vis spectroscopic analysis of reaction components in isolation and combination, and a 1 : 1 stoichiometry between thiolate and Ar–TT$^+$ salt was suggested by Job's method. Formation of aryl radicals was indicated by a radical trap experiment with TEMPO and detection of the corresponding adduct by HRMS.

Determination of the quantum yield (Φ = 89) supported a radical chain mechanism. It was then hypothesized that base-mediated deprotonation of thiols promotes ground-state EDA complex stabilized by π–π interactions, which upon irradiation undergoes homolytic fragmentation to form Ar$^\bullet$, TT, and disulfides. Aryl radicals may subsequently undergo addition to another equivalent of thiolate to form a radical anion adduct capable of reducing Ar–TT$^+$ salts and thus initiating another cycle. Mild conditions and operational simplicity are advantageous features of this system.

A metallaphotoredox-catalyzed (λ_{max} = 450 nm, P = 34 W; PC = [Ir(dtbbpy)(ppy)$_2$]PF$_6$; [M] = CuBr) thioetherification of Ar–TT$^+$ salts was developed by Zha and Ji in 2024.[149] Coupling of 1-thiosugars with (hetero)aryl thianthrenium salts led to the stereoretentive formation of aryl thioglycosides. Several pharmaceutical and agrochemical compounds were thianthrenated and glycosylated, including a gram-scale reaction estrone methyl ether (Scheme 37). Addition of TEMPO led to trace amounts of desired product formation and detection of an aryl radical-trapped adduct by HRMS and ^{1}H NMR analysis. Stern–Volmer experiments demonstrated the most efficient quenching of PC* occurred in the presence of thiosugar and base, suggesting the role of thiolate as the kinetically preferred reducing agent among the redox-active reaction components.

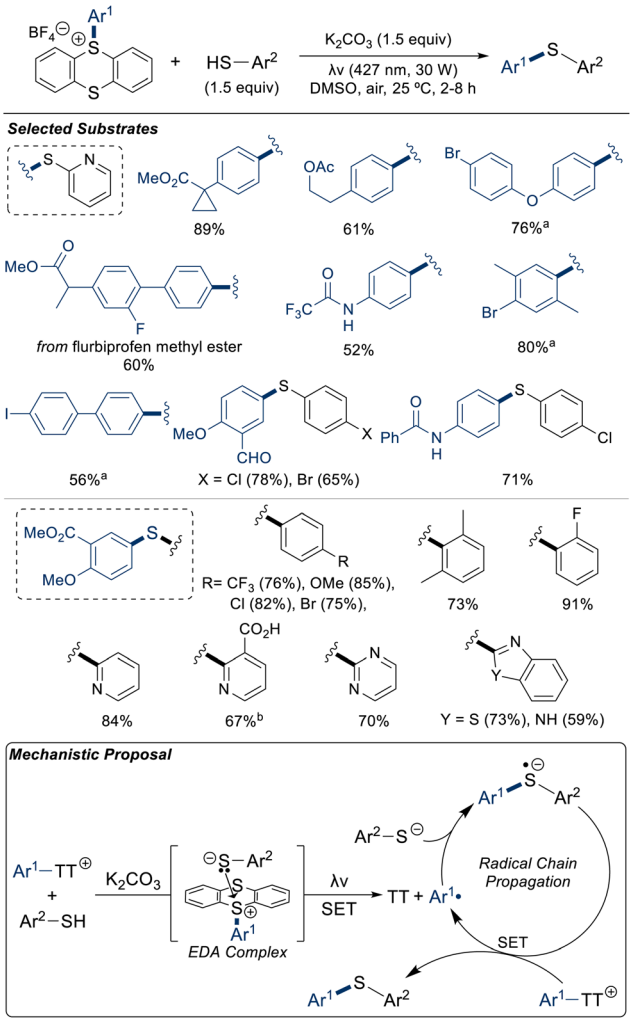

Scheme 36 Thioetherification of aryl thianthrenium salts promoted by a *S*-donor EDA complex. [a]HSAr^2 (1.1 equiv.), K_2CO_3 (1.1 equiv.); [b]K_2CO_3 (2.0 equiv.).

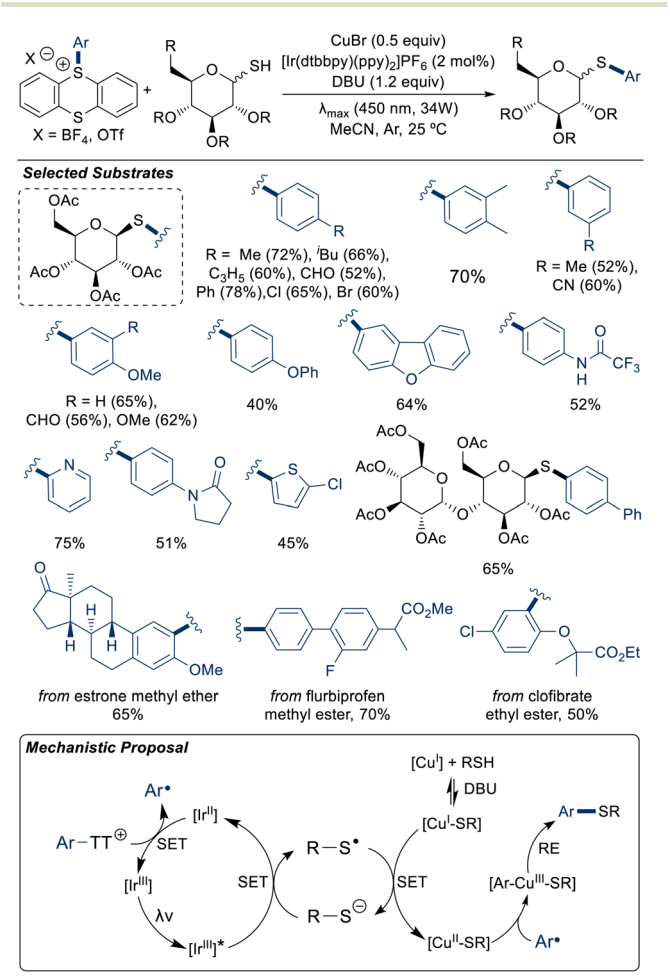

Scheme 37 Metallaphotoredox-catalyzed thioetherification of aryl thianthrenium salts.

Through an on–off experiment in which product formation was inhibited in the absence of light, a self-propagating radical chain mechanism was excluded. It was then proposed that base-mediated ligation of thiosugar to [Cu^{I}] forms a complex that is oxidized to [Cu^{II}-SR] *via* SET with thiol radicals generated in the reduction of [Ir^{III}]*. Aryl radicals oxidatively ligate this complex to generate a [Ar-Cu^{III}-SR] complex before reductive elimination of product.

In 2023, Yang reported a visible-light-promoted (λ = 455 nm, P = 34 W) dithiocarbamoylation of Ar–TT^{+} salts mediated by EDA complex formation in an aqueous medium.[150] This radical three-component coupling of Ar–TT^{+} salts, carbon disulfide, and secondary aryl- or alkyl amines (Scheme 38) was facilitated by surfactant-based (dodecyl trimethyl ammonium chloride; DTAC) micelle formation. In the absence of exogenous surfactant to the model substrates 5-(3-formyl-4-methoxyphenyl)thianthrenium tetrafluoroborate and pyrrolidine, *S*-aryl dithiocarbamoylate yield was reduced from 82% to 65%, improved to 70% in DMSO solvent. A gram-scale reaction of the model system generated product in 63% yield with 96% recovery of TT, and the of natural sunlight as the irradiation source offered 60% isolated product yield. Thianthrenation of fenofibrate and bifonazole enabled conjugation to diethylamine or *N*-methylaniline through a dithiocarbamates linker in moderate to good yield, demonstrating an application of the system to LSF. Radical trap experiments with TEMPO and DPE were indicative of aryl radical formation as the corresponding C_{sp^2}–O–N or C_{sp^2}–C_{sp^2} adducts observed by HRMS with concomitant reduction in product formation. Experimental evidence for the 1 : 1 formation of an EDA complex consisting of a dithiocarbamate anion and Ar–TT^{+} salt was obtained through Job's method and a bathochromic shift in the UV-vis absorption spectrum. Thus, SET within the EDA complex followed by recombination of the dithiocarbamate and aryl radicals was proposed.

Zhang reported the visible-light-promoted (λ = 420 nm, P = 10 W) dithiocarbamoylation of Ar–TT^{+} salts using an EDA complex strategy.[151] Three-component coupling Ar–TT^{+} salts, carbon disulfide, and secondary aryl- or alkyl amines in DMSO/H_2O (1 : 1 v/v) yielded the corresponding *S*-aryl dithiocarbamates (Scheme 39). A gram-scale synthesis using the model substrates *p*-tolylthianthrenium salt and *N*-methylaniline under flow conditions generated product in 66% yield with 90% recovery of TT. Constant irradiation is necessary for product formation, as evidenced by an on–off experiment, a result that would be inconsistent with a chain radical mechanism. Analysis by UV-vis spectroscopy demonstrated the strongest bathochromic shift in a combined solution of the three substrates with base, indicating the contribution of each to the formation of an EDA complex. Job's method suggested a 1 : 1 stoichiometry of dithiocarbamate anion to Ar–TT^{+} salt within the EDA complex. From these experiments, a mechanistic proposal analogous to Yang's was formulated.

A three-component coupling of Ar–TT^{+} salts, amines, and carbon disulfide for the synthesis of *S*-aryl-dithiocarbamates under aerobic conditions and white-light irradiation (color temperature = 4000 K, P = 2 × 40 W) was reported by Chen and Yi in 2024 (Scheme 40).[152] Structurally diverse amines and a selection of electron-deficient arenes were functionalized.

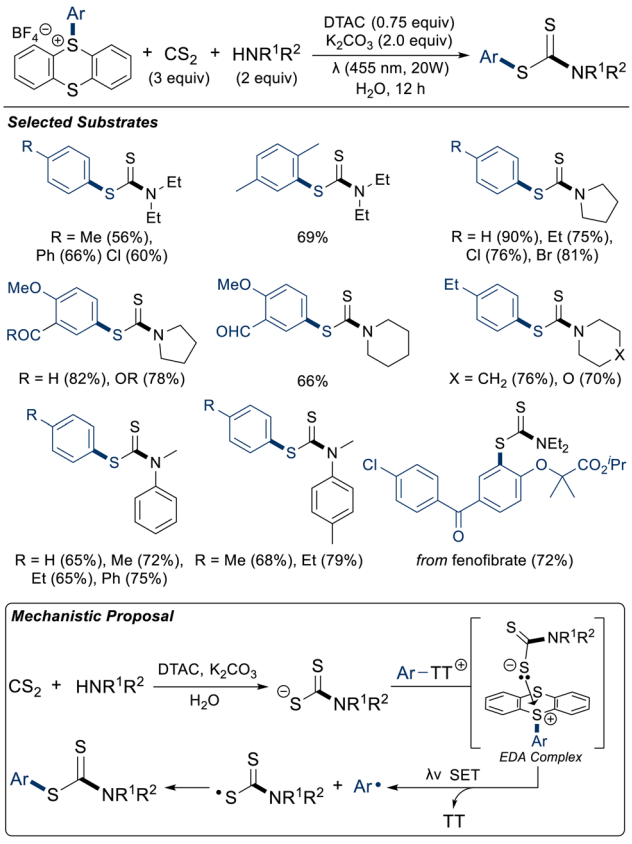

Scheme 38 Dithiocarbamoylation of aryl thianthrenium salts under aqueous conditions.

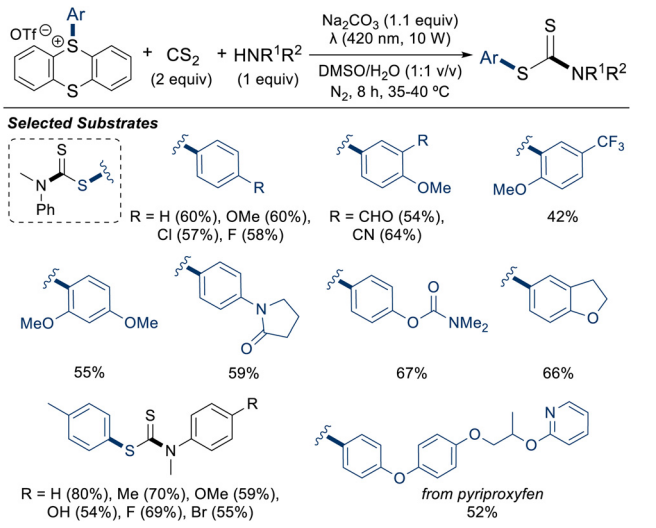

Scheme 39 Dithiocarbamoylation of aryl thianthrenium salts promoted by an S-donor EDA complex.

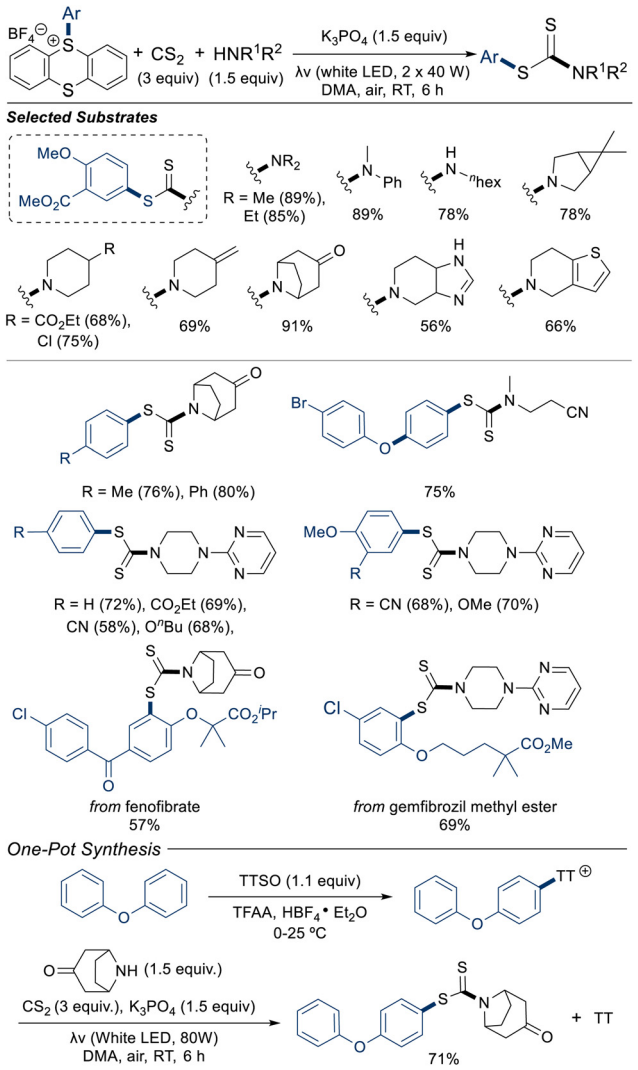

Scheme 40 Dithiocarbamoylation of aryl thianthrenium salts under aerobic conditions.

Thianthrenation of bioactive compounds facilitated their conjugation to amines through a dithiocarbamate linker. In demonstrating green applications of this system, natural sunlight was used as irradiation source and water was utilized as the solvent. One-pot, two-step syntheses were carried out, further enhancing the efficiency of this approach. Design of a continuous flow photoreactor enabled a decagram-scale synthesis with 94% recovery of TT. Spectroscopic analysis revealed the strongest bathochromic shift in the UV-vis absorption profile of a combined solution of the three components with base, suggesting the contribution of each component to the formation of an EDA complex. Absorbance measurements on solutions of 5-(4-phenoxyphenyl)thianthrenium tetrafluoroborate and varying concentrations of morpholine-*N*-dithiocarbamate anion under were suggestive of a 1 : 1 stoichiometry in the EDA complex, as the strongest absorption was observed at a mole fraction of $\chi = 0.5$. Operation of a radical chain mechanism was excluded through an on–off experiment in which product formation was not observed during dark cycles. The proposed mechanism is analogous to those previously discussed for multicomponent dithio-carbamoylation reactions proceeding through an EDA complex.

Wang reported the synthesis of sulfilimines from *N*-Bz-protected aryl sulfenamides and Ar–TT$^+$ salts under visible-light irradiation (λ_{max} = 452 nm, P = 48 W) in the presence of CuCl and DBU at ambient temperature under an inert (N_2) atmosphere (Scheme 41).[153] Electron-rich arenes as well as the pharmaceuticals fenbufen (56%), fenofibrate, gemfibrozil (59%), niflumic acid (COX2 inhibitor), and mexiletine (SCN5A inhibitor, 72%), were thianthrenated and utilized in the transformation. The selected model substrates (80% yield under standard conditions) were transformed in57% yield under air, in 35% yield with phosphate-buffered saline (PBS) as solvent, and in 40% yield with aqueous sodium dodecyl sulfate (SDS; 2 wt%) as solvent, suggesting some tolerance of the system to air and water. Also for the model substrates, the reaction proceeded in 37% yield in the absence of [Cu], suggesting a [Cu]-independent pathway to product formation. Characterization of independent and combined solutions of the reaction components was suggestive of EDA complex formation between deprotonated sulfenamide and the Ar–TT$^+$ salt. It was proposed that, upon irradiation, the EDA complex can decompose into two substrate radicals which recombine to form product. Alternatively, [Cu] may intercept these radicals and facilitate their cross-coupling. Formation of the EDA complex prior pre-

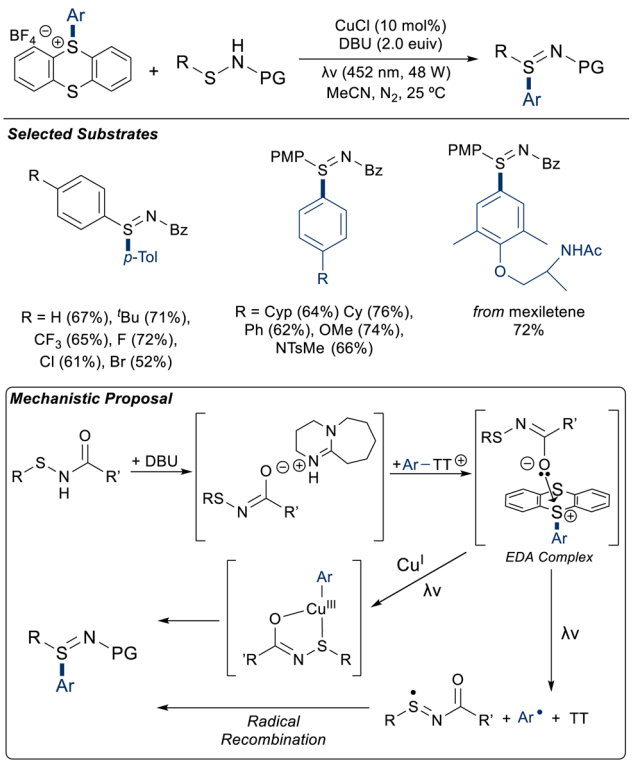

Scheme 41 Copper-catalyzed *S*-arylation of sulfenamides. Cyp = cyclopropyl, Bz = benzoyl.

ceding either pathway was supported by the absence of detectable product formation in the absence of DBU. Toward greater sustainability and scalability, experiments conducted using natural sunlight as the irradiation source (66% yield) or at gram-scale (62% yield) were undertaken, and the nearly quantitative recovery of TT was possible.

Arylation of phosphorothioates in the visible-light (λ = 455 nm, P = 20 W) promoted, [Cu]-catalyzed ([Cu] = $Cu(OAc)_2$, B = K_2HPO_4) synthesis of *S*-aryl phosphorothioates at ambient temperatures under inert (N_2) atmosphere in acetone was reported in 2024.[154] While predominantly electron-rich Ar–TT$^+$ salts were used, electron-withdrawing substituents (–CHO, –CO_2Me, –CN) in the *meta*-position were also tolerated. Bioactive compounds were thianthrenated and used as substrates, including diclofenac amide, fenofibrate, gemfibrozil, and nimesulide. A gram-scale trial with highly efficient recovery of TT, as well as an experiment using natural sunlight irradiation provided favorable results for scalability and sustainability.

Through a three-component synthesis of aryl thioether-substituted imidazoles, Ar–TT$^+$ salts were thioetherified under visible-light irradiation (λ = 455 nm, P = 25 W) and aerobic atmosphere by Yang in 2024.[155] Aryl isothiocyanates, isonitriles, and Ar–TT$^+$ salts were conjugated in the presence of strong base (LiO^{t}Bu) to furnish these trisubstituted N-hetereocycles under mild conditions (Scheme 42). Reaction of 1-fluoro-4-isothiocyanatobenzene, ethyl 2-cyanoacetate, and *p*-tolylthainthrenium tetrafluoroborate at the gram-scale afforded product in 62% yield with 94% recovery of TT.

Extending the reaction time to 3 days, these substrates reacted under natural sunlight irradiation in 72% yield. Radical trap experiments with TEMPO and DPE were suggestive of aryl and thiol radical formation by the detection of the corresponding adducts by HRMS and a significant reduction in the desired product yield. An on–off experiment provided negative evidence for a chain radical mechanism. A UV-vis analysis indicated EDA complex formation by observation of a bathochromic shift when all three substrates are combined in the presence of base. Deprotonation at the α-isocyano position and subsequent [3 + 2] cycloaddition with isothiocyanates establishes the imidazole backbone, and this anionic intermediate is proposed to form an EDA complex with Ar–TT$^+$ salts. Single electron transfer within the complex generates aryl and sulfur-centered radical fragments that may recombine to yield product.

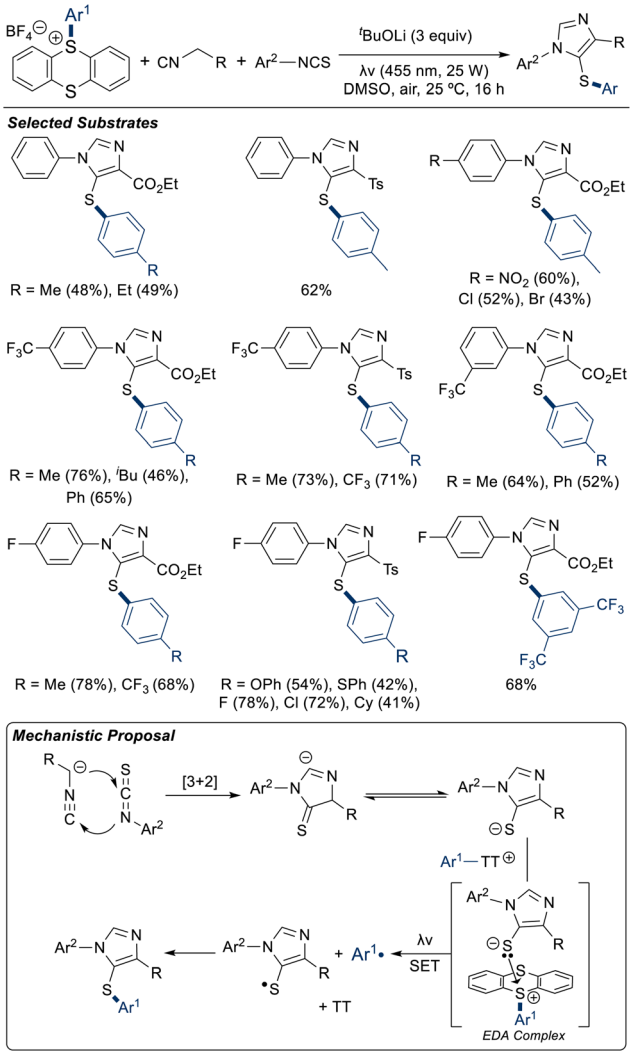

Scheme 42 Three-component synthesis of aryl thioether-substituted imidazoles.

C_{sp^2}–Se bond formation. By parallel strategies, Wu, Zhou, and Wang reported the thiocyanation and selenocyanation of Ar–TT$^+$ salts in 2023.[156] Under visible-light irradiation (λ = 380–390 nm, P = 24 W) and inert atmosphere (N_2) at room temperature, the combination of electron-rich and -poor (hetero)aryl thianthrenium salts and either potassium selenocyanate or copper(I) thiocyanate generated the desired products. Application to the LSF of bioactive compounds, such as boscalid, fenofibrate, and loratadine (H_1-receptor antagonist) was demonstrated (Scheme 43), along with further transformations of select thiocyanated and selenocyanated compounds. A gram-scale synthesis of *p*-tolyl isothiocyanate (67%) was described, and TT was recovered in 94% yield, indicating the capacity for recycling of this byproduct. Absent a bathochromic shift in the UV-vis analysis of the reaction components, formation of an EDA complex was not supported. On–off experiments were consistent with the measured quantum yield for selenocyanation (Φ = 0.26) in that a radical chain mechanism was unlikely. Considering the experimentally determined relative redox potentials of $E_{ox}(TT^{\bullet+}/TT)$ = +0.99 V, $E_{red}(SCN^{\bullet}/SCN^{-})$ = +0.63 V, and $E_{red}(SeCN^{\bullet}/SeCN^{-})$ = +0.31 V *vs.* Fc^+/Fc in MeCN, a mechanism was proposed in which Ar–TT$^+$ salts are photolytically cleaved before radical recombination with thiocyanato or selenocyanato radicals generated through SET with the $TT^{\bullet+}$ fragments.

2.6 Group 17

C_{sp^2}–X bond formation. Select examples of halogenation (X = I, Cl) of Ar–TT$^+$ salts under metallaphotoredox conditions were

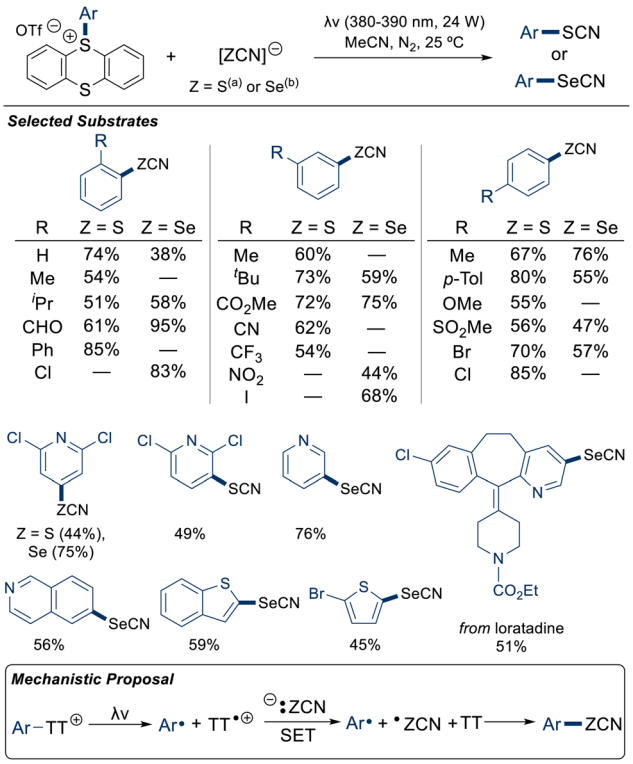

Scheme 43 Thiocyanation and selenocyanation of aryl thianthrenium salts. [a]CuSCN (3.0 equiv.), Na_2CO_3 (4.0 equiv.), 12 h; [b]KSeCN (3.0 equiv.), 24 h.

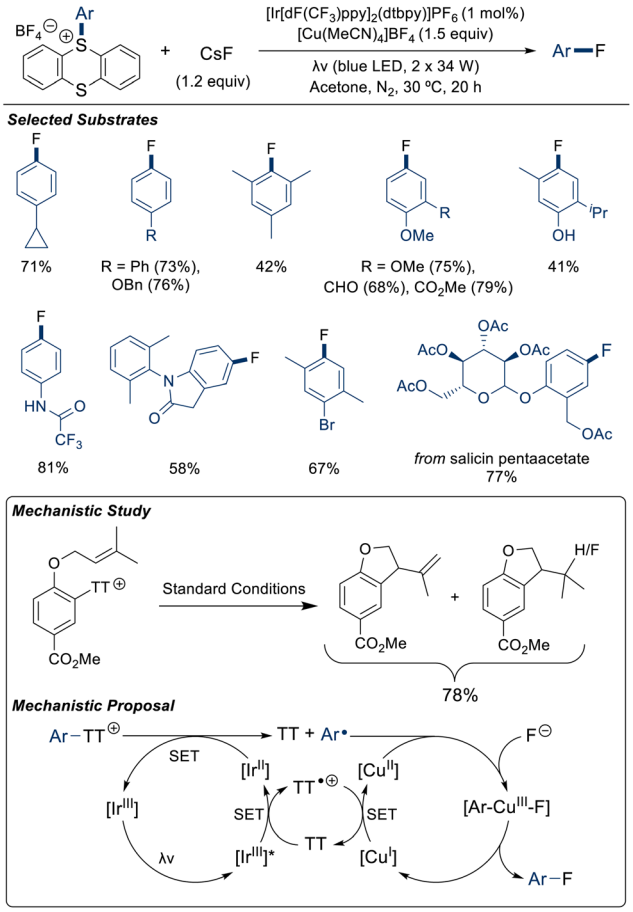

Scheme 44 Fluorination of aryl thianthrenium salts.

described in Ritter's 2019 report.[70] Expanding the scope of these halogenation reactions, a series of late-stage fluorinations was then reported by this group.[52] Under visible-light irradiation (λv = blue LED, P = 2 × 34 W; PC = $[Ir(dF(CF_3)ppy)_2(dtbpy)]PF_6$) in the presence of $[Cu(MeCN)_4]BF_4$, diverse arenes were transformed. Application of this strategy to the LSF of several bioactive compounds was demonstrated (Scheme 44). As has been described in similar systems, the use of stoichiometric [Cu] was useful in reducing the amount of undesired hydrodefunctionalized arene products formed. Stern–Volmer analysis indicated the most efficient quenching of PC* by TT, suggesting a reductive quenching cycle further supported by the directobservation of $TT^{\bullet+}$ by EPR spectroscopy. A radical trap experiment conducted by the addition of TEMPO, as well as a radical clock cyclization experiment, suggested the formation of $Ar^{\bullet}$ intermediates. Determination of a quantum yield of Φ = 0.6 excluded a radical chain mechanism. Therefore, it was hypothesized that $Ar^{\bullet}$ produced by SET with the reduced PC ($[Ir^{II}]$), oxidatively ligate a $[Cu^{II}]$ species furnished from SET with $TT^{\bullet+}$. Coordination of F^- to generate a $[Ar–Cu^{III}–F]$ enables facile reductive elimination of product.

Ritter and Cornella further expanded the scope of their arene halogenation efforts in 2023 through the development of a thermally-promoted, Ni-catalyzed method for chlorination, bromination, and iodination.[157] Treatment with $Ar–TT^+$ salts with $NiCl_2·6H_2O$, Zn^0, and either NaI, NaBr, or TBACl in DMA solvent under argon atmosphere at 25 °C yielded the corresponding haloarenes (Scheme 45). Application to LSF of bioactive compounds was demonstrated. Changing the [Ni] source to $Ni^I(COD)(OPh^*)$ (COD = 1,5-cyclooctadiene, OPh* = $O(^tBu)_3C_6H_2$) without addition of Zn^0 led to production of *N*-(4-iodophenyl)-*N*,4-dimethylbenzenesulfonamide in 76% yield, compared to 95% under standard conditions. The activity of $Ni(COD)_2$ at a 10 mol% loading was attributed to the oxidation of Ni^0 to $[Ni^I]$ by $Ar–TT^+$ salts, as its use in stoichiometric quantity did not furnish product, an effect ascribed to the aggregation of inactive Ni^0 at higher concentrations. Addition of $[Cp_2Fe](BArF4)$ ($BArF_4$ = tetrakis[3,5-bis(trifluoromethyl)phenyl]borate) as oxidant with stoichiometric $Ni(COD)_2$ loading promoted further reactivity (75% yield). Direct observation of $[Ni^I]$ in the presence of $[Cp_2Fe](BAr^F{}_4)$ through EPR spectroscopy further supported the role of Ni^I as the active species. Control experiments in the absence of [Ni] or [Zn] indicated their essential role in the transformation. Although the proposed intermediates were not isolated, a mechanistic hypothesis was proposed on this basis. Reduction of $Ar–TT^+$ salts by $[L–Ni^I–X]$ generates aryl radicals which oxidatively ligate $[L–Ni^{II}–X]^+$ to afford a $[Ar–Ni^{III}–LX]^+$ complex. From this complex, product may be reductively eliminated and the resting catalyst regenerated through anion metathesis.

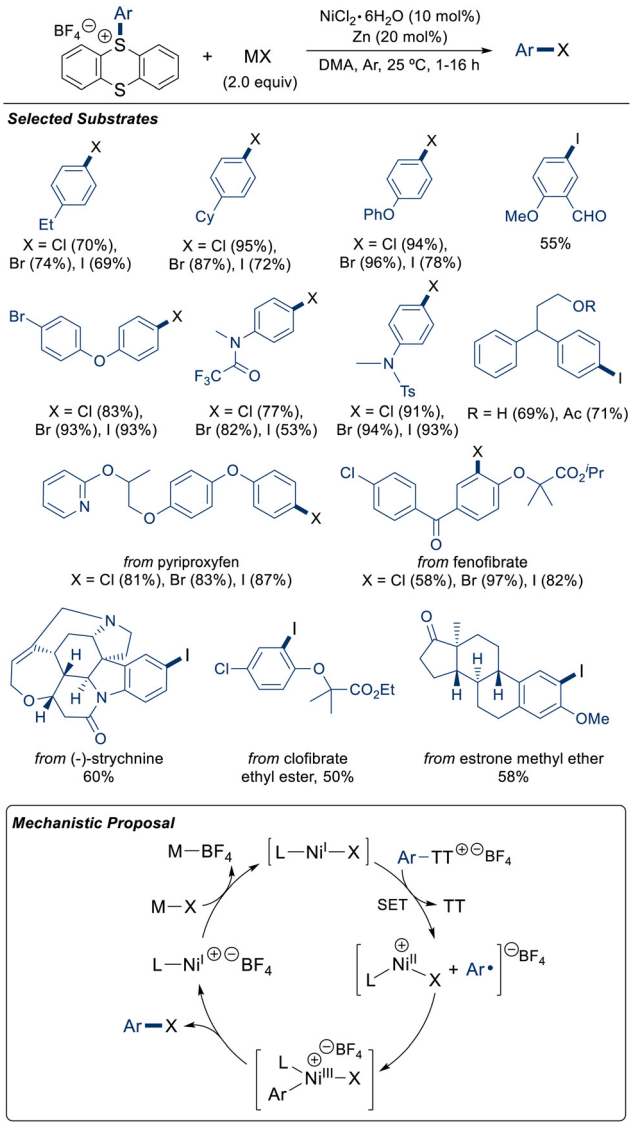

Scheme 45 Halogenation of aryl thianthrenium salts. M = NaI, NaBr, or TBACl.

3. Conclusion

Thianthrenation enables highly regioselective aromatic C_{sp^2}–H activation. Advancements in the preparation and utilization of these reagents recently motivated additional research efforts. Increasingly generalized approaches for their use are thus elaborated.[73] Aryl thianthrenium salts demonstrate divergent reactivity modes across the single- and two-electron regimes as aryl radical precursors, electrophiles, and cross-coupling partners. Here, we review the use of Ar–TT$^+$ salts as aryl radical precursors toward C_{sp^2}–H functionalization with the nonmetal main group elements. Primary methodological advantages of this approach include (1) high regioselectivity observed in aromatic C_{sp^2}–H activation, (2) compatibility of Ar–TT$^+$ salts with thermal, electrochemical, and photochemical energy input, (3) favorable redox properties of thianthrene and Ar–TT$^+$ salts, and (4) the potential for increasingly sustainable synthetic methods.

The origin of regioselectivity in thermally-promoted arene thianthrenation is the reversible formation of a Wheland intermediate followed by an irreversible, selectivity-determining deprotonation. Reversibility in the formation of the Wheland intermediate thermodynamically favors C_{sp^2}–S bond formation at the least sterically-hindered, electronically preferred *para*-position; positive charge accumulation within this intermediate biases the efficiency of this strategy toward electron-donating substituents at the *ortho*- and *para*-positions. Preferential reactivity subsequently occurs at the exocyclic C_{sp^2}–S site as the LUMO demonstrates antibonding character at this site and a dearomative enthalpic penalty is incurred by endocyclic reactivity.

Thianthrene is redox active, twice reversibly oxidized to the mono- and dication, and important implications of this were described in systems where these species functioned as a redox mediator or to sustain photoredox cycles. Further, the reversibility of these redox events enables the recycling of thianthrene and its catalytic reuse in one-pot, two-step, thianthrenation–functionalization reactions, increasing both the efficiency and sustainability of the platform. Formation of EDA complexes between Ar–TT$^+$ salts and electron-donors enables the use of longer irradiation wavelengths, often within the visible region, and thus milder conditions and greater functional group tolerance of these systems. Late-stage functionalization of structurally complex substrates was achieved for a variety of transformations, demonstrating the chemoselectivity advantage of thianthrenation and the mild conditions required to promote radical reactivity of the corresponding Ar–TT$^+$ salts. Achievement of LSF under mild conditions, aerobic atmosphere, aqueous media, and in batch and flow apparati, are promising features for scalability across academia and industry.

As a powerful C_{sp^2}–H functionalization platform, thianthrenation is methodologically limited in the directness of its approach, as is often the case for canonical methods, in that a minimum of two steps are required; activation (thianthrenation) and functionalization. However, further development of one-pot methods may mitigate this inefficiency. Sequential thianthrenation and functionalization of arenes and olefins under electrochemical conditions[18,158] theoretically would enable the catalytic recycling of thianthrene. Development of redox neutral systems, enabled through regeneration of neutral TT, offers an opportunity for increased synthetic efficiency, energy efficiency, and sustainability through waste reduction. Although metallaphotoredox strategies featuring chiral ligand supports on the transition metal catalysts have been used in C_{sp^2}–C_{sp^3} bond-forming systems of Ar–TT$^+$ salts, very few examples of asymmetric catalysis have been reported to date. Nevertheless, this area presents substantial opportunities for further investigation. Further development of multicomponent and radical cascade reactions is desirable for the synthetic utility of multiple-bond formation events in a single reaction which may be otherwise challenging. Thianthrenation

is therefore a promising C_{sp^2}–H activation method that merits additional research.

Author contributions

RAP contributed to the conceptualization, data curation, writing – original draft, writing – review & editing, and visualization. SX contributed to the conceptualization, funding acquisition, supervision, and writing – review & editing. Contributions are listed in accordance with the Elsevier CRediT guidelines.

Conflicts of interest

The authors have no conflicts of interest to declare.

Data availability

No primary research results, software or code have been included and no new data were generated or analysed as part of this review.

Acknowledgements

The authors are grateful for funding support provided by the Welch Foundation (Grant A-2174) and the Department of Chemistry and the Department of Pharmaceutical Sciences at Texas A&M University.

References

1 T. Rogge, N. Kaplaneris, N. Chatani, J. Kim, S. Chang, B. Punji, L. L. Schafer, D. G. Musaev, J. Wencel-Delord, C. A. Roberts, R. Sarpong, Z. E. Wilson, M. A. Brimble, M. J. Johansson and L. Ackermann, C–H activation, *Nat. Rev. Methods Primers*, 2021, **1**, 43.
2 T. Dalton, T. Faber and F. Glorius, C–H Activation: Toward Sustainability and Applications, *ACS Cent. Sci.*, 2021, **7**, 245–261.
3 D. Morton and H. M. L. Davies, Recent Advances in C–H Functionalization, *J. Org. Chem.*, 2016, **81**, 343–350.
4 J. A. Labinger and J. E. Bercaw, Understanding and Exploiting C–H Bond Activation, *Nature*, 2002, **417**, 507–514.
5 K. Godula and D. Sames, C-H Bond Functionalization in Complex Organic Synthesis, *Science*, 2006, **312**, 67–72.
6 R. G. Bergman, C–H activation, *Nature*, 2007, **446**, 391–393.
7 J. He, M. Wasa, K. S. L. Chan, Q. Shao and J.-Q. Yu, Palladium-Catalyzed Transformations of Alkyl C–H Bonds, *Chem. Rev.*, 2017, **117**, 8754–8786.
8 T. W. Lyons and M. S. Sanford, Palladium-Catalyzed Ligand-Directed C–H Functionalization Reactions, *Chem. Rev.*, 2010, **110**, 1147–1169.
9 P. T. Anastas and J. C. Warner, *Green Chemistry: Theory and Practice*, Oxford University Press, 1998.
10 J. W. Lehmann, D. J. Blair and M. D. Burke, Towards the Generalized Iterative Synthesis of Small Molecules, *Nat. Rev. Chem.*, 2018, **2**, 0115.
11 C. N. Prieto Kullmer, J. A. Kautzky, S. W. Krska, T. Nowak, S. D. Dreher and D. W. C. MacMillan, Accelerating Reaction Generality and Mechanistic Insight Through Additive Mapping, *Science*, 2022, **376**, 532–539.
12 Z. Bai and T. Ritter, Applications of Thianthrene Chemistry in Organic Synthesis, *Nat. Synth.*, 2025, **4**, 1187–1199.
13 C. B. Kelly and R. Padilla-Salinas, Late stage C–H functionalization via chalcogen and pnictogen salts, *Chem. Sci.*, 2020, **11**, 10047–10060.
14 F. Berger and T. Ritter, Site-Selective Late-Stage C–H Functionalization via Thianthrenium Salts, *Synlett*, 2021, 339–345.
15 X.-Y. Chen, Y. Wu and P. Wang, Recent Advances in Thianthrenation/Phenoxathiination Enabled Site-Selective Functionalization of Arenes, *Synthesis*, 2022, 3928–3940.
16 H. Meng, M.-S. Liu and W. Shu, Organothianthrenium Salts: Synthesis and Utilization, *Chem. Sci.*, 2022, **13**, 13690–13707.
17 J. Chen, J. Li, M. B. Plutschack, F. Berger and T. Ritter, Regio- and Stereoselective Thianthrenation of Olefins To Access Versatile Alkenyl Electrophiles, *Angew. Chem., Int. Ed.*, 2020, **59**, 5616–5620.
18 D. E. Holst, D. J. Wang, M. J. Kim, I. A. Guzei and Z. K. Wickens, Aziridine Synthesis by Coupling Amines and Alkenes via an Electrogenerated Dication, *Nature*, 2021, **596**, 74–79.
19 F. Juliá, J. Yan, F. Paulus and T. Ritter, Vinyl Thianthrenium Tetrafluoroborate: A Practical and Versatile Vinylating Reagent Made from Ethylene, *J. Am. Chem. Soc.*, 2021, **143**, 12992–12998.
20 D. J. Wang, K. Targos and Z. K. Wickens, Electrochemical Synthesis of Allylic Amines from Terminal Alkenes and Secondary Amines, *J. Am. Chem. Soc.*, 2021, **143**, 21503–21510.
21 M.-S. Liu, H.-W. Du, J.-F. Cui and W. Shu, Intermolecular Metal-Free Cyclopropanation and Aziridination of Alkenes with XH2 (X=N, C) by Thianthrenation, *Angew. Chem., Int. Ed.*, 2022, **61**, e202209929.
22 M.-S. Liu, H.-W. Du and W. Shu, Metal-Free Allylic C–H Nitrogenation, Oxygenation, and Carbonation of Alkenes by Thianthrenation, *Chem. Sci.*, 2022, **13**, 1003–1008.
23 P. Hartmann, K. Bohdan, M. Hommrich, F. Juliá, L. Vogelsang, J. Eirich, R. Zangl, C. Farès, J. B. Jacobs, D. Mukhopadhyay, J. M. Mengeler, A. Vetere, M. S. Sterling, H. Hinrichs, S. Becker, N. Morgner, W. Schrader, I. Finkemeier, K.-J. Dietz, C. Griesinger and T. Ritter, Chemoselective Umpolung of Thiols to

Episulfoniums for Cysteine Bioconjugation, *Nat. Chem.*, 2023, **16**, 380–388.
24 D. E. Holst, C. Dorval, C. K. Winter, I. A. Guzei and Z. K. Wickens, Regiospecific Alkene Aminofunctionalization via an Electrogenerated Dielectrophile, *J. Am. Chem. Soc.*, 2023, **145**, 8299–8307.
25 M. J. Kim, D. J. Wang, K. Targos, U. A. Garcia, A. F. Harris, I. A. Guzei and Z. K. Wickens, Diastereoselective Synthesis of Cyclopropanes from Carbon Pronucleophiles and Alkenes, *Angew. Chem., Int. Ed.*, 2023, **62**, e202303032.
26 M.-S. Liu, H.-W. Du, H. Meng, Y. Xie and W. Shu, Unified Metal-Free Intermolecular Heck-Type Sulfonylation, Cyanation, Amination, Amidation of Alkenes by Thianthrenation, *Nat. Commun.*, 2024, **15**, 529.
27 C. Dorval, A. D. Matthews, K. Targos, S. N. Alektiar, D. E. Holst, Z. Tan, M. Muuronen, J. B. Diccianni, J. E. Gómez, K. M. Sanders, I. A. Guzei and Z. K. Wickens, Unlocking Azole Chemical Space via Modular and Regioselective N-Alkylation, *Nat. Chem.*, 2025, **17**, 1576–1585.
28 P. Hartmann, K. Bohdan, L. Vogelsang, D. Marchionni, C. Preisinger, A. Vetere, K.-J. Dietz and T. Ritter, In Cellulo Cysteine Umpolung for Protein Structure Probing, *J. Am. Chem. Soc.*, 2025, **147**, 35587–35594.
29 K. Huyan, S. Chen and W. Zhao, Diastereoselective Synthesis of Cyclopropyl Diboronates via 1,2-Boronate Rearrangement, *Angew. Chem., Int. Ed.*, 2025, **64**, e202508322.
30 P. J. Verardi, E. A. Ryutov, P. Mukherjee, R. Lalisse, K. Targos, T. Inagaki, M. Kelly, I. A. Guzei, M. Schreier, O. Gutierrez and Z. K. Wickens, Stereo-reversed E2 unlocks Z-selective C–H functionalization, *Science*, 2025, **389**, 1239–1245.
31 M. J. Kim, K. Targos, D. E. Holst, D. J. Wang and Z. K. Wickens, Alkene Thianthrenation Unlocks Diverse Cation Synthons: Recent Progress and New Opportunities, *Angew. Chem., Int. Ed.*, 2024, **63**, e202314904.
32 X. Wu, P. Gao and F. Chen, Synthetic Applications of Sulfonium Salts as Aryl Radical Precursors, *Eur. J. Org. Chem.*, 2023, e202300864.
33 S. Oae, in *Organic Chemistry of Sulfur*, Springer US, 1977, ch. 1, pp. 1–31.
34 R. J. W. Cremlyn, *An Introduction to Organosulfur Chemistry*, Wiley, Chichester, New York, 1996.
35 S. Oae and J. T. Doi, *Organic Sulfur Chemistry: Structure and Mechanism*, CRC Press, Boca Raton, Florida, 1991.
36 B. Meyer, *Sulfur, Energy, and Environment*, Elsevier Science, 2013.
37 K. A. Scott and J. T. Njardarson, Analysis of US FDA-Approved Drugs Containing Sulfur Atoms, *Top. Curr. Chem.*, 2018, **376**, 5.
38 P. Devendar and G.-F. Yang, Sulfur-Containing Agrochemicals, *Top. Curr. Chem.*, 2017, **375**, 82.
39 J. M. Chalker, M. J. H. Worthington, N. A. Lundquist and L. J. Esdaile, Synthesis and Applications of Polymers Made by Inverse Vulcanization, *Top. Curr. Chem.*, 2019, **377**, 16.
40 G. Turkoglu, M. E. Cinar and T. Ozturk, Thiophene-Based Organic Semiconductors, *Top. Curr. Chem.*, 2017, **375**, 84.
41 R. J. Huxtable, *Biochemistry of Sulfur*, Springer US, 2013.
42 N. S. Shlapakov, A. D. Kobelev, J. V. Burykina, Y.-Z. Cheng, S.-L. You and V. P. Ananikov, Sulfur in Waste-Free Sustainable Synthesis: Advancing Carbon–Carbon Coupling Techniques, *Angew. Chem.*, 2024, **136**, e202402109.
43 D. Kaiser, I. Klose, R. Oost, J. Neuhaus and N. Maulide, Bond-Forming and -Breaking Reactions at Sulfur(IV): Sulfoxides, Sulfonium Salts, Sulfur Ylides, and Sulfinate Salts, *Chem. Rev.*, 2019, **119**, 8701–8780.
44 R. S. Glass, Sulfur Radicals and Their Application, *Top. Curr. Chem.*, 2018, **376**, 22.
45 Y.-F. Wei, W.-C. Gao, H.-H. Chang and X. Jiang, Recent Advances in Thiolation via Sulfur Electrophiles, *Org. Chem. Front.*, 2022, **9**, 6684–6707.
46 S. I. Kozhushkov and M. Alcarazo, Synthetic Applications of Sulfonium Salts, *Eur. J. Inorg. Chem.*, 2020, **2020**, 2486–2500.
47 Z. Jin, T. Yu, H. Wang, P. Jia and Y. Huang, Shining Light on Sulfonium Salts and Sulfur Ylides: Recent Advances in Alkylation Under Photoredox Catalysis, *Org. Chem. Front.*, 2024, **11**, 6573–6588.
48 C. Li, Y. Yang, X. Zheng, C. Zhang, H. Cai and W. Lin, Photocatalyzed Sulfoximination/Amidation of (Het)arylethenes Tethered N-tosyl Amide: a Versatile Entry to Sulfoximidoyl β- and γ-Lactams, *Org. Chem. Front.*, 2024, **11**, 4508–4515.
49 K. Kafuta, A. Korzun, M. Böhm, C. Golz and M. Alcarazo, Synthesis, Structure, and Reactivity of 5-(Aryl)dibenzothiophenium Triflates, *Angew. Chem., Int. Ed.*, 2020, **59**, 1950–1955.
50 J.-W. Song, F. Xia, X.-L. Zhang and C.-P. Zhang, Pd-Catalyzed Relay Heck Arylation of Alkenyl Alcohols with Arylsulfonium Salts, *Org. Chem. Front.*, 2024, **11**, 4219–4230.
51 Z.-Y. Tian, Y.-T. Hu, H.-B. Teng and C.-P. Zhang, Application of Arylsulfonium Salts as Arylation Reagents, *Tetrahedron Lett.*, 2018, **59**, 299–309.
52 J. Li, J. Chen, R. Sang, W.-S. Ham, M. B. Plutschack, F. Berger, S. Chabbra, A. Schnegg, C. Genicot and T. Ritter, Photoredox Catalysis with Aryl Sulfonium Salts Enables Site-Selective Late-Stage Fluorination, *Nat. Chem.*, 2020, **12**, 56–62.
53 Y. Cai, T. K. Roy, T. J. Zähringer, B. Lansbergen, C. Kerzig and T. Ritter, Arylthianthrenium Salts for Triplet Energy Transfer Catalysis, *J. Am. Chem. Soc.*, 2024, **146**, 30474–30482.
54 B. Boduszek, H. J. Shine and T. K. Venkatachalam, Reactions of Phenylmagnesium Chloride and Phenyllithium with Thianthrene Cation Radical Perchlorate. Evidence for Electron Transfer: Formation and Decomposition of 5-Substituted Thianthreniumyl Perchlorates, *J. Org. Chem.*, 1989, **54**, 1616–1626.

55 D.-Q. Qian, B. Liu, H. J. Shine, I. Y. Guzman-Jimenez and K. H. Whitmire, Ring-opening reactions of 5-(Aryl) Thianthrenium Bromides with Aryl Thiolates, *J. Phys. Org. Chem.*, 2002, **15**, 139–147.
56 O. Hammerich and V. D. Parker, The Reversible Oxidation of Aromatic Cation Radicals to Dications. Solvents of Low Nucleophilicity, *Electrochim. Acta*, 1973, **18**, 537–541.
57 H. J. Shine and L. Piette, Ion-radicals. The Reaction of Thioaromatic Compounds with Acids. II. Diphenyl Disulfide, Thianthrene and Thianthrene Oxides, *J. Am. Chem. Soc.*, 1962, **84**, 4798–4806.
58 M. Kinoshita and H. Akamatu, The Electron Spin Resonance Absorption of the Complexes of Aromatic Sulfur Compounds with Lewis Acids, *Bull. Chem. Soc. Jpn.*, 1962, **35**, 1040–1041.
59 E. Lucken, 1, 4-Dithiinium Radical-Cations, *J. Chem. Soc.*, 1962, 4963–4965.
60 H. Bock, A. Rauschenbach, C. Näther, M. Kleine and Z. Havlas, Thianthren-Radikalkation-Tetrachloroaluminat, *Chem. Ber.*, 1994, **127**, 2043–2049.
61 H. J. Shine and J. J. Silber, Ion Radicals. XXII. Reaction of Thianthrenium Perchlorate (C12H8S2+ClO4-) with Aromatics, *J. Org. Chem.*, 1971, **36**, 2923–2926.
62 K. Kim, V. Hull and H. J. Shine, Ion radicals. XXIX. Reaction of Thianthrene Cation Radical Perchlorate with Some Benzene Derivatives, *J. Org. Chem.*, 1974, **39**, 2534–2537.
63 W. K. Lee, B. Liu, C. W. Park, H. J. Shine, I. Y. Guzman and K. H. Whitmire, Addition of Thianthrene Cation Radical to Cycloalkenes. An Unexpected Monoadduct, *J. Org. Chem.*, 1999, **64**, 9206–9210.
64 D.-Q. Qian, H. J. Shine, I. Y. Guzman-Jimenez, J. H. Thurston and K. H. Whitmire, Mono-and Bisadducts From the Addition of Thianthrene Cation Radical Salts to Cycloalkenes and Alkenes, *J. Org. Chem.*, 2002, **67**, 4030–4039.
65 H. J. Shine, P. Rangappa, J. N. Marx, D. C. Shelly, T. Ould-Ely and K. H. Whitmire, Adducts of Thianthrene-and Phenoxathiin Cation Radical Salts with Symmetrical Alkynes. Structure and Formation of Cumulenes on Alumina Leading to α-Diketones, α-Hydroxyalkynes, and α-Acetamidoalkynes, *J. Org. Chem.*, 2005, **70**, 3877–3883.
66 P. Rangappa, H. J. Shine, J. N. Marx, T. Ould-Ely, A. T. Kelly and K. H. Whitmire, Adducts of Thianthrene-and Phenoxathiin Cation Radical Tetrafluoroborates to 1-Alkynes. Structures and Formation of 1-(5-Thianthreniumyl)- and 1-(10-Phenoxathiiniumyl)alkynes on Alumina Leading to α-Ketoylides and α-Ketols, *J. Org. Chem.*, 2005, **70**, 9764–9770.
67 H. J. Shine, B.-J. Zhao, J. N. Marx, T. Ould-Ely and K. H. Whitmire, Decomposition of Alkene Adducts of Thianthrene Cation Radical in Nitrile Solvents. Formation of Alkyl-2-Oxazolines and a New Class of Four-Component Products: 5-[(1-Alkoxyalkylidene) Ammonio] Alkylthianthrenium Diperchlorates, *J. Org. Chem.*, 2004, **69**, 9255–9261.
68 B.-J. Zhao, D. H. Evans, N. A. Macías-Ruvalcaba and H. J. Shine, Reaction of Thianthrene and Phenoxathiin Cation Radicals with 2, 3-Dimethyl-2-Butene. Chemical and Electrochemical Studies, *J. Org. Chem.*, 2006, **71**, 3737–3742.
69 B. Boduszek and H. J. Shine, Preparation of Solid Thianthrene Cation Radical Tetrafluoroborate, *J. Org. Chem.*, 1988, **53**, 5142–5143.
70 F. Berger, M. B. Plutschack, J. Riegger, W. Yu, S. Speicher, M. Ho, N. Frank and T. Ritter, Site-Selective and Versatile Aromatic C–H Functionalization by Thianthrenation, *Nature*, 2019, **567**, 223–228.
71 F. Juliá, Q. Shao, M. Duan, M. B. Plutschack, F. Berger, J. Mateos, C. Lu, X.-S. Xue, K. N. Houk and T. Ritter, High Site Selectivity in Electrophilic Aromatic Substitutions: Mechanism of C–H Thianthrenation, *J. Am. Chem. Soc.*, 2021, **143**, 16041–16054.
72 J. Wu, Z. Wang, X.-Y. Chen, Y. Wu, D. Wang, Q. Peng and P. Wang, Para-Selective Borylation of Monosubstituted Benzenes using a Transient Mediator, *Sci. China:Chem.*, 2020, **63**, 336–340.
73 D. Ahmadli, S. Müller, Y. Xie, T. Smejkal, S. Jaeckh, A. V. Iosub, S. R. Williams and T. Ritter, Standardized Approach for Diversification of Complex Small Molecules via Aryl Thianthrenium Salts, *J. Am. Chem. Soc.*, 2025, **147**, 4268–4283.
74 R. A. Naumann, M. A. Clerk, R. E. Hernandez and N. A. Romero, Electrochemical C–H Functionalization and Defunctionalization of Polystyrene, *J. Am. Chem. Soc.*, 2025, **147**, 37272–37279.
75 U. Svanholm, O. Hammerich and V. D. Parker, Kinetics and Mechanisms of the Reactions of Organic Cation Radicals and Dications. II. Anisylation of Thianthrene Cation Radical, *J. Am. Chem. Soc.*, 1975, **97**, 101–106.
76 X.-Y. Chen, Y.-N. Li, Y. Wu, J. Bai, Y. Guo and P. Wang, Cu-Mediated Thianthrenation and Phenoxathiination of Arylborons, *J. Am. Chem. Soc.*, 2023, **145**, 10431–10440.
77 Z. He and P. Dydio, Photoinduced Cu(II)-Mediated Decarboxylative Thianthrenation of Aryl and Heteroaryl Carboxylic Acids, *Angew. Chem., Int. Ed.*, 2024, **63**, e202410616.
78 N. Kvasovs and V. Gevorgyan, Contemporary Methods for Generation of Aryl Radicals, *Chem. Soc. Rev.*, 2021, **50**, 2244–2259.
79 X. Zeng, The Strategies Towards Electrochemical Generation of Aryl Radicals, *Chem. – Eur. J.*, 2024, **30**, e202402220.
80 K. Grudzień, A. Zlobin, J. Zadworny, K. Rybicka-Jasińska and B. Sadowski, Modern Photo-and Electrochemical Approaches to Aryl Radical Generation, *Org. Chem. Front.*, 2024, **11**, 5232–5277.
81 E. L. S. de Souza and C. C. Oliveira, Selective Radical Transformations with Aryldiazonium Salts, *Eur. J. Org. Chem.*, 2023, e202300073.
82 X. Tian, Y. Liu, S. Yakubov, J. Schütte, S. Chiba and J. P. Barham, Photo- and Electro-Chemical Strategies for

the Activations of Strong Chemical Bonds, *Chem. Soc. Rev.*, 2024, **53**, 263–316.
83 P. Allongue, M. Delamar, B. Desbat, O. Fagebaume, R. Hitmi, J. Pinson and J.-M. Savéant, Covalent Modification of Carbon Surfaces by Aryl Radicals Generated from the Electrochemical Reduction of Diazonium Salts, *J. Am. Chem. Soc.*, 1997, **119**, 201–207.
84 M. Sheng, D. Frurip and D. Gorman, Reactive Chemical Hazards of Diazonium Salts, *J. Loss Prev. Process Ind.*, 2015, **38**, 114–118.
85 K. H. Vase, A. H. Holm, K. Norrman, S. U. Pedersen and K. Daasbjerg, Covalent Grafting of Glassy Carbon Electrodes with Diaryliodonium Salts: New Aspects, *Langmuir*, 2007, **23**, 3786–3793.
86 E. Linde, S. Mondal and B. Olofsson, Advancements in the Synthesis of Diaryliodonium Salts: Updated Protocols, *Adv. Synth. Catal.*, 2023, **365**, 2751–2756.
87 D. Le Count and J. Reid, Iodonium Salt Synthesis. Evidence for the Formation of Isomers in the Synthesis of Diaryliodonium Salts, *J. Chem. Soc. C*, 1967, 1298–1301.
88 Z. Tang, M. Guan, T. Wang, G. Yu, J. Qin, J. Lan and R. Yan, Palladium-Catalyzed Catellani-type Selective C–H Silylation of Aryl-TT Salts, *Org. Chem. Front.*, 2025, **12**, 2260–2265.
89 C. Chen, J.-P. Liu, X.-Y. Hu, Z.-Y. Wang, X.-X. Zhang, J.-H. Song, Y.-P. Zhu, C. Ni and B. Zhu, Palladium-catalyzed Site-Selective C–H Polyfluoroarylation of Arenes via Aryl Thianthrenium Salts, *Org. Chem. Front.*, 2025, **12**, 4997–5002.
90 Y. Ji, A. Jaafar, C. Gimbert-Suriñach, M. Ribagorda, A. Vallribera, A. Granados and M. J. Cabrera-Afonso, Photocatalyst-Free Light-Mediated Three-Component Alkoxy-, Hydroxy-, and Azidotrifluoromethylation of Alkenes, *Org. Chem. Front.*, 2024, **11**, 6660–6665.
91 L. van Dalsen, R. E. Brown, J. A. Rossi-Ashton and D. J. Procter, Sulfonium Salts as Acceptors in Electron Donor-Acceptor Complexes, *Angew. Chem., Int. Ed.*, 2023, **62**, e202303104.
92 R. I. Patel, B. Saxena and A. Sharma, Photoactivation of Thianthrenium Salts: An Electron-Donor–Acceptor (EDA)-Complex Approach, *J. Org. Chem.*, 2025, **90**, 6617–6643.
93 W. Li, J. Rabeah, F. Bourriquen, D. Yang, C. Kreyenschulte, N. Rockstroh, H. Lund, S. Bartling, A.-E. Surkus, K. Junge, A. Brückner, A. Lei and M. Beller, Scalable and Selective Deuteration of (Hetero)Arenes, *Nat. Chem.*, 2022, **14**, 334–341.
94 S. Kopf, F. Bourriquen, W. Li, H. Neumann, K. Junge and M. Beller, Recent Developments for the Deuterium and Tritium Labeling of Organic Molecules, *Chem. Rev.*, 2022, **122**, 6634–6718.
95 D. Zhao, R. Petzold, J. Yan, D. Muri and T. Ritter, Tritiation of Aryl Thianthrenium Salts with a Molecular Palladium Catalyst, *Nature*, 2021, **600**, 444–449.
96 Q. Wang, W. Xiao, H. He, J. Guo, M. Wang, M. Ma and B. Zhao, Regioselective Deuteration of Arenes Enabled by Simple Heterogeneous Palladium Catalysis, *J. Org. Chem.*, 2023, **88**, 10818–10827.
97 Z.-H. Lin, Y.-F. Yao and C.-P. Zhang, Deuteration of Arylthianthren-5-ium Salts in CD3OD, *Org. Lett.*, 2022, **24**, 8417–8422.
98 S. J. Blanksby and G. B. Ellison, Bond Dissociation Energies of Organic Molecules, *Acc. Chem. Res.*, 2003, **36**, 255–263.
99 K. Sun, C. Ge, X. Chen, B. Yu, L. Qu and B. Yu, Energy-Transfer-Enabled Photocatalytic Transformations of Aryl Thianthrenium Salts, *Nat. Commun.*, 2024, **15**, 9693.
100 V. Balzani, P. Ceroni and A. Juris, in *Photochemistry and Photophysics: Concepts, Research, Applications*, John Wiley & Sons, 1 edn, 2014, ch. 6, pp. 139–168.
101 N. Miyaura, in *Cross-Coupling Reactions: A Practical Guide*, ed. N. Miyaura, Springer Berlin Heidelberg, Berlin, Heidelberg, 2002, pp. 11–59.
102 J. F. Hartwig, Regioselectivity of the Borylation of Alkanes and Arenes, *Chem. Soc. Rev.*, 2011, **40**, 1992–2002.
103 I. A. I. Mkhalid, J. H. Barnard, T. B. Marder, J. M. Murphy and J. F. Hartwig, C–H Activation for the Construction of C–B Bonds, *Chem. Rev.*, 2010, **110**, 890–931.
104 M. M. M. Hassan, S. Guria, S. Dey, J. Das and B. Chattopadhyay, Transition Metal–Catalyzed Remote C—H Borylation: An Emerging Synthetic Tool, *Sci. Adv.*, 2023, **9**, eadg3311.
105 Y.-M. Tian, X.-N. Guo, H. Braunschweig, U. Radius and T. B. Marder, Photoinduced Borylation for the Synthesis of Organoboron Compounds, *Chem. Rev.*, 2021, **121**, 3561–3597.
106 T. Liu, Y.-P. Cai and Q.-H. Song, Visible-Light-Mediated Borylation of Arenes via an Electron Donor–Acceptor Complex of Thianthrenium Salts, *J. Org. Chem.*, 2025, **90**, 6569–6576.
107 S. Pimparkar, A. Koodan, S. Maiti, N. S. Ahmed, M. M. M. Mostafa and D. Maiti, C–CN bond formation: an overview of diverse strategies, *Chem. Commun.*, 2021, **57**, 2210–2232.
108 G. Zhang, Z. Luo, C. Guan, X. Zhang and C. Ding, Nickel-Catalyzed Selective C–H Cyanation via Aromatic Thianthrenium Salts, *J. Org. Chem.*, 2023, **88**, 9249–9256.
109 K. Cheng, E. W. Webb, G. D. Bowden, J. S. Wright, X. Shao, M. S. Sanford and P. J. H. Scott, Photo- and Cu-Mediated 11C Cyanation of (Hetero)Aryl Thianthrenium Salts, *Org. Lett.*, 2024, **26**, 3419–3423.
110 G. Boscutti, M. Huiban and J. Passchier, Use of Carbon-11 Labelled Tool Compounds in Support of Drug Development, *Drug Discovery Today:Technol.*, 2017, **25**, 3–10.
111 Y.-F. Zhang and Z.-J. Shi, Upgrading Cross-Coupling Reactions for Biaryl Syntheses, *Acc. Chem. Res.*, 2018, **52**, 161–169.
112 E. M. Alvarez, T. Karl, F. Berger, L. Torkowski and T. Ritter, Late-Stage Heteroarylation of Hetero(aryl)sulfonium Salts Activated by α-Amino Alkyl Radicals, *Angew. Chem., Int. Ed.*, 2021, **60**, 13609–13613.

113 Y. Zhao, C. Yu, W. Liang and F. W. Patureau, Photochemical (Hetero-)Arylation of Aryl Sulfonium Salts, *Org. Lett.*, 2021, **23**, 6232–6236.

114 A. Shi, P. Xiang, Y. Wu, C. Ge, Y. Liu, K. Sun and B. Yu, Visible-Light-Promoted Metal-Free 3-Arylation of 2-Aryl-2H-indazoles with Triarylsulfonium Salts, *Synlett*, 2022, 457–464.

115 Z. Wang, J. Wang, Z. Yang, X. Li, K. Cheng and W. Liu, Photoinduced Cu-Catalyzed C2-H Functionalization of Azoles using Aryl Thianthrenium Salts, *Adv. Synth. Catal.*, 2025, **367**, e202401378.

116 K. Sun, A. Shi, Y. Liu, X. Chen, P. Xiang, X. Wang, L. Qu and B. Yu, A General Electron Donor–Acceptor Complex for Photoactivation of Arenes via Thianthrenation, *Chem. Sci.*, 2022, **13**, 5659–5666.

117 S. Yang, X. Tan, D. Liu, H. Jiang and W. Wu, Visible Light–Induced Arylation/Alkylation/Phosphorylation of Isocyanides via EDA Complex Activation, *Chin. J. Chem.*, 2025, **43**, 1379–1384.

118 F. Ye, F. Berger, H. Jia, J. Ford, A. Wortman, J. Börgel, C. Genicot and T. Ritter, Aryl Sulfonium Salts for Site-Selective Late-Stage Trifluoromethylation, *Angew. Chem., Int. Ed.*, 2019, **58**, 14615–14619.

119 Y.-L. Zhang, G.-H. Wang, Y. Wu, C.-Y. Zhu and P. Wang, Construction of α-Amino Azines via Thianthrenation-Enabled Photocatalyzed Hydroarylation of Azine-Substituted Enamides with Arenes, *Org. Lett.*, 2021, **23**, 8522–8526.

120 Y. Cai and T. Ritter, Meerwein-type Bromoarylation with Arylthianthrenium Salts, *Angew. Chem., Int. Ed.*, 2022, **61**, e202209882.

121 Y. Cai, S. Chatterjee and T. Ritter, Photoinduced Copper-Catalyzed Late-Stage Azidoarylation of Alkenes via Arylthianthrenium Salts, *J. Am. Chem. Soc.*, 2023, **145**, 13542–13548.

122 H. J. Timpe and K. P. Kronfeld, Light-Induced Polymer and Polymerization Reactions XXXIII: Direct Photoinitiation of Methyl Methacrylate Polymerization by Excited States of Ketones, *J. Photochem. Photobiol., A*, 1989, **46**, 253–267.

123 C. B. Tripathi, T. Ohtani, M. T. Corbett and T. Ooi, Photoredox Ketone Catalysis for the Direct C–H Imidation and Acyloxylation of Arenes, *Chem. Sci.*, 2017, **8**, 5622–5627.

124 P. Sarró, A. Gallego-Gamo, R. Pleixats, A. Vallribera, C. Gimbert-Suriñach and A. Granados, Access to Benzyl Oxindoles via Electron Donor-Acceptor Complex Photoactivation Using Thianthrenium Salts and Potassium Carbonate, *Adv. Synth. Catal.*, 2024, **366**, 2587–2595.

125 B. Mondal, A. Chatterjee, N. C. Saha, M. Jana and J. Saha, Thianthrenation-Promoted Photoinduced Alkene Difunctionalization and Aryl Allylation with Morita–Baylis–Hillman Adducts, *Chem. Commun.*, 2024, **60**, 7184–7187.

126 Q. Wu, X. Li, J. Ma, Y. Shi, J. Lv and D. Yang, Arylcyanation of Styrenes by Photoactive Electron Donor–Acceptor Complexes/Copper Catalysis, *Org. Lett.*, 2024, **26**, 7949–7955.

127 Q. Wu, X. Li, J. Lv, Y. Shi and D. Yang, Photoredox/Copper Dual-Catalyzed Regioselective 1,4-Arylcyanation of 1,3-Enynes for Multifunctionalized Allenyl Nitriles, *Org. Lett.*, 2025, **27**, 7703–7708.

128 N. Kaplaneris, M. Akdeniz, M. Fillols, F. Arrighi, F. Raymenants, G. Sanil, D. T. Gryko and T. Noël, Photocatalytic Functionalization of Dehydroalanine-Derived Peptides in Batch and Flow, *Angew. Chem., Int. Ed.*, 2024, **63**, e202403271.

129 H. Ma, D. Zhang, B. Cheng, L. Wang, B. Xu, S. Wang, S. Zhang, J. Lv, B. König and G. Zhang, Photoredox/Copper Cooperatively Catalyzed Arylalkynylation of [1.1.1] Propellane, *Org. Lett.*, 2025, **27**, 3446–3451.

130 D.-S. Ji, Y. Ye, P. Zhang, C. Zhou, Y. Yuan, X. Bao and C. Huo, Visible-Light-Induced NHC-Catalyzed Carboacylation Reaction of Alkenes from Aryl Thianthrenium Salts and Aldehydes, *Org. Lett.*, 2025, **27**, 2247–2255.

131 K. Liu, M. Schwenzer and A. Studer, Radical NHC Catalysis, *ACS Catal.*, 2022, **12**, 11984–11999.

132 P. S. Engl, A. P. Häring, F. Berger, G. Berger, A. Pérez-Bitrián and T. Ritter, C–N Cross-Couplings for Site-Selective Late-Stage Diversification via Aryl Sulfonium Salts, *J. Am. Chem. Soc.*, 2019, **141**, 13346–13351.

133 X. Tan, W. Xiong, B. Zhu, H. Liu, W. Wu and H. Jiang, Photoinduced Arene C–H Amination with Ammonia: A Practical and Regioselective Strategy for Primary Amines, *Adv. Synth. Catal.*, 2023, **365**, 2165–2170.

134 S. Ni, R. Halder, D. Ahmadli, E. J. Reijerse, J. Cornella and T. Ritter, C–Heteroatom Coupling with Electron-Rich Aryls Enabled by Nickel Catalysis and Light, *Nat. Catal.*, 2024, **7**, 733–741.

135 H. Xu, X. Li, Y. Dong, S. Ji, J. Zuo, J. Lv and D. Yang, Thianthrenium-Enabled Phosphorylation of Aryl C–H Bonds via Electron Donor–Acceptor Complex Photoactivation, *Org. Lett.*, 2023, **25**, 3784–3789.

136 A. Gallego-Gamo, D. Reyes-Mesa, A. Guinart-Guillem, R. Pleixats, C. Gimbert-Suriñach, A. Vallribera and A. Granados, Site-Selective and Metal-Free C–H Phosphonation of Arenes via Photoactivation of Thianthrenium Salts, *RSC Adv.*, 2023, **13**, 23359–23364.

137 W. Liu, H. Hou, H. Jing, S. Huang, W. Ou and C. Su, Photoinduced Phosphination of Arenes Enabled by an Electron Donor–Acceptor Complex Using Thianthrenium Salts, *Org. Lett.*, 2023, **25**, 8350–8355.

138 M. Mato, P. C. Bruzzese, F. Takahashi, M. Leutzsch, E. J. Reijerse, A. Schnegg and J. Cornella, Oxidative Addition of Aryl Electrophiles into a Red-Light-Active Bismuthinidene, *J. Am. Chem. Soc.*, 2023, **145**, 18742–18747.

139 R. Sang, S. E. Korkis, W. Su, F. Ye, P. S. Engl, F. Berger and T. Ritter, Site-Selective C-H Oxygenation via Aryl Sulfonium Salts, *Angew. Chem., Int. Ed.*, 2019, **58**, 16161–16166.

140 Y. Zhao, C. Yu, W. Liang, I. L. Atodiresei and F. W. Patureau, TEMPO-Mediated Late Stage Photochemical Hydroxylation of Biaryl Sulfonium Salts, *Chem. Commun.*, 2022, **58**, 2846–2849.

141 Y. Guo, L. Wei, Z. Wen, H. Jiang and C. Qi, Photoredox-Catalyzed Coupling of Aryl Sulfonium Salts with CO2 and Amines to Access O-Aryl Carbamates, *Chem. Commun.*, 2023, **59**, 764–767.

142 A. Granados, M. J. Cabrera-Afonso, M. Escolano, S. O. Badir and G. A. Molander, Thianthrenium-Enabled Sulfonylation via Electron Donor-Acceptor Complex Photoactivation, *Chem. Catal.*, 2022, **2**, 898–907.

143 F.-S. He, P. Bao, Z. Tang, F. Yu, W.-P. Deng and J. Wu, Photoredox-Catalyzed α-Sulfonylation of Ketones from Sulfur Dioxide and Thianthrenium Salts, *Org. Lett.*, 2022, **24**, 2955–2960.

144 Q. Li, J. Huang, Z. Cao, J. Zhang and J. Wu, Photoredox-Catalyzed Reaction of Thianthrenium Salts, Sulfur Dioxide and Hydrazines, *Org. Chem. Front.*, 2022, **9**, 3781–3785.

145 X. Kong, Y. Chen, Q. Liu, W. Wang, S. Zhang, Q. Zhang, X. Chen, Y.-Q. Xu and Z.-Y. Cao, Selective Fluorosulfonylation of Thianthrenium Salts Enabled by Electrochemistry, *Org. Lett.*, 2023, **25**, 581–586.

146 H. Xu, X. Li, Y. Wang, X. Song, Y. Shi, J. Lv and D. Yang, Arylthianthrenium Salts as the Aryl Sources: Visible Light/Copper Catalysis-Enabled Intermolecular Azidosulfonylation of Alkenes, *Org. Lett.*, 2024, **26**, 1845–1850.

147 H. Ma, Y. Li, P. Wang, J. Ye, J. Zhang, G. Liu and J. Wu, Photoredox-Catalyzed Intermolecular Azidosulfonylation of Alkenes with DABCO·(SO2)2, Trimethylsilyl Azide and Thianthrenium salts, *Org. Chem. Front.*, 2023, **10**, 866–871.

148 M. J. Cabrera-Afonso, A. Granados and G. A. Molander, Sustainable Thioetherification via Electron Donor–Acceptor Photoactivation Using Thianthrenium Salts, *Angew. Chem., Int. Ed.*, 2022, **61**, e202202706.

149 Y. Fang, Q. Liang, L. Shi, J. Wen, X. Liu, X. Hong, X. Zha and F. Ji, Site-Selective S-Arylation of 1-Thiosugars with Aryl Thianthrenium Salts through Copper(I)-Mediated, Photoredox- Catalyzed Reactions, *Adv. Synth. Catal.*, 2024, **366**, 2344–2351.

150 H. Xu, X. Li, J. Ma, J. Zuo, X. Song, J. Lv and D. Yang, An Electron Donor–Acceptor Photoactivation Strategy for the Synthesis of S-aryl Dithiocarbamates Using Thianthrenium Salts Under Mild Aqueous Micellar Conditions, *Chin. Chem. Lett.*, 2023, **34**, 108403.

151 M. Liu, Y. Qian, Y. Wu and F. Zhang, Multicomponent Synthesis of Di-Aryl Dithiocarbamates via Electron Donor–Acceptor Photoactivation with Thianthrenium Salts, *Green Chem.*, 2023, **25**, 3852–3856.

152 Y. Tang, Y. Cai, Z. Xie, Z. Gao, X. Chen and J. Yi, Multicomponent Reactions to Access S-aryl Dithiocarbamates via an Electron Donor–Acceptor Complex Under Open-to-Air Conditions, *Org. Biomol. Chem.*, 2024, **22**, 1378–1385.

153 X. Zhuang, H. Li, Z. Feng and H. Wang, Visible-Light-Mediated Copper-Catalyzed S-Arylation of Sulfenamides with Aryl Thianthrenium Salts, *Org. Lett.*, 2025, **27**, 4886–4892.

154 G. Guo, J. Ma, Y. Dong, Q. Wu, J. Lv, Y. Shi and D. Yang, Visible Light/Copper Catalysis-Enabled Arylation and Alkenylation of Phosphorothioates via Site-Selective C–H Thianthrenation, *Org. Lett.*, 2024, **26**, 8382–8388.

155 J. Zuo, X. Li, Y. Shi, J. Lv and D. Yang, Synthesis of Sulfur-Containing Trisubstituted Imidazoles by One-Pot, Multicomponent Reaction via Electron Donor–Acceptor Complex Photoactivation, *Org. Lett.*, 2024, **26**, 3541–3546.

156 X.-Y. Chen, X. Kuang, Y. Wu, J. Zhou and P. Wang, Thianthrene Radical Cation as a Transient SET Mediator: Photoinduced Thiocyanation and Selenocyanation of Arylthianthrenium Salts, *Chin. J. Chem.*, 2023, **41**, 1979–1986.

157 S. Ni, J. Yan, S. Tewari, E. J. Reijerse, T. Ritter and J. Cornella, Nickel Meets Aryl Thianthrenium Salts: Ni(I)-Catalyzed Halogenation of Arenes, *J. Am. Chem. Soc.*, 2023, **145**, 9988–9993.

158 T. Michiyuki and L. Ackermann, Electrochemical Preparation and Transformation of Sulfonium Salts, *ChemElectroChem*, 2025, **12**, e202400711.

